Università degli Studi di Padova

Department of Cardiac, Thoracic and Vascular Sciences

Ph.D. Course in: Traslational Specialistic Medicine “G.B Morgagni”

Curriculum: Neurosciences

Series XXXI

STRUCTURAL BRAIN PATTERNS IN ANOREXIA NERVOSA: A MULTIMODAL MRI EVALUATION

Coordinator: Prof.ssa Annalisa Angelini

Supervisor: Prof.ssa Angela Favaro

Ph.D. Student: Enrico Collantoni

ABSTRACT

Introduction.

Cortical and white matter structural abnormalities in Anorexia Nervosa (AN) have been recently investigated, but no attempt has been made to explore the organizational patterns that govern the relationships between different brain areas and to characterize the neurobiology of the disorder in the different stages of its course. Aims of the present work are to characterize cortical and white matter network architecture by means of different structural indices and computational techniques, to observe the presence of any correlation between clinical variables and networks characteristics and to investigate the structural organizational patterns in the different stage of AN course.

Methods and Materials.

38 patients with acute AN, 38 healthy controls and 20 patients in full remission from AN were included in this study. All participants underwent high-resolution MRI. An analysis of cortical structural co-variance was performed using cortical thickness and gyrification indices. The anatomical complexity of the cortex was explored by means of Fractal Dimension (FD). Connectomic tools were applied to DTI tractography data to investigate the white matter network architecture.

Results.

Patients with AN showed unbalanced integration and segregation properties in cortical thickness, gyrification and DTI networks both on global and regional levels. Patients with a poor outcome at a three years follow-up assessment showed higher segregation measures and lower small-worldness in the gyrification network. The FD analysis revealed a reduced cortical complexity in the AN group.

Discussion.

Alterations in structural covariance patterns in AN are likely to reflect the metabolic consequences of the disorder as well as deviations in normal developmental trajectories. Lower FD in AN indicates a reduction of cortical complexity in the acute stages of the disorder and evidenced that this structural index is sensitive to the effects of malnutrition.

INDEX

INTRODUCTION

ANOREXIA NERVOSA

Anorexia Nervosa (AN) is a severe psychiatric disorder of multifactorial etiology that typically develops during adolescence, is characterized by a high female/male ratio and by high co-morbidity and mortality rates. From a psychopathological point of view, pivotal elements of the disorder are an intense fear of weight gain and a distortion of the body image, which results in an extreme caloric restriction and in other compensatory behaviors such as purging or excessive exercise (American Psychiatric Association, 2013; Zipfel et al., 2015).

The incidence rates in AN have been estimated at 490 per 100000 person-years in a large community study (Keski-Rahkonen et al., 2007), with the highest incidence rates among females aged 14 to 19 years (Javaras et al., 2015). The lifetime-prevalence of AN substantially changed after the introduction of DSM-5 diagnostic criteria. In particular, the transition from DSM-IV to DSM-5 has caused increased diagnosis rates in the full-threshold diagnoses and a reduction of sub-threshold diagnoses (Smink, van Hoeken, & Hoek, 2013). Using DSM-5 criteria, a recent research estimated a lifetime-prevalence of AN at 3.6% in a sample of 16-20 years old female population (Mustelin et al., 2016). In the last three decades the AN incidence seems to have reached a plateau, but a decrease in its age of onset has been highlighted (Angela Favaro, Caregaro, Tenconi, Bosello, & Santonastaso, 2009).

AN is characterized by variable clinical course and outcome. The clinical course of AN is often relapsing and protracted, leading to high rates of disability and to high burdens on families, society and national health systems. Across studies examining patients 10 to 20 years after diagnosis, just under half of patients achieved full recovery, another third remained symptomatic but demonstrated some improvement, and 20% remained chronically ill (Steinhausen, 2002). The prognosis of AN is strongly influenced by the time between the onset and its recognition. Early recognition and early treatment seem to predict more favorable outcomes, while long delays between onset of illness and initiation of

treatment is associated with worse course and outcome (Steinhausen, 2002). In AN, mortality rates are higher than in any other psychiatric disorder, mainly as the result of the serious clinical complications. A large meta-analysis conducted on a total of 35 studies and on 6009 subjects evidenced an annual mortality rate of 5.10 deaths per 1000 person-years, of which 1.3 deaths resulted from suicide (Arcelus, Mitchell, Wales, & Nielsen, 2011). Also suicide attempts are frequently reported in AN. A study on a large cohort of AN patient (n=432) reported that 17% of them endorsed at least one suicide attempt (Bulik et al., 2008), and a review conducted in 2006 by Franko and Keel reported that clinical correlates of suicide attempts included purging behaviors, depression, substance abuse and history of childhood physical or sexual abuse (Franko & Keel, 2006).

Many studies have reported elevated co-morbidity rates in individuals with AN, also evidencing that the ability to identify the presence of co-morbidities is of high importance for addressing therapeutic choices (Salbach-Andrae et al., 2008). The most common psychiatric disorders that occur with AN are Major Depressive Disorder, with reported lifetime prevalence rates ranging from 9,5% to 64,7% in those with restrictive AN and from 50 to 71,3% in those with AN binge-purge subtype (Fernandez-Aranda et al., 2007). Anxiety Disorders and Obsessive-Compulsive disorders are also frequently diagnosed in comorbidity with AN (Halmi et al., 2003; Swinbourne et al., 2012). The onset of anxiety disorders often precedes the onset of AN and their frequency among AN patients ranges from 25% to 75%. With regard to OCD symptoms, 68% of AN patients of the restrictive type and 79,1% of those of the binge eating/purging type present lifetime obsessions and compulsions (Halmi et al., 2003).

THE ROLE OF STRUCTURAL NEUROIMAING IN THE UNDERSTANTING OF THE PATHOGENETIC PATHWAYS TO ANOREXIA NERVOSA

The etiology of AN is complex and multifactorial and the role of the involved factors should be distinguished in predisposing, precipitating and perpetuating. Either biological and genetical, as well as psychological and sociocultural factors (Rose & Frampton, 2011) have a role.

In last years, advances in neuroimaging techniques, alongside the presence of increasingly powerful computational methods, have allowed great progresses in the identification of the neurobiological substrates that characterize AN etiology and progression (Guido K. W. Frank, Favaro, Marsh, Ehrlich, & Lawson, 2018; Guido K.W. Frank, 2014). In this context, structural neuroimaging has the advantage of evaluating substrates that are not influenced by acute emotional and motivational states (J. A. King, Frank, Thompson, & Ehrlich, 2018). However, since to date the long-term effects of weight loss and starvation on the brains of patients with EDs are largely unknown, studies conducted in currently ill or in recovered patients are intrinsically limited in describing cause-effects relationships, because it is not possible to disentangle structural alterations pre-existent to the disorder from the consequences of malnutrition. In other words, research should address not only the role of genetic and environmental risk factors on the brain, but also the effects of the disorder on developmental trajectories, in order to fully understand the pathogenetic pathways to disease, and to distinguish causes from consequences (Angela Favaro, 2013).

The main challenge with the interpretation of structural neuroimaging findings in AN is in the ability to recognize which pathogenic mechanisms underlie specific brain alterations. In fact, alterations in the brain structure could result from multiple causes that can in turn act differently depending on the stage of the disorder in which they occur. Coherently with this, is particularly important to adopt a staging model of AN that could help in distinguishing those factors that contribute to the onset of the disorder from those that are caused by the disorder itself in a neurodevelopment context (Angela Favaro, 2013). A proper staging of the course of AN is also important from a therapeutic perspective, since it allows to design treatment programs tailored to the phase of the illness (Treasure, Stein, & Maguire, 2015).

To date, structural neuroimaging studies in AN focused on Gray Matter (GM) or White Matter (WM) evaluation. GM evaluations used both Voxel Based Morphometry (VBM) and Surface Based Morphometry approaches (SBM) (J. A. King et al., 2018; J Seitz, Herpertz-Dahlmann, & Konrad, 2016; Titova, Hjorth, Schiöth, & Brooks, 2013). VMB allows to investigate cortical volume and density, while

SBM allows to estimate Cortical Thickness and Gyrification indices. WM estimations mainly focused on Fractional Anisotropy (FA) (Landman et al., 2007). FA describes how diffusive processes vary in the different spatial directions and is a good marker of WM integrity. An increase in FA (FA values range from 0 to 1) reflects an increased diffusivity in the direction parallel to the fiber and a reduced diffusivity in the perpendicular directions. Alterations in FA values can reflect different pathogenetic processes, such as inflammation, edema, demyelination, gliosis and axonal loss (Agarwal et al., 2009; Dong et al., 2004).

A novel approach in the neuroimaging of AN consists in applying connectomic measures to structural indices, in order to investigate the structural architecture of neural circuits and to describe the mutual relationships between different brain areas (Sporns, 2010). From a neurobiological perspective, neurocircuits represents a highly sensitive interface between biological and environmental factors, being continuously modeled accordingly to developmental demands and to external contingencies. Infancy and adolescence are very important and peculiar developmental windows, as they are characterized by greater brain plasticity rates (DeFelipe, 2006). During these critical periods, the exposure to specific risk factors may have important effects on neurocircuit modeling, that may results in conditions of vulnerability (Angela Favaro, 2013). A connectomic approach is particularly useful in understanding changes in both local and global brain dynamics that are associated with a pathological process or behavior in a neurodevelopment context (Morgan, White, Bullmore, & Vértes, 2018).

STATE OF THE ART IN THE STRUCTURAL NEUROIMAGING IN ANOREXIA NERVOSA

GREY MATTER EVALUATION

The study of the brain macrostructure requires T1-weighted MRI. For the evaluation of grey matter, two methods can be identified: voxel-based morphometry (VBM) (Ashburner & Friston, 2000) and surface-based analysis (SBA) (B. Fischl & Dale, 2000; Bruce Fischl, Sereno, & Dale, 1999).

In VBM, two quantities are used to measure morphometric properties: volume and concentration (i.e. the amount of gray matter per unit of intracranial volume). This technique performs a non-linear registration to spatially normalize the T1-weighted image of a subject to a group template and to establish a voxel-per-voxel correspondence across subjects. This process creates a map of how far each voxel in the input image must move to land at the matching point in the template image. Then, these deformed brain images are segmented in different tissue classes and smoothed so that each voxel represents the average of itself and its neighbors. A voxel-wise statistical analysis is performed to compare brains from different subjects.

In SBA, the morphometric measures are computed by geometrically modelling the cortical surface. In particular, in SBA, the cortex is modeled as a mesh of triangles whose vertices are used as coordinates. The knowledge of these coordinates allows the spatial manipulation of the cortex and the computation of different morphometric measures. For example, the cortical surface area can be computed by summing up the areas of the triangles, the cortical thickness is computed as the distance between the white and pial surfaces and the curvature is a measure of how sharply the cortex is folded at each point.

VBM studies in AN have been exhaustively meta-analyzed (Jochen Seitz et al., 2014). The two most comprehensive meta-analyses conducted to date showed quite consistent results and identified a marked reduction in GM in patients with acute AN (Jochen Seitz et al., 2014; Titova et al., 2013). The main concerns with VMB studies in AN are represented by the small sample sizes and by the heterogeneity of age in the experimental samples. Overall, studies on adolescents showed more homogeneous results and more pronounced GM volume changes in comparison to adult ones. The regions that have been shown to be more susceptible to GM changes appeared to be Cingulate Gyrus, Hippocampus and Midbrain. With some exceptions, recovered AN patients tend to show nearly normalized brain volumes after weight gain. Short-term weight gain in longitudinal studies resulted in about half of GM and CSF changes being normalized relatively quickly upon initial weight gain (on average after 4 months) (Jochen Seitz et al., 2014).

SBM studies in AN are inconsistent as regards findings, methodological approaches and recruitment criteria.

A significant reduction of cortical thickness in underweight patients with AN was reported by different studies, although it has not been always replicated (Bär, de la Cruz, Berger, Schultz, & Wagner, 2015; Bernardoni et al., 2016; Lavagnino et al., 2016) . Inconsistent findings across different studies were probably due to differences in experimental samples. The duration of the disease and the age of the patients are likely to be the main sources of these differences. There is to date only one longitudinal observation estimating cortical thickness in patients with AN. This longitudinal study showed a substantial restoration of CT after an average of three months of weight recovery (Bernardoni et al., 2016). Regional findings showed reduced CT mainly in parietal and frontal regions (Bär et al., 2015; Fuglset et al., 2016) but involved brain areas are quite heterogeneous across studies. Lavagnino et al. (2018), in a recent study, performed a region-based analysis that showed a mixed pattern with AN patients showing higher values of cortical thickness in comparison to healthy controls in orbital and insular areas and lower values in superior frontal cortex.

Regarding cortical gyrification, Favaro et al. (Angela Favaro, Tenconi, Degortes, Manara, & Santonastaso, 2015) observed the presence of significant alterations in the parietal and frontal cortex of adult patients with AN; hypogyrification in these areas was not correlated with weight loss, body mass index, cortical thickness or dehydration (Angela Favaro et al., 2015). Furthermore, these alterations were not present in patients with a good clinical outcome, regardless of their body weight and recovery status. On the contrary, in a mixed sample of adolescents and adults, Bernardoni et al. (Bernardoni et al., 2018a) found that an almost complete normalization of cortical folding after weight gain and weight restoration was the main predictor of increased gyrification during treatment (Bernardoni et al., 2018a).

WHITE MATTER EVALUATION

In recent years, a marked increase in studies evaluating white matter in AN by means of Diffusion Tensor Imaging (DTI) has been observed. However, these studies considered low and heterogeneous samples and used different multi-subjects analysis approaches (Voxel-Based Morphometry, Tract-Based Spatial Statistics, Probabilistic and Deterministic Tractography). Furthermore, a recent research has raised methodological issues in the investigation of the fornix, which is shown to be structurally altered in five DTI studies in AN. In fact, in acute AN, the increased volume of the ventricles seems to lead to a partial volume effect (PVE) that alters the diffusion index of the fornix (Kaufmann et al., 2017). For all these reasons, the results of DTI studies in AN should be interpreted with caution.

Overall, DTI studies in patients with acute AN evidenced heterogeneus FA alteration in several WM fiber tracts, suggesting the presence of a lower WM integrity. A recent research, conducted by Philippou and colleagues on a sample of 26 patients with restrictive AN showed widespread WM alteration, with largest differences in Corona Radiata, Corpus Callosum and Superior Longitudinal Fasciculus (Phillipou et al., 2018). Alterations in these regions were replicated by another recent TBSS analysis (Gaudio et al., 2017). Interestingly, in a longitudinal analysis, Vogel and colleagues observed FA alterations in similar areas than Philippou et al. and Gaudio et al., but with a different direction (increased FA in Corona Radiata, Corpus Callosum, Anterior and Posterior Thalamic Radiation, Anterior and Posterior limb of internal capsula, inferior longitudinal fasciculus) (Vogel et al., 2016). Increased FA was also observed by Frank et al. (Guido K.W. Frank, Shott, Hagman, & Yang, 2013) Travis et al. (2015) and Cha et al. (Cha et al., 2016), who evidenced complex patterns of FA alterations in AN. Frank and colleagues found higher FA in left superior longitudinal fasciculus, bilateral anterior corona radiata, bilateral inferior fronto-occipital fasciculus, and lower FA in left fornix, bilateral cingulum, right forceps major, right superior, left posterior corona radiata in AN patients when compared to healthy controls. Travis and colleagues (2015) evidenced increased FA in anterior thalamic radiations and in left anterior superior longitudinal fasciculus, and lower FA in right anterior superior longitudinal fasciculus, in fimbria-fornix and in the

motor subdivision of corpus-callosum in patients with AN with respect to healthy controls. The studies that showed patterns of increased FA in patients with AN are all conducted on adolescent patients with relatively short illness duration and are likely to reflect a sort of reaction of the developing brain to the toxic effects of malnutrition, dehydration or starvation. To investigate whether the nature of DTI findings reflected state or trait disorder related features, few studies to date have focused on patients recovered from AN. Among them, only one evidenced the presence of WM alterations in patients recovered from AN, while the others reported no differences in WM structures between recovered patients and healthy controls. A recent longitudinal observation focused on a sample of 46 patients with AN before and after a partial weight restoration (at least 10% of BMI increase). The study replicated findings about reduced FA in the fornix and corpus callosum and found an increased FA in the corticospinal tract in the acute state of malnutrition. All these alterations normalized with weight gain at the follow up assessment (Boehm et al., 2016). The normalization of DTI alterations with weight recovery confirms the results of another longitudinal observation conducted by Vogel and colleagues, but not the findings of Cha and collaborators, who found a persistence of higher FA values in regions near to the lateral Orbito Frontal Cortex and in the Nucleus Accumbens in recovered AN patients (Cha et al., 2016; Vogel et al., 2016).

A meta-analysis conducted by our research-group in 10 DTI studies in AN identified two clusters of decreased FA in patients with AN that are located in the left caudate and in left thalamus (Meneguzzo & Collantoni et al., in prep.). In the following Table, the studies that investigated WM in patients with AN to date are reported.

Table 1. DTI studies in AN

Study	Diagnosis/ Diagnostic criteria	N AN	N HC	Age AN	Age HC	BMI AN at the scan	BMI HC	Illness duration Years(DS)	Medicated
Bang et al., 2017	recAN DSM IV	22	22	27.62 (5.06)	26.10 (4.75)	20.45 (1.69)	21.83 (1.80)	2.83 (2.31)	3/22
	No differences AN-HC.								
Shott et al., 2016	recAN DSM IV	24	24	30.3 (8.1)	27.4 (6.3)	20.83 (2.37)	21.64 (1.26)	5.90 (5.21)	6/24
	recAN showed increased white matter connectivity between bilateral insula regions and ventral striatum left insula and middle orbitofrontal cortex and right insula and medial prefrontal cortex. FA was reduced in recAN compared with HC in anterior corona radiata, external capsule, and cerebellum including the corticopontine tract, corpus callosum, anterior thalamic radiation, inferior, and middle cerebellar peduncle as well as inferior fronto-occipital and uncinate fasciculus.								
Zhang et al., 2016	recAN DSM IV	24 (23 f/ 1 m)	31	21.33 (4.54)	20.90 (3.91)	20.13 (1.51)	21.99 (3.02)	6.01 (2.87)	none
	No differences in mean total fiber count between groups. recAN showed abnormal modularity involving frontal, basal ganglia, and posterior cingulate nodes.								
Yau et al., 2013	recAN DSM IV	12	10	28.7 (7.9)	26.7 (5.4)	21.2 (1.5)	22.0 (1.1)	5.67 (5.21)	none
	No differences in FA. recAN showed lower mean diffusivity in frontal, parietal and cingulum white matter relative to control women.								
Hayes et al., 2015	AN DSM IV-TR	8	8	35 (11)	36 (9)	n/a	n/a	16 (6)	8/8
	Reduced FA in AN in bilateral anterior limb of capsula interna, left inferior fronto-occipital fasciculus, right anterior cingulum. Increased FA in AN in the left fornix crus. Deterministic multitensor tractography suggested increased white matter connectivity in prefrontal and left occipitoparietal corticies and decreased in thalamus in AN.								
Frank et al.,2013	AN DSM IV	19	22	15.4 (1.4)	14.8 (1.8)	16.2 (1.1)	21.3 (1.9)		11/19
	Reduction of FA in AN in left fornix, bilateral cingulum, right forcepts major, right superior and left posterior corona radiata. Increased in AN in left superior longitudinal fasciculus, bilateral anterior corona radiata and bilateral inferior fronto-occipital fasciculus.								
Philippou et al., 2018	AN DSM-5	23	26	22.01 (5.42)	22.61 (3.12)	16.71 (1.18)	22.83 (3.38)	5.35 (4.62)	n/a
	Widespread FA decreases with one significant cluster that encompassed the corpus callosum, the left and right corona radiate, the superior longitudinal fasciculus and the right posterior thalamic radiation.								
Gaudio et al., 2017	AN DSM-IV-TR	18	16	15.7 (1.6)	16.3 (1.5)	16.2 (1.2)	21.1 (1.9)	0.41 (0.15)	none
	FA reduced in AN in the left anterior and superior corona radiata and left superior longitudinal fasciculus.								
Hu et al., 2017	AN DSM-IV	8	14	17.6 (2.2)	19.1 (3.1)	14.3 (1.3)	20.1 (1.7)	0.87 (0.52)	n/a
	AN patients revealed a decrease in FA in the left superior frontal gyrus, medial frontal gyrus, anterior cingulate cortex, middle frontal gyrus, inferior frontal gyrus, thalamus, and bilateral								

	insula. Positive correlations between the mean FA value of the left inferior frontal gyrus, insula as well as thalamus and BMI in AN patients.								
Kaufmann et al., 2017	AN DSM 5	25	25	22.8 (4.8)	23.36 (3.4)	13.83 (1.33)	21.07 (1.93)	6.8 (4.9)	11/25
	Reduced FA in the fornix in AN, but disappeared completely after correcting for free water.								
Canna et al., 2017	AN DSM 5	16	16	25.3 (1.6)	26.1 (3.5)	16,8 (1,6)	21.1 (1.6)	AN: 7.9 (6.9)	none
	No significant differences in the mean FA of the corpus callosum.								
Cha et al., 2016	AN DSM 5	22	18	19.5 (2.42)	20.5 (2.95)	17.3 (1.24)	21.2 (1.63)	n/a	none
	An increase in FA was observed in the dorsolateral PFC, superior frontal gyrus, and cerebellum; a decrease in FA was observed in the cerebellum. Mean FA of the whole brain white matter did not significantly differ between the groups.								
Vogel et al., 2016	AN DSM IV	22	21	15.03 (1.60)	15.17 (1.28)	15.36 (1.08)	20.34 (2.59)	1 (1)	2/22
	Increased FA in bilateral frontal, parietal and temporal areas (including the bilateral superior region of corona radiata, corpus callosum anterior, anterior and posterior thalamic radiation, anterior and posterior limb of the internal capsule as well as the left inferior longitudinal fasciculus) in AN patients at admission compared to controls. Exploratory longitudinal analysis showed this FA increase to be partially normalized after weight rehabilitation.								
Pfuhl et al., 2016	AN DSM IV	35	35	16.1 (2.8)	16.4 (2.6)	14.70 (1.31)	20.75 (2.98)	n/a	none
	No differences AN-HC.								
Frank et al., 2016	AN DSM IV	26	26	23.23 (5.26)	24.39 (3.49)	16.23 (1.09)	21.61 (1.21)	6.62 (5.65)	16/26
	AN subjects had greater structural connectivity in pathways between insula, orbitofrontal cortex and ventral striatum, but lower connectivity from orbitofrontal cortexand amygdala to the hypothalamus								
Travis et al., 2015	AN DSM IV	15	15	16.6 ± 1.4	17.1 ± 1.3	16.0 (1.2)	21.4 (2.1)	1.36 (0.95)	2/15
	Reduced FA in AN in right anterior superior longitudinal fasciculus, bilateral fimbria fornix, motor subdivision of corpus callosum. Increased FA in AN in right anterior thalamic radiation, left anterior superior longitudinal fasciculus.								
Nagahara et al., 2014	AN DSM IV	17	18	23.8 (6.68)	26.2 (5.6)	13.6 (1.3)	19.9 (2.0)	4.93 (4.9)	6/17
	AN patients showed a significantly lower FA value in the left cerebellum. Significant positive correlations between the mean FA value of the left cerebellar hemisphere cluster and BMI, as well as between the mean MD value of the cluster in the anterior body of the fornix and the duration of illness								
Via et al., 2014	AN DSM IV	19	19	28.37 (9.55)	28.63 (8.58)	17.03 (1.09)	21.09 (1.80)	6.53 (6.03)	5/19
	AN patients showed significant FA decreases in the parietal part of the left superior longitudinal fasciculus (included the temporoparietal junction and surrounded the posterior insular cortex and the temporal and parietal opercula).								
Frieling et al., 2012	AN DSM IV	12	20	26.84 (6.94)	24.80 (2.60)	15.18 (1.39)	19.60 (0.94)		
	AN showed bilateral reductions of FA maps in the posterior thalamic radiation which includes the optic radiation, and the left mediodorsal thalamus.								

Kazlouski et al., 2011	AN DSM IV	16	17	23.9 (7)	25.1 (4)	16.5 (1)	21.5 (1)	7.5 (8)	8/16
	AN showed clusters of significantly reduced FA in the bilateral fimbria- fornix, fronto-occipital fasciculus, and in posterior cingulum WM. In the AN group, Harm Avoidance was predicted by left and right fimbria-fornix FA.								
von Schwanenflug et al., 2018	AN DSM IV	56	56	15.9 (2.9)	16.2 (2.9)	14.66 (1.34)	20.62 (2.44)	1.21 (0.91)	n/a
	FA was significantly reduced in the callosal body in AN.								

NEW PARADIGMS AND FUTURE DIRECTIONS IN STRUCTURAL NEUROIMAGING: FROM STRUCTURE TO NETWORKS

The hypothesis that psychiatric disorders arise from a disrupted organization of interconnected neural systems is not new, and has been supported by several studies that investigated the functional connectivity patterns between distinct brain areas. The idea that the complex cognitive, emotional and behavioral alterations that characterize psychiatric disorders derive from a complex alteration of neural connectivity arose a huge interest in recent years and highlighted the potentialities of applying network neurosciences tools to psychiatric research (Fornito, Zalesky, & Breakspear, 2015). Within neuroimaging research, the study of brain networks proceeded on two distinct methodological lines: the first focuses on small networks of different brain regions by means of correlation analysis or independent component analysis (Damoiseaux et al., 2006; Fox et al., 2005), while the second focuses on the studies of large networks by means of complex system science tools (Bullmore & Sporns, 2009; Rubinov & Sporns, 2010; Sporns, 2006). Since the brain is a complex system per definition, the use of complex system science to evaluate its architecture seems to be particularly appropriate and is having an ever-increasing application (Danielle S Bassett & Sporns, 2017; Fröhlich, 2016). A specific characteristic of complex systems is that they display organized structural and functional patterns that results from a selective coupling between different elements. These patterns are achieved by means of an intricate system of different types of connectivity that are displayed on different scales, from micro- to macro-scales.

A mathematical description of complex systems of interconnected elements is provided by Graph Theory (Boccaletti, Latora, Moreno, Chavez, & Hwang, 2006). A graph consists of a connection matrix which describes pairwise relationships between discrete entities that are called nodes. Connections between nodes are called edges. Edges can be either directed, if the direction of the interaction between two nodes is specified, or undirected, if the interaction between the nodes has no direction. A graph can be represented both graphically, by nodes (eg, circles) and edges (eg, arrows or lines), or

mathematically by an adjacency matrix (which can be also called connection matrix). In this n-b-n adjacency matrix (where n is the number of nodes) each node is defined by a row and a corresponding column. In undirected networks, the adjacency matrix is symmetrical (Rubinov & Sporns, 2010).
From a graph, a lot of parameters can be obtained by applying a set of different mathematical formulae. One of the most relevant parameters of a graph is the degree. The degree of a node is the number of connections that connect it to other nodes. The degree distribution of a real network is estimated from the degree of all nodes of the network, and indicates the range on which the degree of the nodes that constitute the network varies. Nodes can be connected by single edges (neighbor nodes) or by sequences of intermediate nodes and links. Ordered sequences of unique edges and intermediate nodes are called paths, while sequences of non-unique edges are called walks. The correlation between the degrees of connected nodes is defined as assortativity. Positive assortativity values indicate that high-degree nodes are likely to connect to each other, while negative values of assortativity indicate that nodes with high degree tend to connect with nodes with low degree (Noldus & Mieghem, 2014).
The measures that characterize a network can be distinguished and classified in:

1. *Local segregation properties* that quantify the tendency of a network to form regions of nodes that are strongly interconnected with each other and poorly connected to the other nodes of the graph.
2. *Global integration properties* that quantify how much a network is capable of a globally distributed and efficient communication.
3. *Influence and Centrality measures* that analyze the role that some nodes assume within the network, according to their relevance in managing connectivity and information transmission.

Integration measures:

1. **Path length** is the minimum number of edges that must be traversed to go from one node to another. A measure of the typical separation between two nodes in the graph is given by the

average shortest path length, also known as characteristic path length. Characteristic path length is defined as the mean of geodesic lengths over all couples of nodes (Boccaletti et al., 2006).

2. **Global efficiency** is a measure of efficient information transfer and is inversely related to path length. A fully connected network has maximal global efficiency, while in a fully disconnected network the global efficiency has a minimal value (Latora & Marchiori, 2001).

Segregation measures:

1. The **clustering coefficient** of a node indicates the density of connections between the neighbors of the node. The clustering coefficient of a network is computed as the average of clustering coefficients across nodes (Onnela, Saramäki, Kertész, & Kaski, 2005).

2. **Local efficiency** has a role similar to the clustering coefficient, representing a nodal measure of the average efficiency within a local subgraph (Latora & Marchiori, 2001).

3. The **modularity** measures the correlation between the probability of having an edge that connect two nodes and the probability that those nodes are parts of the same community. The most important algorithm for the computation of modularity is the Girvan Newman (GN) one, which works by recursively removing the edges with the highest betweenness until a good separation in single communities is found (Newman & Girvan, 2004). Modules are defined as local communities of highly interconnected nodes which are poorly connected with other regions.

Centrality and influence measures:

In a network, some nodes are more densely connected, able to promote integrative processes and influential than others. Such nodes are defined as “hubs” (Martijn P. van den Heuvel & Sporns, 2013).

Hubs can be identified by several parameters. The simplest index used to identify a hub is the degree. Nodes with a high degree manage more connections and are likely to influence many other network nodes. Nodes with a high degree can handle connections with different modules or within a single module. Hubs that have many inter-modules interactions are called connector hubs and have a high participation coefficient, while hubs that have many intra-modules connections are called provincial hubs and have a low participation coefficient. Other measures of centrality are based on the idea that a node is as influential as it can exert a control over the flow of information (Sporns, 2010). From these, the betweenness centrality estimates the relevance of a node as the fraction of all shortest paths in the network that pass through that node. Nodes with high betweenness centrality are crossed by many short paths and exert a high influence over the information stream. Brain Hubs were demonstrated to form a so-called "rich club", that is characterized by the tendency of high degree-nodes to be more densely connected among themselves than with nodes with a lower degree. Rich club regions, computed by DTI techniques, include the superior parietal cortex, the precuneus, the superior frontal cortex, the putamen, the hippocampus and thalamus in both right and left hemispheres (M. P. van den Heuvel & Sporns, 2011).

Small world properties:

Small-world properties combine high clusterization levels and short path length characteristics. In a network with small-world properties all nodes are linked through relatively few intermediate steps, even though most nodes maintain only few direct connections and mainly with their neighbors. A small-world network is placed in an intermediate position between regular and irregular networks and is mathematically characterized by an equal combination of their characteristics. Small-world brain networks exhibit the ability to use a relatively small number of long-distance connections to synchronize the overall information flow and the advantage to use local connections to locally processing the information (Danielle Smith Bassett & Bullmore, 2006a; Watts & Strogatz, 1998).

Structural network extraction:

Structural brain networks can be mapped by means of different parameters. Studies that investigate the architecture of the brain cortex compute structural connection patterns from cross-correlations in cortical thickness or gyrification data, while studies that investigate white matter architecture uses diffusion imaging and tractography data. The computation of a structural network entails different steps. The first requires the parcellation of the brain in different areas. Different anatomical parcellation schemes are specifically available for this purpose. Step 2 requires the choice of the metrics on which connectivity can be estimated (cortical thickness, gyrification, DTI). Step 3 requires the computation of an association matrix with the correlation values between different brain areas. Step 4 requires the choice of a threshold to generate an adjacency matrix from the association matrix: different thresholds will generate graphs of different sparsity or connection density, and so network properties can be explored over a range of different thresholds. At step 5 network parameters can be computed by comparing the observed network with the "null" distribution of equivalent parameters estimated in random networks (with the same number of nodes and connections) (Patric Hagmann et al., 2007; Rubinov & Sporns, 2010).

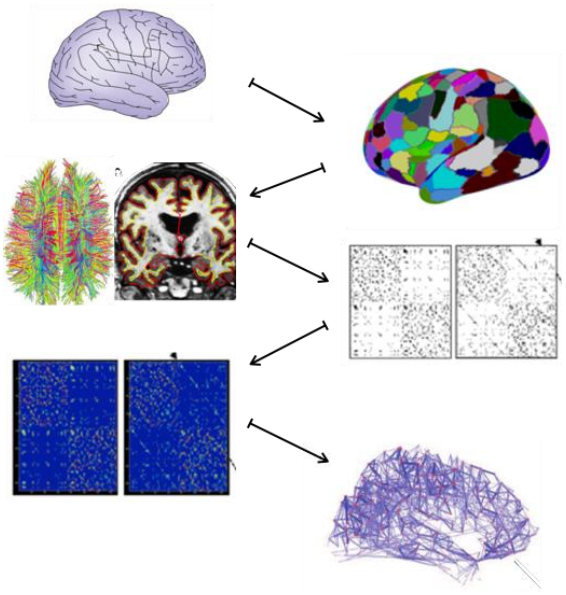

Figure 1. Main steps involved in the computation of structural networks

Cortical structural co-variance patterns

The opportunity to use graph theory tools to investigate the cortical structural patterns derives from the observation that inter-individual differences in the structure of a brain region often covary with inter-individual differences in other brain regions (P Lerch et al., 2006). This phenomenon, known as structural co-variance, is likely to reflect different cellular and molecular mechanisms that arise from connectivity processes (Gong, He, Chen, & Evans, 2012). Several observations highlighted that the synapses between neurons have a NMNDA-dependent trophic effect on neuronal development, and that synchronous firing induces neuroplasticity and synaptogenesis (Burgoyne, Graham, & Cambray-Deakin, 1993). At the microanatomic level, these mechanisms are evidenced to determine coordinated grow processes and to shape the structural inter-relations between different neural communities (Katz & Shatz, 1996).

More in details, coordinated neurodevelopment could arise both from activity-independent and activity-dependent processes: 1) *activity-independent processes* rely mainly on genetic factors. For example, correlated genetic influences have been showed to contribute to the formation of structural correlations between areas of the frontal-parietal network (Rimol et al., 2010; Schmitt et al., 2008; Thompson et al., 2001), and the 5-HTTLPR polymorphism of the gene for the serotonin transporter was observed to contribute in the determination of structural co-variance patterns between the amygdala and the anterior cingulate cortex (Pezawas et al., 2005). 2) *Activity-dependent mechanisms* rely mainly on cognitive and behavioral processes. Obviously, the relations between structural co-variance patterns and cognition/behaviors are partially genetically determined, but the brain morphology, as well as the inter-relations between different areas, have been demonstrated to be specifically modified by learning and training mechanisms (Hyde et al., 2009; Lv et al., 2008; Maguire et al., 2000).

From a psychiatric perspective, the investigation of how the patterns of structural inter-regional correlation emerge during childhood, adolescence and the first adulthood is particularly interesting.

During these periods, neuroplasticity mechanisms are fundamental for driving the fine-tune of the brain maturation accordingly to experiences-driven stimuli (experience-expectant plasticity), and any alterations in their progression could be involved in determining the emergence of several psychiatric conditions (Hensch, 2004a).

Over the most intense phases of neurodevelopment, axonal connections continuously undergo forming and reforming processes, sharing mutually trophic effects and leading to synchronized maturational changes. From a structural perspective, the periods of greater maturational changes are characterized by a combination of synaptic pruning and myelination. Interestingly, the processes that determine a reduction in cortical thickness during adolescence - i.e. synaptic pruning - seem to be particularly important in shaping the structural co-variance between different brain regions (Zielinski, Gennatas, Zhou, & Seeley, 2010). Moreover, maturational transformations are largely determined by functional needs and are characterized by different timing and speed-rates during development.

A longitudinal study that investigate the development of structural covariance networks showed an increase of integration properties during late childhood (from 8,5 to 11,3 years) and an opposed maturational pattern from 11 to 15 years (increase of segregation properties) (Khundrakpam et al., 2013). During the adulthood, the curve tends to stabilize. This study also highlighted that connectivity patterns showed a shift in regional maturation patterns. In fact, early connectivity was showed to establish mainly in primary sensorimotor areas, while later developmental phases were characterized by greater connectivity processes in paralimbic and association regions. A change in structural co-variance patterns during development is confirmed by a recent research conducted by Khundrakpam et al. (2013), who observed a peak in the number of hubs during late childhood and a shift in their distribution toward frontal regions during adolescence. In another longitudinal observation, Alexander-Bloch and colleagues (Alexander-Bloch, Raznahan, Bullmore, & Giedd, 2013) considered a large sample of young people (aged 9-22 years at enrollment) who underwent a different MRI scans over a follow-up

period of 6-12 years. Their findings support the hypothesis that correlated anatomical structure between brain regions results from similarities in developmental trajectories.

Structural co-variance studies conducted on psychiatric populations showed mixed results. Patients with Schizophrenia showed increased segregation properties (increased clustering) and lower integration characteristics (longer path length) in cortical thickness covariance network (Collin et al., 2013; Y. Zhang et al., 2012). The distribution of the most central nodes also appears to be altered in patients with schizophrenia, with a decrease in frontal hubs and an increase in primary sensory and/or paralimbic nodes (Alexander-Bloch, Giedd, & Bullmore, 2013a; Rubinov & Bullmore, 2013). Studies evaluating co-variance gyrification patterns in schizophrenia evidenced alterations in regional topological properties, with increased segregation of insula and dorsolateral prefrontal cortex and reduced integration of structures around the central sulcus and lateral occipital cortex (Palaniyappan, Park, Balain, Dangi, & Liddle, 2015). Moreover, patients with first episode psychosis who showed a poor treatment response had higher segregation and reduced integration properties in the global gyrification covariance network when compared to healthy controls and to patients who showed good response to therapy (Palaniyappan et al., 2016a). Covariance network computed with cortical thickness indices in patients with MDD showed higher clusterization and lower small-world properties. Furthermore, patients with major depression showed altered nodal centrality in different components of the Default Mode, Salience and Central Executive Networks. Depression severity scores were shown to correlate with alterations in nodes within the default mode and executive networks (Wang et al., 2016). In Obsessive-Compulsive Disorder, a network approach with cortical thickness measures evidenced the presence of alterations in node efficiency that was mainly located in sensory-motor regions. No differences were detected at a global level in a comparison between patients with OCD and healthy controls (Kim, Jung, Kim, Jang, & Kwon, 2013).

White matter co-variance patterns

Recent advances in diffusion MRI and tractography methods allow to map structural connectivity by tracing white-matter fibers with deterministic or probabilistic approaches (Descoteaux, Deriche, Knösche, & Anwander, 2009). Studies that compared anatomical tract tracing and DTI in non-human species found a considerable agreement between the two approaches and demonstrated that DTI is a valid and reliable method to non-invasively investigate the structure and the orientation of white matter tracts (Danielle S Bassett & Sporns, 2017; Dauguet et al., 2007). The application of DTI techniques to the study of developmental changes showed a progressive decrease in diffusivity and an increase in anisotropy with age. These changes are likely to reflect an increase in myelination rates and continue until early adulthood (Morgan et al., 2018).

Studies evaluating structural connectivity by means of DTI during development in healthy subjects evidenced non-uniform maturational changes. Wierenga and colleagues (2016), found a gradual strengthening in frontal and parietal intra-lobes connectivity and lower changes in subcortical, temporal and occipital regions in the age range of 7 to 23. Furthermore, they reported a decrease in overall path length and an increase in nodes strength with age. The observation of a progressive increase in integration characteristic of the network (increment in global efficiency, nodal strength, number of modules), alongside a reduction in segregation properties (decrease in local clustering and modularity) during development is replicated by several papers (Cao, Huang, Peng, Dong, & He, 2016). The increase of integration and robustness characteristics during maturational trajectories probably reflects the refinement of connectivity patterns that sustain the dynamic modeling of brain circuits.

Notably, during development, it was shown that the increase in fractional anisotropy correlated with changes in network properties. This observation allows to hypothesize that the maturation of the network is probably sustained by processes that lead to a change in WM structure such as synaptogenesis, myelination and synaptic pruning (Cao et al., 2016; Tau & Peterson, 2010).

Graph theoretical analysis on DTI measures in patients with schizophrenia revealed a preserved small-world organization but an impaired connectivity in a distributed network of nodes that include medial frontal, parietal/occipital and the left temporal lobe. Schizophrenic patients also showed a less efficient connectivity architecture at a global level. An analysis of hubs distribution in schizophrenia revealed a reduction in rich club density, that was associated with lower levels of global communication properties and with a reduced hubs centrality (Martijn P. Van Den Heuvel et al., 2013). In Major Depressive Disorder, a connectome analysis on DTI data evidenced the presence of lowered structural connectivity in areas of the default mode network and in regions associated to emotional and cognitive processing. The global network characteristics were demonstrated to be conserved in patients with MDD (Korgaonkar, Fornito, Williams, & Grieve, 2014). An abnormal white matter connectivity, by means of graph theory, was also evidenced in patients with ADHD in several brain networks encompassing cortico-cortical, subcortical, cerebellar and frontostriatal circuits. Moreover, different connectivity patterns were evidenced to characterize different clinical ADHD subtypes (Hong et al., 2014).

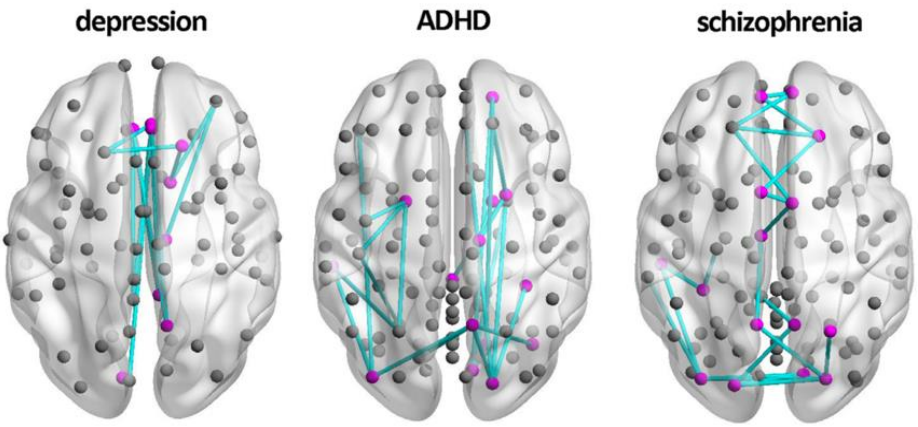

Figure 2. Connectome maps measured with DTI in patients with major depression, ADHD and schizophrenia. The depression data were first described by Korgaonkar et al. (2014), the the ADHD findings by Hong et al. (2014), and the changes in schizophrenia by Zalesky et al. (2011).

Economy of the brain organization – a developmental perspective in the evaluation of psychiatric disorders

The idea that the topological organization of the brain requires a trade-off between complexity and containment of the wiring cost is not recent. Between the end of the nineteenth and the beginning of the twentieth century, Ramon Y Cajal clearly proposed that the evolution of neuronal morphology and connectivity is closely linked to the need to preserve basic resources such as space and biological material: "all the various conformations of the neuron and its various components are simply morphological adaptations governed by laws of conservation for time, space and material" (Sporns, 2010).

The recent ever-increasing application of complex networks science to the study of the brain has resumed and expanded this concept, allowing to highlight that the organization of the brain arises from the negotiation between more parsimonious segregation properties and more expensive integration characteristics. The Small-World organization of the brain sustains this integration/segregation trade-off and allows the co-existence of both intra and extra-modular connections (Danielle Smith Bassett & Bullmore, 2006b).

Different developmental and anatomical mechanisms are involved in determining the wiring of neural networks according to energy saving and space optimization needs. For example, as previously described, the macroscopic network organization in modules and clusters successfully sustains this functional and structural demand. Another developmental mechanism that is supposed to fundamentally contribute in optimizing the length and the wiring cost of neural connections is cortical folding. It has been hypothesized that the convolution of the cortex derives from tension-based processes due to the physical force exerted by axonal connectivity (Van Essen, n.d.). The development of cortical gyrification would therefore results in an optimization of the axonal conduction cost, as well as in an increase of brain complexity.

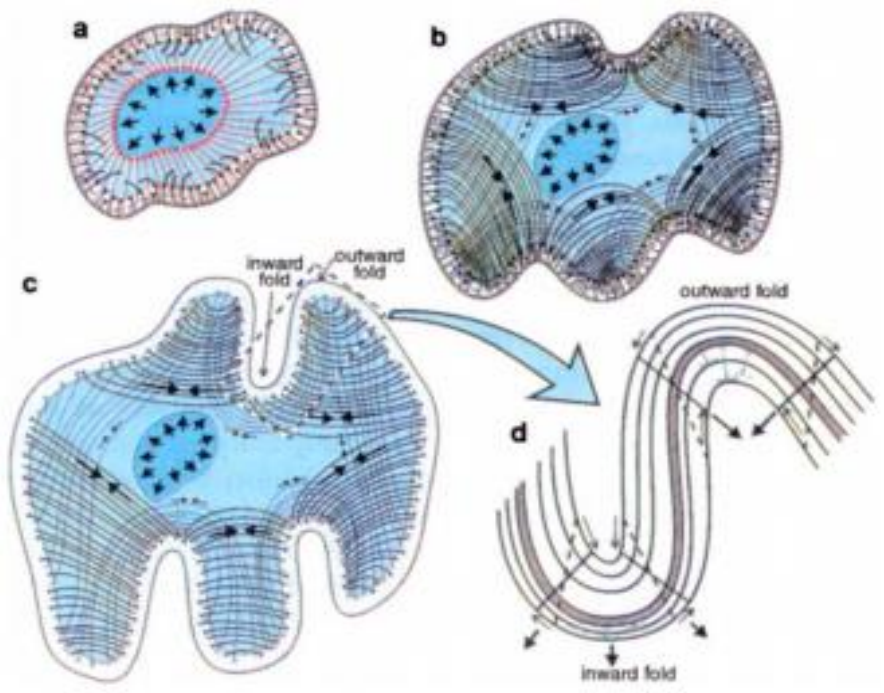

Figure 3. a) the cortical sheet is physically tethered from only one side, initially by radial glial processes. b) specific cortico-cortical projectons are established. b) and c) tension along obliquely oriented axonal trajectories between nearby cortical areas would generate tangential force components that tend to induce folds at specific locations in relation to areal boundaries. Outward folds tend to occur between neighboring areas that are only weakly interconnected d) along inward folds, cells in deep layers shoud be stretched radially, making these layers thinner. In outward folds cells in deep layers shoud be stretched radially, making these layers thicker.
Figure taken from Van Essen, 1997.

The identification and the evaluation of possible alterations in the architecture of the brain both at regional and global levels requires the application of different tools that can explore different aspects of the network organization.

While graph theory indices provide a good description of the rules that govern the anatomical correlations between different areas at a macroscopic level (Bullmore & Sporns, 2009), the characterization of the hierarchical and multilevel organization of the brain, of its convolutive patterns and of its macroscopic and microscopic complexity can be provided by other specific measures (i.e. gyrification, fractal dimension) (Benoit B. Mandelbrot, 1983).

The study of the maturation of connectivity patterns is very important in a psychiatric perspective, since most of the etiopathogenetic factors that determine psychiatric disorders are likely to intervene during the first two decades of life (Paus, Keshavan, & Giedd, 2008). A description of the organization of the connectome using graph theory tools allowed to conceptualize a theoretical model for psychiatric illnesses, called "developmental miswiring" – i.e., the abnormal development of neural interactions in the connectome (DiMartino et al., 2014). The evaluation of anomalies in developmental trajectories differentiate between processes that alter the timing of networks maturation from processes that alter the nature of specific developmental mechanisms. The ability to exactly individuate the nature of developmental alterations requires to know the rules that govern the normal wiring of the connectome at the different stages of brain maturation. For this purpose, an increasing number of efforts are directed to characterize the organizing principles of the normal connectome by means of longitudinal MRI studies in pediatric populations (Collin & Van Den Heuvel, 2013; P Hagmann et al., 2010; Menon, 2013).

The key brain maturational mechanisms that, if altered, may lead to a developmental miswiring and to the emergence of neurologic and psychiatric symptoms have been recently investigated. A recent review provides a comprehensive description of the five fundamental processes that characterize normal neuro-developmental trajectories (DiMartino et al., 2014):

1- *Shift from short to long-range connectivity*: a continuous shift from short-length to long-length connectivity patterns occurs from infancy to early adulthood. Although this change is gradual during maturation, it appears to be prominent in the first two years of life (Gao, Alcauter, Elton, et al., 2015; Gao, Alcauter, Smith, Gilmore, & Lin, 2015; Yap et al., 2011).

2- *Community structure changes*: the application of graph theory tools to the study of brain development has allowed to observe a dynamic change in the composition of segregation and integration properties. In infancy, a prevalence in connections between anatomically proximal

regions is observed, while more distributed properties emerge with age (Fair et al., 2007; Fransson, Åden, Blennow, & Lagercrantz, 2011; Thomason et al., 2014).

3- *Maximizing the cost-efficiency of information transfer*: graph theory allows to assess the efficiency of the flow of information between neurons both at global and regional levels. While global efficiency seems to remain quite stable across developmental phases, local efficiency is showed to increase across childhood (Cao et al., 2014; Dennis et al., 2013). A fundamental role in the determination of local efficiency is played by brain hubs, that constitute the structural and functional backbone of brain connectivity. During development, a shift in hubs location is observed: during infancy hubs are preferentially located in primary sensory and in motor areas, whereas in first adulthood they are preferentially located in posterior cingulate, insula and in other heteromodal/associative regions (Fransson et al., 2011). Interestingly, hub-regions appears to be particularly vulnerable in neurological as in psychiatric conditions. One meta-analysis conducted by Crossley and colleagues (2014) on more than 20,000 patients, evidenced that gray matter lesions were more likely to occur in hub regions than in non-hub ones over 26 different neurological and psychiatric disorders. Hub regions are particularly expensive elements within the connectome, since they manage a lot of information. Because of their centrality, integrativity and energetic cost, brain hubs are particularly vulnerable to pathogenic processes that affect the brain. Furthermore, when affected by disease-related processes, they are likely to spread damages in other brain regions. The exact role of hub-regions in the pathogenesis of psychiatric disorders is still to clarify, but preliminary observations in schizophrenia highlighted a compensatory over-activation of high degree nodes during the first phases of the disorder, followed by a later functional deterioration (Crossley et al., 2016; Fornito et al., 2015).

4- *From subcortico-cortical to cortico-cortical connectivity*: in childhood, subcortical-cortical connections tend to be stronger, while in adulthood, a shift in cortico-cortical connectivity is observed (Greene et al., 2014; Supekar, Musen, & Menon, 2009).

5- *Interhemispheric connectivity*: the development of both inter-hemispheric and intra-hemispheric connectivity is crucial during brain maturation. Structural and functional MRI studies focused mainly on corpus callosum changes and in hemispheric specialization during development. During brain maturation, a progressive increase in hemispheric specialization is observed. This process is necessary to support, both structurally and functionally, a specific subset of functions and determines a gradual inter-hemispheric asymmetry (Tzourio-Mazoyer, 2016).

Among psychiatric disorders, Anorexia Nervosa offers a unique and fascinating model, because it is likely to have a neurodevelopmental origin, but also is associated to severe metabolic alterations that might interfere with the neurodevelopmental trajectory given that the onset is often during adolescence or first adulthood. These metabolic repercussions can critically alter the balance between the energy optimization needs and the global integration properties of the brain network. Thus, the application of multimodal imaging and computational techniques to the study of AN could be particularly useful to explore not only the complex nature of its neurobiological underpinnings, but also the consequences of starvation and malnutrition on brain maturation.

Brain structural complexity

The complexity of central nervous system arises from its organization in interconnected elements that can be studied on different scales, from the microscopic (molecules and cells) to the macroscopic (brain areas and their relationship to behavior and diseases) (Fröhlich, 2016) . As previously described, the application of graph theory to neuroimaging data allows to investigate the neural architecture on a macroscopic level, and is not able to offer a detailed anatomical description of the brain structure. The possibility to describe the brain anatomical complexity by means of neuroimaging tools is a fascinating and tricky challenge, given the complex rules that shape its structure. The Euclidean geometry demonstrated great limits in describing very complex structures, and for this reason, in recent

years, alternative geometrical models have been considered. Among these, fractals geometry was specifically proposed for its ability to capture complex and convoluted structures that are characterized by a multilevel and hierarchical organization (Mandelbrot, 1983).

From a mathematical point of view, fractal objects result from the iterative repetition of equal parts over infinity length scales and are characterized by "self-similarity". This mathematical approach allows to describe and quantify the complexity of several natural objects with an irregular morphology, and is particularly useful to quantify the complexity of the brain cortex. Fractal geometry estimates the complexity of a structure by means of a specific index, called fractal dimension (D) (Jelinek & Fernandez, 1998; Dušan Ristanović & Milošević, 2012). D quantifies the geometrical complexity of an object by describing its space-filling properties. The most frequently used method to compute D is the box-counting algorithm, that allows to measure the level of occupancy of an analyzed object regardless of its fractal or non-fractal nature. The box-counting method works by reiteratively covering fractal objects by means of meshes of differently dimensioned squares, and then counting the number of squares occupied by the studied figure (Di Ieva, 2016; Dusan Ristanović, Stefanović, & Puskas, 2013). From this computation, a logarithmic function is extracted, and the slope of the function is referred as fractal dimension (D). The convoluted pattern of the brain cortex is particularly suited to be studied by fractal geometry tools, which were successfully integrated in the surface-based computation of MRI images (R. D. King, Brown, Hwang, Jeon, & George, 2010). Intuitively, since gyrification is the main source of cortical complexity, FD could be considered an indirect measure of cortical folding. Different literature observations show that FD correlate not only with the gyrification index but also with cortical thickness (Madan & Kensinger, 2016). This is a very interesting finding, since FD may be able to integrate the information given by cortical thickness and gyrification, also providing further and non-redundant information. The use of this parameter appears to be particularly useful in the study of neurodegenerative processes, where the effect of the decrease in cortical thickness is observed to be complementary with the impact of the reduction in cortical convolution.

As previously stated for the application of connectomic tools to structural neuroimaging in AN, the application of FD to surface-based processed MRI images in this disorder could represents an interesting research perspective, since it is an uncommon condition in which a reduction of cortical thickness and gyrification does not occur in degenerative neurological conditions or in elderly populations.

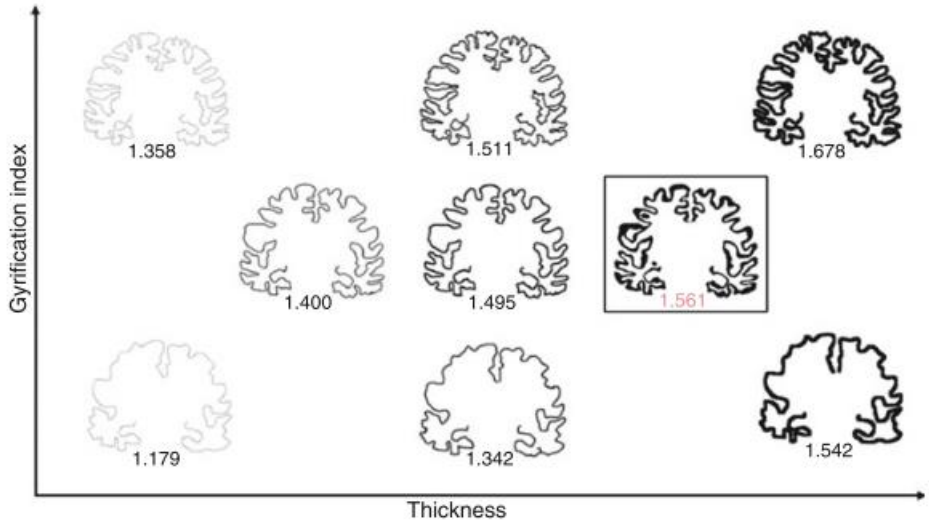

Figure 4. The effects of cortical thickness and gyrification index on measured fractal dimensionality. A coronal slice from a control subject and its fractal dimension is seen in the box. The remaining cortical ribbons are artificial data demonstrating fractal dimension changes with variation in cortical thickness, gyrification index, and the combination of the two. The fractal dimension of each slice is indicated by the number below the slice. Changes in cortical thickness are seen on the horizontal axis with increasing thickness towards the right. Changes in the gyrification index are seen on the vertical axis with values increasing upwards. Thinning of the cortical ribbon and lowering the gyrification index both decrease fractal dimensionality (From King et al., 2010)

Main research questions

Aims of the present work are to characterize cortical and white matter network architecture by means of different structural indices and computational techniques, to observe the presence of any correlation between clinical variables and networks characteristics and to investigate the structural organizational patterns in the different stage of AN course.

We hypothesize that cortical architecture and white matter connectivity patterns are altered in patients with AN. We also hypothesize the presence of specific alterations in covariance patterns of areas that are crucially involved in the neurobiology of the disorder and the presence of specific correlations between structural abnormalities in AN and specific clinical variables of the disorder.

Small-world properties of brain morphological characteristics in Anorexia Nervosa

INTRODUCTION

Anorexia Nervosa (AN) is a disabling psychiatric disorder that typically develops in female individuals during adolescence or early adulthood and is characterized by important psychopathological, cognitive, medical and neurobiological abnormalities (Zipfel et al., 2015).

From a neurobiological perspective, in recent years many efforts have been made to describe brain volumetric and morphological characteristics in AN, and to characterize them according to the course of the disease and to different clinical variables. Since AN often has its onset in adolescence (Favaro et al., 2009), a neurodevelopmental approach is of particular relevance in order to understand both the role of early etiopathogenetic factors (Favaro et al., 2006) and the consequences of malnutrition on maturational trajectories.

The possibility to describe changes of morphological and structural brain features over neurodevelopmental trajectories allows better interpretation of how their alterations can impact on different psychiatric conditions.

The study of cortical thickness and gyrification indices are very promising within this context, since their modifications through the stages of brain maturation and their ability to capture anatomical and structural cortical properties are increasingly characterized (J. A. King et al., 2018). During neurodevelopment, cortical thickness reflects processes that determine a progressive reorganization of grey matter structure, following the demands for greater plasticity in childhood and the subsequent need for higher synaptic stability in later phases. Gyrification, on the other hand, begins prior to birth to shape an efficient architecture that shows great structural stability over time, with the exception of a gradual decrease in the amount of cortical complexity during adolescence (White, Su, Schmidt, Kao, & Sapiro, 2010).

The different stability of these two structural parameters along neurodevelopmental trajectories is explained by their different sensitivity to environmental influences; cortical thickness is in fact more influenced by environmental exposures than gyrification, which maintains a more constant configuration during development (Armstrong, Schleicher, Omran, Curtis, & Zilles, 1995; Thambisetty et al., 2010).

Previous literature on brain morphology in patients with AN is inconsistent as regards findings, methodology approaches and recruitment criteria. A significant reduction of cortical thickness in underweight patients with AN was found by two studies, which did not detect a direct correlation between cortical thickness and body mass index (BMI) (Bär et al., 2015; J. A. King et al., 2015). Furthermore, in a longitudinal study, Bernardoni and colleagues (Bernardoni et al., 2016) observed a substantial normalization of thickness after an average of three months of weight restoration (Bernardoni et al., 2016). On the contrary, Lavagnino and colleagues (Lavagnino et al., 2016), while observing a correlation between cortical thickness and BMI in the AN group, did not find any differences between patients and controls (Lavagnino et al., 2016). Moreover, in a recent study, a comparison between patients with AN (both acute and recovered) and healthy women revealed higher cortical thickness values in orbitofrontal areas (Lavagnino et al., 2018).

Regarding cortical gyrification, Favaro et al. (Favaro et al., 2013) observed the presence of significant alterations in the parietal and frontal cortex of adult patients with AN; hypogyrification in these areas was not correlated with weight loss, body mass index, cortical thickness or dehydration (Favaro et al., 2013). Furthermore, these alterations were not present in patients with a good clinical outcome, regardless of their body weight and recovery status. On the contrary, in a mixed sample of adolescents and adults, Bernardoni et al. (Bernardoni et al., 2018a) found that an almost complete normalization of cortical folding after weight gain and weight restoration was the main predictor of increased gyrification during treatment (Bernardoni et al., 2018a).

In the context of clinical neurosciences, evaluation of the morphological and structural parameters of the cerebral cortex on the basis of their covariance patterns is becoming increasingly important since it can reveal an inter-regional structural dependence, which derives from a complex mixture of developmental, genetic and environmental factors (Alexander-Bloch, Giedd, & Bullmore, 2013b). The possibility of characterizing the topology of cortical structural and morphological networks provides an insight into the ways in which the architecture of cortical connectivity negotiates the trade-off between network wiring cost and topological complexity and allows a very promising perspective on the study of psychiatric illnesses (Bullmore & Sporns, 2012; Fornito, Bullmore, & Zalesky, 2017). One of the most promising potentials of complex network sciences is in fact related to its applicability for uncovering developmental mechanisms that lead to aberrant brain network organization and for tracking the progression of disease in degenerative disorders (Fornito & Bullmore, 2015). The topological complexity of brain networks lies mainly in the need to mediate the presence of locally and globally distributed connections and to support, during neurodevelopment, the shift from a modular and segregated organization to a more globally integrated one. This integrated configuration fulfills the maturation of high order association areas and of higher cognitive abilities. In this perspective, it is of great interest to explore the connectomic characteristics of Anorexia Nervosa: a disorder that is hypothesized to have an early neurodevelopmental origin (Favaro et al., 2013), but also represents a potential restraint for brain maturational trajectories due to starvation and consequent malnutrition. Our purpose in this paper is therefore to apply the tools provided by connectomics and graph theory to deepen our knowledge of the neurobiological complexity of AN, by trying to define any abnormalities in covariation patterns of gyrification and cortical thickness and then to assess the rules that govern the structural cortical topological interaction in the disorder. The secondary aim of the present study was to compare covariation patterns of the same brain characteristics between patients who have recovered at a 3-year follow-up and those who have not. We hypothesized that graph theory metrics in AN would support a

delay in neurodevelopmental trajectories in both cortical measurements, with higher network segregation parameters and lower integrative properties in patients with AN compared to HC.

METHODS AND MATERIALS

The sample included was the same as a previous study (Favaro et al., 2013). A total of 58 patients with AN (38 with acute AN and 20 fully recovered) and 38 HC participated. Definition of full recovery was: 1) having had AN (according to DSM-5 criteria) in their lifetime; 2) being asymptomatic for at least 6 months at the time of scanning (mean remission time: 38.5 months (standard deviation=33.2; range 6-96). Amenorrhea, food restriction, bingeing, excessive exercise, fasting and purging in the last 6-months were exclusion criteria for the recovered AN group and none of the subjects of this group relapsed in the year following scanning. Table 1 describes the main characteristics of the sample. Exclusion criteria for both patients with AN and HC were male gender, history of head trauma or injury with loss of consciousness, history of any serious neurological or medical illness, active use of systemic steroids, pregnancy, active suicidality or major depression, history of substance/alcohol abuse or dependence, bipolar disorder or schizophrenia spectrum disorder, moderate mental impairment (IQ<60) or learning disabilities, use of medications other than antidepressants, and known contraindications to conventional MRI. History of any psychiatric disorder and any first-degree relatives with an eating disorder were additional exclusion criteria for HC.

When recruiting subjects, some individuals were not included in the study: five AN patients, because of antipsychotic medication and/or severe comorbidity; one AN patient and one healthy subject, because of previous head trauma; and one AN patient, 3 recovered AN and 2 healthy subjects, who were not available to undergo MRI scanning when scheduled. The final sample comprised of 96 women (38 with AN, 20 recovered from AN, and 38 HC). No further subject was excluded due to problems with scan acquisition, gross brain alterations, or motion artifacts.

The experimental sample was composed of different diagnostic subtypes: 32 subjects (84%) were restrictive AN, 6 patients were binge eating/purging AN subtype and 7 patients presented restrictive AN subtype with a history of binge eating or purging behavior. 14 AN patients and 4 recovered women were under drug treatment with antidepressants at the time of scanning (acute AN: 1 patient mirtazapine, 2 paroxetine, 2 escitalopram, 1 fluoxetine, 8 sertraline; recovered AN: 4 sertraline). Ethical permission was obtained from the ethics committee of the Hospital of Padova. After completely describing the study to the subjects, informed written informed consent was obtained.

Table 2. Baseline characteristics of the three groups

	AN patients (n=38)	Recovered AN patients (n=20)	Healthy women (n=38)	AN vs. HW	Recovered AN vs. HW
	mean (SD)	mean (SD)	mean (SD)	z (p)	z (p)
Age	26.1 (7.2)	26.3 (7.1)	25.3 (6.3)	0.38 (0.701)	0.44 (0.659)
Age at onset	18.3 (5.1)	17.7 (3.2)	=	=	=
Duration of illness (months)	78.6 (81.3)	45.7 (65.0)	=	=	=
Duration of recovery (months)	=	45.4 (46.8)	=	=	=
Baseline BMI	15.8 (1.8)	19.6 (1.6)	21.7 (2.9)	7.42 (0.000)	3.09 (0.002)
Lowest BMI	14.0 (1.8)	15.7 (1.4)	19.8 (2.5)	7.17 (0.000)	5.35 (0.000)
Education	14.2 (2.2)	14.2 (2.7)	15.5 (2.3)	2.63 (0.009)	1.94 (0.053)
Edinburgh laterality index	57.2 (37.6)	60.6 (35.2)	55.1 (42.0)	0.52 (0.603)	0.32 (0.749)
Left cortical thickness	2.45 (0.14)	2.52 (0.10)	2.53 (0.09)	2.65 (0.008)	0.23 (0.819)
Right cortical thickness	2.44 (0.14)	2.51 (0.11)	2.52 (0.08)	2.86 (0.004)	0.34 (0.731)
Left gyrification	2.85 (0.09)	2.90 (0.09)	2.90 (0.11)	1.97 (0.048)	0.23 (0.819)
Right gyrification	2.85 (0.10)	2.90 (0.09)	2.90 (0.12)	1.83 (0.067)	0.07 (0.941)

According to the false discovery rate method, differences are significant at $p<0.027$

Clinical Assessment and Follow-up

All subjects were investigated for AN diagnosis with a diagnostic interview according to the Eating Disorders Section of the Structured Clinical Interview for DSM-5 (American Psychiatric Association, 2013) and, also, a semi-structured interview was used in order to collect socio-demographic and clinical variables (Favaro et al., 2012, 2013). More information about subjects' psychopathology was achieved using the Hopkins Symptoms Checklist (Derogatis, Lipman, Rickels, Uhlenhuth, & Covi, 1974) and the Eating Disorders Inventory (Garner, Olmstead, & Polivy, 1983) in order to gather depressive and obsessive-compulsive symptoms, as well as those regarding eating disorders. Furthermore, the Edinburgh Handedness Inventory (Oldfield, 1971) was used to assess handedness.

All subjects were recruited at the Hospital of Padova Eating Disorder Unit, fulfilled the diagnosis for AN according to DSM-IV criteria and were medically stable at the time of scanning. Most patients had restricting type anorexia nervosa at the time of scanning (see Supplementary Materials). Follow-up for acute AN patients was performed about 3 years later (average 3.4 years, range 1.7-3.9). A semi-structured interview, the Eating Disorders Section of the Structured Clinical Interview for DSM-IV, as well as information from informants, were used to achieve diagnostic information at follow up. Full recovery was defined as: normal range weight, regular menses, absence of binge/purge/avoidance or restrictive eating behavior, absence of excessive physical activity, body dissatisfaction or drive to thinness for at least 3 months before the evaluation. Table 2 shows the baseline characteristics of the two groups with a different outcome at follow up.

Table 3. Baseline data of the two outcome groups

	AN patients with recovery at follow-up (n=13)	AN patients without recovery (n=24)	
	mean (SD)	mean (SD)	z (p)
Age	25.5 (6.8)	26.7 (7.5)	0.33 (0.74)
Age at onset	20.8 (6.5)	17.1 (3.8)	2.26 (0.02)*
Duration of illness (months)	40.0 (46.2)	101.2 (89.8)	2.10 (0.04)
Baseline BMI	14.9 (1.75)	16.2 (1.6)	2.23 (0.03)
Lowest BMI	14.4 (2.0)	13.7 (1.7)	1.13 (0.26)
Duration follow-up (years)	3.2 (0.6)	3.5 (0.5)	1.48 (0.14)
Final BMI	19.6 (2.1)	17.7 (4.3)	3.66 (<0.001)*

According to the false discovery rate method, differences are significant at $p<0.027$

MRI Data Acquisition

Scans were collected using a Philips Achieva 1.5 Tesla scanner equipped for echo-planar imaging. High-resolution 3D T1-weighted anatomical images were acquired using a gradient-echo sequence (repetition-time=20 sec, echo time=3.78 msec, flip angle= 20°, 160 sagittal slices, acquisition voxel size=1×0.66×0.66 mm, field of view 21-22 cm).

Data Processing and Statistics

Data processing was performed using the FreeSurfer package (Martinos Center for Biomedical Imaging, Massachusetts General Hospital, Boston) version 5.3.0. The preprocessing was carried out according to the standard description using the following steps: skull-stripping and intensity correction, gray matter–white matter boundary determination for each cortical hemisphere using tissue intensity and

neighborhood constraints, and finally, tessellation of the resulting surface boundary to generate multiple vertices across the whole brain before inflating.

After cortical reconstruction, the cortex was divided into units based on individual gyral and sulcal structures (Destrieux, Fischl, Dale, & Halgren, 2010). The local Gyrification Index (lGI) was measured at thousands of points of the reconstructed cortical surface using previously validated algorithms (Schaer et al., 2008). In each vertex, lGI is computed within 25-mm circular regions of interest and represents the degree of cortical folding that quantifies the amount of cortex buried with in the sulcal folds in the surrounding circular region. An overall hemispheric lGI value was automatically computed. Vertex-wise measurements of cortical thickness (B. Fischl & Dale, 2000) were also estimated (Destrieux et al., 2010; B. Fischl & Dale, 2000). Surface reconstruction and segmentation were manually inspected and minor manual intervention was performed when necessary, according to FreeSurfer user guidelines. The local Gyrification Index (lGI) was developed to take account of the three-dimensional nature of the cortical surface and was introduced in order to replace the previous two-dimensional linear gyrification measures, more susceptible to different kinds of bias. The lGI is a measure of cortical folding and was calculate at thousands of points of the reconstructed cortical surface using already validated algorithms (Schaer et al., 2008).

Properties of the Connectome and group comparison

Covariance patterns within connectome are described using integration and segregation properties, which are quantified using various graph theory indices. Segregation indicates a modular development of related brain regions, while integration results from maturational processes affecting the entire brain. Integration was measured using Global Efficiency and Characteristic Path Length; segregation was measured using Clustering Coefficient, Modularity and Local Efficiency. We also quantified Small-World Index (SWI), a measure of the balance between integration and segregation. All topological properties

were computed using Graph Analysis Toolbox (GAT) (http://brainlens.org/tools. html) (Hosseini, Hoeft, & Kesler, 2012).

Between group comparison was performed 2 groups at time, both for cortical thickness and for gyrification indices (AN vs HC, AN-rec vs HC, poor-outcome vs good-outcome). Significant differences between topological parameters were investigated using a nonparametric permutation test with 1000 repetition. The numerosity of the original groups were maintained in each repetition by the randomly reassignment of the regional data (or residuals) of each participant to one of the two group analyzed, so as to obtain an association matrix for each random group. Then, a range threshold of 0.1 to 0.5 with increments of 0.05 were applied to each random group in order to estimate the binary adjacency matrices. Topological measurements were calculated for all networks and the full density range were used in order to compare differences in network measurements. For each iteration, the values of each random group across the range of density were plotted and the differences of the different areas under the obtained curves were used in order to compute topological proprieties. p values were obtain by comparing the results from the actual differences in the curve functions obtained and the null distribution of differences. This nonparametric permutation test compared the shapes of the curves derived from multiple threshold points (and so from multiple comparisons) and is based on functional data analysis (FDA) that allowed to overcome limitations driven by the sensitivity of the analysis methodology.

Constructing Cortical Thickness-based Networks

A 148×148 Pearson's correlation matrix of Cortical Thickness indices of each parcellated brain region was used to create a binary adjacency matrix for each group. Age, Edinburgh Handedness Inventory score and mean cortical thickness index were used as covariates.

A range of thresholds determined by connection densities (proportions of connections present in a graph to all possible connections) varying from 0.1 to 0.5 (increments of 0.05) was used to compare the properties of emerging networks.

Constructing Gyrification-Based Networks

A 148×148 Pearson's correlation matrix of gyrification indices of each parcellated brain region was used to create a binary adjacency matrix for each group. Age, intracranial volume, Edinburgh Handedness Inventory score and mean overall gyrification index were used as covariates.

A range of thresholds determined by connection densities (proportions of connections present in a graph to all possible connections) varying from 0.1 to 0.5 (increments of 0.05) was used to compare the properties of emerging networks.

Comparing network measures between patients with different outcome profiles at follow up, the minimum density at which fully connected graph was observed was 0.20. Between these groups, the range of thresholds used to compare the properties of the networks varied from 0.2 and 0.5 (increments of 0.05).

Statistics

Group comparisons were performed by means of nonparametric statistical tests, with false discovery rate methods to control for multiple comparisons.

RESULTS

Table 1 shows the main clinical characteristics of the 3 groups involved in the study, including average cortical thickness and gyrification index as found in Favaro et al (Favaro et al., 2013). Differences in vertex-wise analyses were reported in our previous paper (Favaro et al., 2013).

Cortical thickness based networks

Main findings regarding the properties of cortical thickness based networks are reported in Table 3. Hub distribution is described in Supplementary Materials.

Patients with AN vs. HC

Patients with acute AN showed increased segregation measures in terms of Mean Local Efficiency, Clustering and Modularity in comparison to HC (Table 3), while, on the contrary, they revealed significantly lower patterns of integration as measured by Global Efficiency.

Both AN patients and HC reported average values of small-wordless greater than 1, but the small-world index was significantly higher in patients with acute AN than in HC (Table 3). No regional differences were detected either in the segregation or in the integration indices. Figure n.5 graphically represents differences in clustering coefficient, mean local efficiency, small-world index and modularity between AN group and HC.

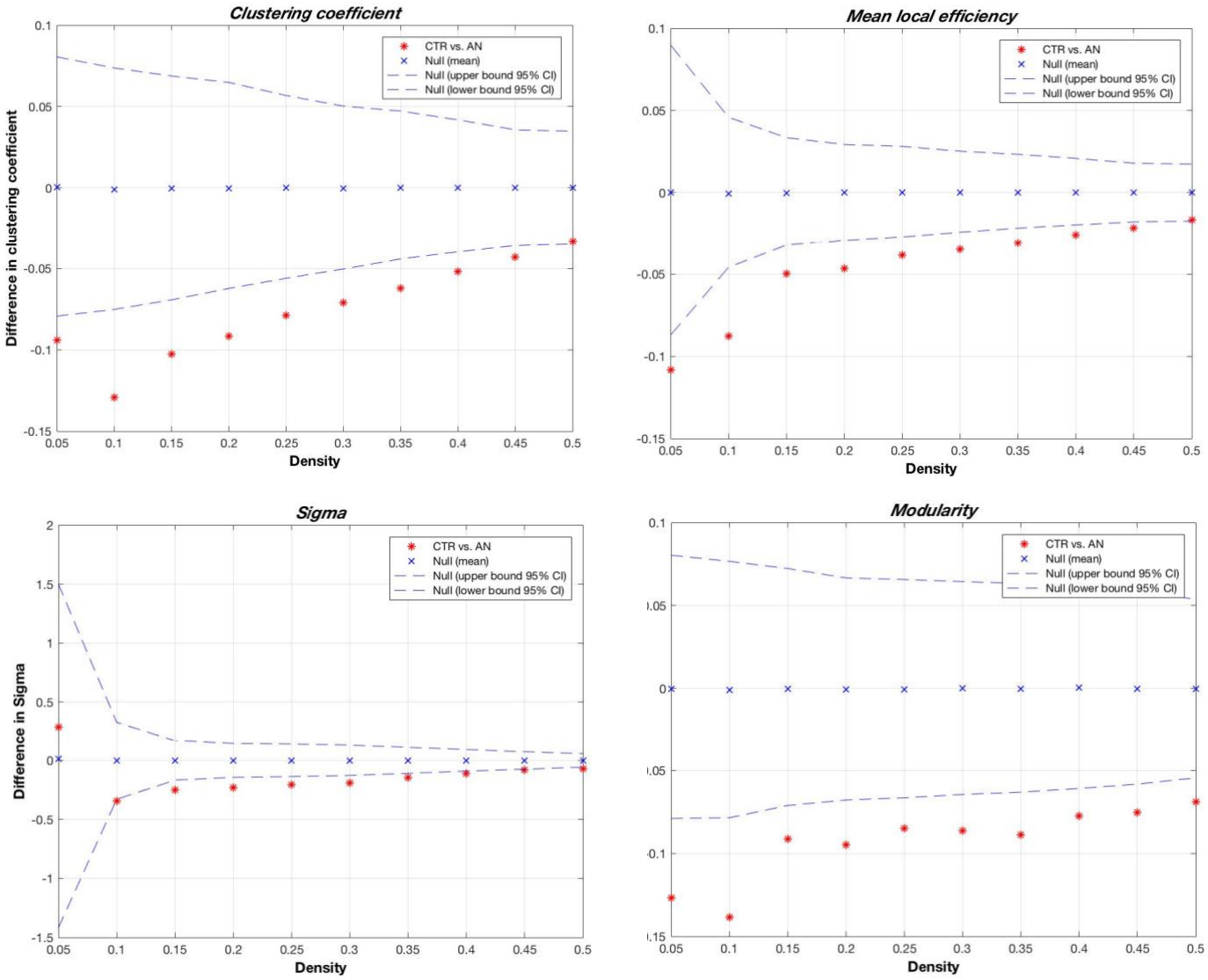

Figure 5. Differences in clustering coefficient, mean local efficiency, small-world index and modularity between AN patients and HC.

Patients recovered from AN vs. HC

No differences emerged in the comparison between the recovered AN and the healthy control group in any integration and segregation parameters in either overall or regional networks analysis. In recovered patients, mean small-world index was 1.63 (SD=0.53). With regard to segregation measures, mean clustering coefficient was 0.45 (SD=0.09), mean local efficiency is 0.71 (SD=0.07) and mean modularity was 0.28 (SD=0.09), whereas with regard to integration measures, mean global efficiency is 0.64 (SD=0.09), and mean characteristic path length was 1.77 (SD=0.26).

Table 4. Topological properties of Cortical Thickness-based connectome

		AN (n=38)	HC (n=38)	Poor outcome (n=24)	Good outcome (n=13)	FDA permutation test (p-values)
		Mean (SD)	Mean (SD)	Mean (SD)	Mean (SD)	
Small-world index		1.64 (0.46)	1.45 (0.38)	1.66 (0.47)	1.73 (0.55)	AN>HC (0.0001)
Measure of segregation						
	Clustering Coefficient	0.47 (0.08)	0.39 (0.11)	0.47 (0.08)	0.47 (0.78)	AN>HC (0.008)
	Mean local efficiency	0.72 (0.07)	0.68 (0.09)	0.63 (0.09)	0.63 (0.09)	AN>HC (0.005)
	Modularity	0.28 (0.09)	0.19 (0.07)	0.27 (0.08)	0.27 (0.09)	AN>HC (0.006)
Measures of integration						
	Global efficiency	0.63 (0.09)	0.64 (0.08)	0.63 (0.09)	0.63 (0.09)	AN<HC (0.02)
	Characteristic path lenght	1.78 (0.29)	1.74 (0.22)	1.78 (0.28)	1.79 (0.29)	AN>HC (0.03)

According to the false discovery rate method, differences are significant at p<0.027

Good outcome patients vs. poor outcome patients

Patients with a poor outcome and those with a good outcome at a 3-year follow-up assessment did not show differences in global network properties. A regional analysis of the between-group differences revealed a significantly higher clustering coefficient of the orbital part of the left inferior frontal gyrus in the poor outcome group (FDR-corrected permutation-based *p* values: <0,001) while patients with a

good outcome show a higher degree in the same area (FDR-corrected permutation-based *p* values: <0,001).

Gyrification based networks

Main findings regarding the properties of gyrification based networks are reported in Table 4. Hub distribution is described in Supplementary Materials.

Patients with AN vs. HC

No differences were detected in integration and segregation measures between patients with AN and HC. Both AN patients, HC and recovered AN patients showed small-worldness greater than 1. However, the small-world index was significantly higher in patients with acute AN than in HC (Table 4).

Patients recovered from AN vs. HC

No statistically significant differences were detected in the gyrification based network in the comparison between recovered AN patients and HC. In recovered patients, mean small-world index was 1.81 (SD=0.59). With regard to segregation measures, mean clustering coefficient was 0.54 (SD=0.05), mean local efficiency was 0.76 (SD=0.04) and mean modularity was 0.32 (SD=0.11), whereas with regard to integration measures, mean global efficiency was 0.62 (SD=0.10), and mean characteristic path length was 1.84 (SD=0.36).

Good outcome patients vs. poor outcome patients

Patients with a poor outcome showed significantly higher clustering and trends towards significantly higher mean local efficiency and characteristic path length when compared to patients with a good outcome (Table 4). At a regional level, the poor outcome group revealed a higher normalized degree index in the inferior part of the right circular sulcus of the insula (FDR-corrected permutation-based *p*

values: <0,001) and a higher normalized clustering of the left superior temporal sulcus (FDR-corrected permutation-based *p* values: <0,001).

Both groups showed small-worldness greater than 1, but the small-world index was significantly higher in the good outcome group.

Table 5. Topological properties of Gyrification-based connectome

		AN (n=38)	HW (n=38)	Poor outcome AN (n=24)	Good outcome AN (n=13)	FDA permutation test (p-values)
		Mean (SD)	Mean (SD)	Mean (SD)	Mean (SD)	
Small-world index		1.91 (0.75)	1.75 (0.66)	1.12 (0.01)	1.51 (0.31)	AN>HC (0.019); Good>poor-outcome (0.02)
Measures of segregation						
	Clustering Coeffficient	0.53 (0.05)	0.48 (0.06)	0.64 (0.05)	0.57 (0.05)	Poor>good-outcome (0.02)
	Mean local efficiency	0.75 (0.04)	0.73 (0.04)	0.81 (0.04)	0.78 (0.02)	Poor>good-outcome (0.03)
	Modularity	0.32 (0.12)	0.29 (0.11)	0.20 (0.05)	0.26 (0.08)	=
Measures of integration						
	Global efficiency	0.62 (0.10)	0.63 (0.09)	0.65 (0.08)	0.66 (0.07)	=
	Characteristic path lenght	1.84 (0.37)	1.80 (0.31)	1.77 (0.25)	1.68 (0.17)	Poor>good-outcome (0.04)

According to false discovery rate method, differences are significant at p<0.029

Hubs distribution in cortical thickness-and gyrification-based connectomes

Differences in Hubs distribution were detected in the comparisons between different groups both on cortical thickness and on gyrification based networks. Hubs distribution is reported in tables …

Table 6. Hubs distribution in cortical thickness-based connectome. Comparison between AN patients and HC.

NET HUBS DEGREE (AN)	**NET HUBS DEGREE (HC)**
L- Paracentral lobule and sulcus	L-Middle frontal sulcus
L- Middle frontal gyrus	L- Planum temporale or temporal plane of the superior temporal gyrus
L- Orbital sulci (H-shaped sulci)	L-Transverse temporal sulcus
R- Middle-anterior part of the cingulate gyrus and sulcus (aMCC)	R-Paracentral lobule and sulcus
R-Long insular gyrus and central sulcus of the insula	R-Short insular gyri
R- Postcentral gyrus	R- Postcentral gyrus
R-Superior frontal sulcus	R-Lateral aspect of the superior temporal gyrus
	R- Temporal pole
NET HUBS BETWENNESS (AN)	**NET HUBS BETWENNESS (AN)**
L- Paracentral lobule and sulcus	L- Middle-anterior part of the cingulate gyrus and sulcus (aMCC)
L- Anterior part of the cingulate gyrus and sulcus(ACC)	L- Middle frontal gyrus (F2)
L- Posterior-dorsal part of the cingulate gyrus(dPCC)	L- Postcentral gyrus
L- Middle temporal gyrus (T2)	L- Planum polare of the superior temporal gyrus
R- Long insular gyrus and central sulcus of the insula	L- Superior occipital sulcus and transverse occipital sulcus
R- Middle occipital sulcus and lunatus sulcus	L- Transverse temporal sulcus
R- Anterior occipital sulcus and preoccipital notch (temporo-occipital incisure)	R- Short insular gyri
R- Fronto-marginal gyrus (of Wernicke) and sulcus	R- Postcentral gyrus
	R- Lateral aspect of the superior temporal gyrus

Table 7. Hubs distribution in gyrification-based connectome. Comparison between AN patients and HC.

NET HUBS DEGREE (AN)	NET HUBS DEGREE (HC)
L- Subcentral gyrus (central operculum) and sulci	L-Opercular part of the inferior frontal gyrus
L- Long insular gyrus and central sulcus of the insula	R- Opercular part of the inferior frontal gyrus
L- Lateral occupito-temporal gyris (fusiform gyrus)	R-Triangular part of the inferior frontal gyrus
R- Subcentral gyrus (central operculum) and sulci	R-Vertical ramus of the anterior segment of the lateral sulcus (or fissure)
	R- Superior segment of the circular sulcus of the insula
	R- Suborbital sulcus
NET HUBS BETWENNESS (AN)	**NET HUBS BETWENNESS (HC)**
L- Lateral occipito-temporal gyrus (fusiform gyrus, O4-T4)	L- Anterior part of the cingulate gyrus and sulcus(ACC)
L- Supramarginal gyrus	L- Inferior temporal gyrus (T3)
R- Superior occipital gyrus (O1)	L- Anterior transverse collateral sulcus
R- Orbital gyri	L- Posterior transverse collateral sulcus
R- Supramarginal gyrus	R- Middle-anterior part of the cingulate gyrus and sulcus (aMCC)
R- Anterior transverse collateral sulcus	R- Supramarginal gyrus
R- Lateral orbital sulcus	R- Intraparietal sulcus (interparietal sulcus) and transverse parietal sulci
R- Medial orbital sulcus (olfactory sulcus)	R- Inferior part of the precentral sulcus
R- Superior temporal sulcus (parallel sulcus)	

Table 8. Hubs distribution in cortical thickness-based connectome. Comparison between AN-rec patients and HC.

NET HUBS DEGREE (AN-rec)	NET HUBS DEGREE (HC)
L- Middle-posterior part of the cingulate gyrus and sulcus (pMCC)	L- Long insular gyrus and central sulcus of the insula
L- Straight gyrus, Gyrus rectus	L- Planum polare of the superior temporal gyrus
L- Marginal branch (or part) of the cingulate sulcus	L- Posterior ramus (or segment) of the lateral sulcus (or fissure)
R- Posterior-ventral part of the cingulate gyrus (vPCC, isthmus of the cingulate gyrus)	L- Superior temporal sulcus (parallel sulcus)
R- Anterior transverse temporal gyrus (of Heschl)	L- Transverse temporal sulcus
R- Superior occipital sulcus and transverse occipital sulcus	R- Superior parietal lobule (lateral part of P1)
	R- Postcentral gyrus
	R- Anterior transverse temporal gyrus (of Heschl)
NET HUBS BETWENNESS (AN)	**NET HUBS BETWENNESS (HC)**
L- Anterior part of the cingulate gyrus and sulcus (ACC)	L- Long insular gyrus and central sulcus of the insula
L- Posterior-ventral part of the cingulate gyrus (vPCC, isthmus of the cingulate gyrus)	L- Postcentral gyrus
L- Calcarine sulcus	L- Planum polare of the superior temporal gyrus
L- Marginal branch (or part) of the cingulate sulcus	L- Posterior ramus (or segment) of the lateral sulcus (or fissure)
R- Cuneus	L- Superior temporal sulcus (parallel sulcus)
R- Posterior transverse collateral sulcus	L- Transverse temporal sulcus
R- Middle frontal sulcus	R- Superior parietal lobule (lateral part of P1)
R- Pericallosal sulcus (S of corpus callosum)	R- Anterior transverse temporal gyrus (of Heschl)

Table 9. Hubs distribution in gyrirification-based connectome. Comparison between AN-rec patients and HC.

NET HUBS DEGREE (AN-rec)	NET HUBS DEGREE (CTR)
L- Middle-anterior part of the cingulate gyrus and sulcus (aMCC)	L- Opercular part of the inferior frontal gyrus
L- Calcarine sulcus	R- Triangular part of the inferior frontal gyrus
R- Middle-anterior part of the cingulate gyrus and sulcus (aMCC)	R- Medial orbital sulcus (olfactory sulcus)
R- Straight gyrus, Gyrus rectus	
R- Medial orbital sulcus (olfactory sulcus)	
NET HUBS BETWENNESS (AN)	**NET HUBS BETWENNESS (AN)**
L- Precuneus (medial part of P1)	L- Anterior part of the cingulate gyrus and sulcus (ACC)
L-Short insular gyri	L- Planum temporale or temporal plane of the superior temporal gyrus
L- Vertical ramus of the anterior segment of the lateral sulcus (or fissure)	L- Postcentral sulcus
R- Long insular gyrus and central sulcus of the insula	R- Middle-anterior part of the cingulate gyrus and sulcus (aMCC)
R- Occipital pole	R- Lingual gyrus, ligual part of the medial occipito-temporal gyrus, (O5)
R- Calcarine sulcus	R- Orbital gyri
	R- Intraparietal sulcus (interparietal sulcus) and transverse parietal sulci
	R- Superior occipital sulcus and transverse occipital sulcus

Table 10. Hubs distribution in cortical thickness-based connectome. Comparison between patients with a good outcome and patients with a poor outcome.

NET HUBS DEGREE (good-outcome group)	**NET HUBS DEGREE (poor-outcome group)**
L- Middle frontal sulcus	L- Middle-anterior part of the cingulate gyrus and sulcus (aMCC)
L- Inferior part of the precentral sulcus	L- Superior parietal lobule (lateral part of P1)
R- Angular gyrus	L- Intraparietal sulcus (interparietal sulcus) and transverse parietal sulci
R- Middle frontal gyrus (F2)	R- Postcentral gyrus
R- Sulcus intermedius primus (of Jensen)	R- Superior frontal sulcus
	R- Anterior occipital sulcus and preoccipital notch(temporo-occipital incisure)
NET HUBS BETWENNESS (good-outcome group)	**NET HUBS BETWENNESS (poor-outcome group)**
L-Middle-anterior part of the cingulate gyrus and sulcus (aMCC)	L- Posterior-dorsal part of the cingulate gyrus(dPCC)
L- Anterior transverse temporal gyrus (of Heschl)	L- Inferior segment of the circular sulcus of the insula
L- Occipital pole	L- Superior segment of the circular sulcus of the insula
L- Temporal pole	L- Sulcus intermedius primus (of Jensen)
L- Middle frontal gyrus (F2)	R- Occipital pole
L- Lateral orbital sulcus	R- Superior frontal gyrus (F1)
L- Parieto-occipital sulcus (or fissure)	R- Middle occipital sulcus and lunatus sulcus
R- Inferior segment of the circular sulcus of the insula	R- Anterior occipital sulcus and preoccipital notch(temporo-occipital incisure)
R- Medial orbital sulcus (olfactory sulcus)	

Table 11. Hubs distribution in gyrification-based connectome. Comparison between patients with a good outcome and

NET HUBS DEGREE (good-outcome group)	**NET HUBS DEGREE (poor-outcome group)**
L- Opercular part of the inferior frontal gyrus	L- Anterior transverse temporal gyrus (of Heschl)
L- Lateral aspect of the superior temporal gyrus	R- Opercular part of the inferior frontal gyrus
R- Lateral orbital sulcus	
NET HUBS BETWENNESS (good-outcome group)	**NET HUBS BETWENNESS (poor-outcome group)**
L- Opercular part of the inferior frontal gyrus	L- Posterior ramus (or segment) of the lateral sulcus (or fissure)
L- Lateral aspect of the superior temporal gyrus	L- Marginal branch (or part) of the cingulate sulcus
L- Inferior frontal sulcus	L- Subparietal sulcus
L- Superior temporal sulcus (parallel sulcus)	R- Anterior part of the cingulate gyrus and sulcus(ACC)
R- Middle-posterior part of the cingulate gyrus and sulcus (pMCC)	R- Opercular part of the inferior frontal gyrus
R- Opercular part of the inferior frontal gyrus	R- Lateral occipito-temporal gyrus (fusiform gyrus, O4-T4)
R- Subcallosal area, subcallosal gyrus	R- Pericallosal sulcus (S of corpus callosum)
R- Lateral orbital sulcus	

DISCUSSION

In the last decade many advances have been made in the description of the organizational principles that govern the anatomy and the topology of brain structural covariance networks and in establishing the relationship between them and functional connectivity patterns (Alexander-Bloch, Giedd, et al., 2013b). Regional and global structural brain features undergo profound modifications during development and establish their covariance properties following complex trajectories that are influenced by both genetic predisposition and environmental influences. The biological mechanisms underlying thickness and gyrification correlation among cortical areas might impact at different developmental stages and their properties should reflect the different mechanisms that influence the cortical connective architecture. Several studies have examined thickness and gyrification covariance patterns in psychiatric diseases in order to understand whether disruptions in segregation and integration properties are measurable and to investigate the candidate biological and developmental underpinnings that may explain such alterations (Buchy et al., 2017; Chen et al., 2014; Griffiths et al., 2016; Palaniyappan et al., 2016b, 2015; Saad et al., 2017).

In this study we use a connectomic approach by means of cortical thickness and gyrification data to study the cortical structural architecture in AN and to evaluate the presence of any imbalance in the overall cortical network properties and in regional subnetwork patterns.

Our results highlighted the presence of a significantly higher segregation of the overall cortical thickness network in the acute AN group in comparison to the healthy control group. AN patients in particular showed higher local efficiency, modularity and clustering coefficients, which indicate the presence of a more topologically localized and less densely distributed connective organization. On the contrary, gyrification patterns did not show significant differences between the acute AN and the HC group. The observation that cortical thickness networks showed more significant alterations than gyrification based networks in acute AN patients is probably due to their different developmental trajectory and to their

different sensitivity to environmental changes. While convolution of the cortical surface begins prior to birth, establishing its main patterns principally in the fetal and neonatal stages, cortical thickness undergoes profound modification during later developmental phases, probably as the result of a fine tuning process between brain structure and function (Hensch, 2004b).

Evidence in the literature regarding the evolution of cortical thickness networks suggests that structural networks exhibit a global efficient small-world and modular organization by the time of birth and indicates a delayed increase of their integrative properties, which follows maturation of high order association areas and refinement of higher cognitive abilities (Cao et al., 2016; Morgan et al., 2018).

In acute AN patients, our results highlight the presence of significantly higher small-world properties in cortical thickness and in gyrification-based networks. These findings could represent the consequence of processes that tend to reduce the wiring cost of the global network and could indicate the presence of a more economical and less random cortical structural architecture. We can also hypothesize that this configuration could represent a consequence of the energy saving needs imposed by AN in the acute stage and that the presence of increased small-world properties is due to the attempt to maintain an adequate network efficiency despite starvation and malnutrition. This finding is also consistent with the clinical observation that many patients describe increased functioning during starvation, at least in the initial stages, and better ability in managing emotions, which is considered a maintenance factor (Brockmeyer et a l., 2012).

The present study excludes the presence of any regional differences (which have been found in other psychiatric diagnoses) in integration and segregation properties, suggesting that the disorder impacts only the global covariation patterns estimated on cortical thickness indices. These results allow us to hypothesize that the acute effect of the disease could determine a global network readjustment that follows energy saving purposes. Therefore, AN could impact the balance between the wiring cost of the network and its integrative communication demand, supporting a less expensive connective architecture reconfiguration.

To better understand the impact of AN on the cortical structural connectivity architecture and on their developmental trajectories we evaluated a sample of AN recovered patients, without finding significant alterations either in gyrification or in cortical thickness covariance networks. These results seem to confirm the sensitivity of the overall cortical thickness network to the acute effects of the disease.
The second objective of our study was to explore the impact of gyrification and cortical thickness patterns in predicting outcome at follow up, evaluating the presence of possible differences in cortical connectivity patterns between “good prognosis” and “poor prognosis” patients. The absence of significant differences in the overall cortical thickness network properties between the two groups examined is consistent with a high cortical thickness sensitivity to the acute effects of AN, which homogeneously impact the cortical thickness covariance patterns in the acute stage of the disease. However, regional analysis showed a non-homogeneous pattern, with a significantly lower number of connected edges (lower degree) and higher regional clustering of the orbital part of the left inferior frontal gyrus in the poor-outcome group. Inferior frontal gyrus is involved in numerous executive functions, playing a critical role mainly in cognitive control and in response inhibition. Proper maturation of inhibitory abilities is particularly crucial during adolescence, given the detrimental role of high levels of impulsivity during this critical developmental period. Interestingly, the transition from adolescence to adulthood is characterized by profound differences in the spatial localization of inhibitory processing, with a higher recruitment of right IFG in adulthood and a more left dominant processing at younger ages (Vara, Pang, Vidal, Anagnostou, & Taylor, 2014).
Adolescent individuals with AN show a bilateral decrease in gray matter volume in the IFG and the volume of this area was found to negatively correlate with both age and age of onset of the disorder (Fujisawa et al., 2015). Our observation of higher segregation in the IFG in the group of patients with a poor outcome is consistent with the idea that a lower integration of maturation of this area could mediate for prognostically unfavorable characteristics of the disorder.

Analysis of the role of gyrification-based networks in predicting the outcome at follow up showed the presence of a more clustered, segregated and less efficient overall covariance network in the poor-outcome group. Since gyrification patterns seem to develop mainly during the prenatal stages, our results are in line with others that support a neurodevelopmental hypothesis for AN and suggest a role of early maturational processes in the characterization of a subgroup of patients with low response to treatments.

Structural networks are proven to have an intimate relationship with functional cortical interconnectivity and a fundamental role in the way in which cortical regions structurally mature in relation to one another (Khundrakpam et al., 2013; Raznahan et al., 2011). We can hypothesize that the higher global segregation of the poor-outcome group and its lower global efficiency could reduce the response to treatment by limiting the dynamic functional reconfiguration of the network and the information exchange between topologically distant brain areas.

The finding of a lower integration of gyrification indices in mediating the prognosis of AN is in line and expands the previous observation of a lower cortical gyrification in AN patients who show a poor outcome at a 3-year follow up (Angela Favaro, Tenconi, Degortes, Manara, & Santonastaso, 2015). In particular, since lower structural integration is likely to indicate a slowdown in the maturation of connectivity patterns during development, the opportunity to disentangle the role of neurodevelopment trajectories on the onset of AN and the impact that the disorder itself has on neurodevelopmental trajectories seems to be particularly relevant from a clinical point of view.

From a regional perspective, patients with a bad prognosis show an increased clustering of the left superior temporal sulcus, a higher-order processing region that has a key role in diverse aspects of social perception and cognition, including the perception of faces, voices and understanding the actions and mental states of others (Vander Wyk, Hudac, Carter, Sobel, & Pelphrey, 2009; Zilbovicius et al., 2006). The higher clusterization of this area in AN patients who have a poor response to treatment indicates, in this clinical population, a preponderance of segregative network characteristics.

Patients with a poor outcome also have a reduced degree of the right insula, when compared with patients with good prognosis, which indicates a reduced centrality of an area with high integrative functions (Craig, 2009). These regional differences are consistent with the high segregation of gyrification covariance networks in patients with bad prognosis and suggest a role of highly connected areas such as the insula and superior temporal sulcus in determining or mediating the resistance of the disorder to conventional treatments.

This study has several strengths, as well as important limitations, which should be taken into consideration. It is the first to analyze the relationships between different cortical structural indices using a connectomic framework in AN, and to describe the relationship between structural covariation patterns and subsequent outcomes of the disorder. However, particular caution must be applied in interpreting brain findings in AN samples, for which it is often difficult to disentangle the effects of early developmental factors on the brain and the consequences of starvation.

In conclusion, the present study highlights the presence of higher segregation and lower integration characteristics in the global cortical thickness-based network in patients with acute AN when compared to HC. These higher segregation characteristics could be due to a maturational delay, which would affect normal development trajectories, or to a protective and energy saving adaptation to the disease. However, the presence of small-world properties in AN patients guarantees the presence of non-random and balanced network properties, in line with the high level of functioning that characterizes patients with AN even in their malnourished status. The differences evidenced between cortical thickness and gyrification networks in acute AN patients and the observation of a more clustered and segregated gyrification network in patients with a bad prognosis suggest that the covariation patterns of these two parameters should be further investigated using longitudinal observations in order not only to better understand the long-term consequences of malnutrition, but also to explore the possibility of using gyrification and its pattern of covariance network as a measure of outcome.

Reduced cortical complexity in Anorexia Nervosa: a Fractal Dimension analysis

INTRODUCTION

Anorexia nervosa (AN) is a severe psychiatric disorder with a typical onset during adolescence (Angela Favaro et al., 2009), characterized by severe and prolonged alterations of energy intake and high levels of mortality. Although there is a notable interest in understanding the effects of starvation on the brain structure of these patients, a full characterization of brain changes is still at its first stages (Jochen Seitz et al., 2014). The onset of AN typically occurs when neurodevelopment is still ongoing (Connan, Campbell, Katzman, Lightman, & Treasure, 2003) and it is possible that the effects of malnutrition have a different impact in brain areas that are in a sensitive period of growth at the time of AN onset. Moreover, there are some evidences that prenatal and perinatal factors are involved in the etiopathogenesis of AN and, for this reason, it is not easy to understand how much brain structural alterations in patients with AN precede the onset or are a consequence of the disorder.

Most studies to date employed a Voxel Based Morphometry approach and found a globally reduced GM volume, but inconsistent results emerged in the identification of specific regional changes in AN (Jochen Seitz et al., 2014). In addition, only few studies found a significant correlation with body weight or amount of weight loss, and almost none with age of onset or duration of illness (J Seitz et al., 2016). The use of a Surface Based Morphometry approach did not result in more consistent findings (Bernardoni et al., 2016; Fuglset et al., 2016; J. A. King et al., 2015; Lavagnino et al., 2016, 2018). Generally, a reduction of cortical thickness is described in the different studies, but the extent of the reduction varies from almost the whole cortex to about a quarter or one third (Bernardoni et al., 2016; Fuglset et al., 2016). Other surface-based methods, such as local gyrification index and cortical folding, have been employed to describe brain cortical changes in patients with AN (Bernardoni et al., 2018b; Angela Favaro et al., 2015; Schultz et al., 2017). Both measures displayed significant alterations in acute patients, but the

interpretation of these findings are not clear, since gyrification tends to develop early in childhood and its alteration is usually attributed to prenatal or very early insults (White et al., 2010).

A novel way to quantify and analyze the cortex from a morphological and structural point of view has been recently offered by fractal geometry (Kiselev, Hahn, & Auer, 2003), which is specifically designed for the analysis of complex structural and morphological patterns (Madan & Kensinger, 2016). The application of fractal geometry to neuroscience is consistent with the evidence, already highlighted by the increasing application of complex network science to neuroimaging data, that the central nervous system is organized in nested and hierarchical organization patterns that need to balance both regularity and randomness (Di Ieva, 2016). This multi-level structural organization of the brain seems to be well-described by fractal geometry, which is based on the concept of "self-similarity" (Mandelbrot, 1983). Since the fractal properties of the cerebral cortex arise secondary to folding (Hofman, 1991) structural MRI studies used fractal dimensionality to quantify the morphological complexity of the cortex and its convolutional properties both in clinical and non-clinical samples (Cook et al., 1995; Nenadic, Yotter, Sauer, & Gaser, 2014; Sandu et al., 2008).

Two types of fractal dimensionality can be considered, depending on whether the volume of the gray matter is included in the computation. Incorporating the volume of the grey matter into the computation ensures that changes in cortical thickness are directly integrated within the fractal dimensionality estimation. Thus, interestingly, fractal dimension appears to co-vary with both cortical thickness and gyrification (R. D. King et al., 2010). Furthermore, it also appears to demonstrate a great sensitivity to cortical atrophy and to age-related differences (Madan & Kensinger, 2016). Cortical complexity measured by means of FD has shown both global and regional alterations when examined in different psychiatric disorders such as ADHD, schizophrenia, bipolar and obsessive-compulsive disorders (Ha et al., 2005; Li et al., 2007; Nenadic et al., 2014; Sandu et al., 2008; Squarcina et al., 2015).

In this study, we explored - for the first time - the use of FD to describe the brain cortical alterations in patients with AN. We hypothesize a reduction of cortical complexity in acute underweight patients and an improvement of this feature after remission.

METHODS AND MATERIALS

The sample included was the same as a previous study (Favaro et al., 2013). 38 patients with acute AN, 38 HC and 20 patients in full remission from AN were included in this study. Patients who recovered from AN had full AN in their lifetime, but were asymptomatic from at least 6 months at the time of scanning [mean remission time: 38.5 months (standard deviation533.2); range 6–96]. The main characteristics of the sample are reported in table 12. Exclusion criteria for the recovered group were amenorrhea, food restriction, bingeing, excessive exercise, fasting and purging in the last 6-months. None of the recovered patients relapsed in the year following the study. Exclusion criteria for all subjects were male gender, history of head trauma or injury with loss of consciousness, history of any serious neurological or medical illness, active use of systemic steroids, pregnancy, active suicidality or major depression, history of substance/alcohol abuse or dependence, bipolar disorder or schizophrenia spectrum disorder, moderate mental impairment (IQ<60) or learning disabilities, use of medications other than antidepressants, and known contraindications to conventional MRI. For healthy women, additional exclusion criteria were history of any psychiatric disorder and the presence of first-degree relatives with an eating disorder.

At the time of recruitment, some individuals were excluded from the study: five AN patients was under antipsychotic medication and/or reported severe comorbidity; one AN patient and one healthy subject reported a previous head trauma; one AN patient, 3 recovered AN and 2 healthy subjects were not available to undergo MRI scanning when scheduled. The final sample comprised of 96 women (38 with AN, 20 recovered from AN, and 38 HC). No further subject was excluded due to problems with scan acquisition, gross brain alterations, or motion artifacts.

Ethical permission was obtained from the ethics committee of the Padova Hospital. After completely describing the study to the subjects, informed written informed consent was obtained.

Table 12. Sample characteristics

	AN (n=38) Mean	SD	Recovered AN (n=20) Mean	SD	HC (n=38) Mean	SD	AN vs. HC *t* (p)	Rec.AN vs. HC *t* (p)
Age (years)	26,1	7,2	26,3	7,0	25,2	6,7	0,54 (0,59)	0,59 (0,56)
Baseline Body mass index (kg/m^2)	16,0	1,8	19,6	1,6	21,6	3,0	10,51 (<0,001)	2,91 (0,005)
Lowest Body mass index (kg/m^2)	14,0	1,8	15,7	1,4	19,8	2,5	11,56 (<0,001)	6,71 (<0,001)
Weight loss (kg)	7,1	2,8	5,2	3,1	3,4	1,7	7,01 (<0,001)	2,95 (0,005)
Age of onset (years)	18,3	5,0	17,7	3,2	-	-	-	-
Duration of illness (months)	78,6	81,2	45,7	65,0	-	-	-	-
Duration of recovery (months)			45,4	47,0	-	-	-	-
Edinburgh laterality index	57,1	37,5	60,0	35,2	55,0	42,0	0,23 (0,82)	0,50 (0,62)
Education (years)	14,2	2,2	14,1	2,6	15,4	2,3	2,44 (0,02)	1,97 (0,05)
Drive to thinness	9,9	6,1	-	-	2,3	4,2	6,22 (<0,001)	-
Depression	1,4	0,8	-	-	0,7	0,6	4,06 (<0,001)	-
Trait anxiety	56,6	9,7	-	-	39,3	9,6	7,82 (<0,001)	-

Clinical assessment and Follow-up

A diagnostic interview according to the Eating Disorders Section of the Structured Clinical Interview for DSM-5 (American Psychiatric Association, 2013) was performed in all subjects. A semi-structured interview was also used to collect socio-demographic and clinical variables (Favaro et al., 2012, 2013). The Hopkins Symptoms Checklist (Derogatis et al., 1974) to assess depressive and obsessive-compulsive symptoms, the Eating Disorders Inventory (Garner et al., 1983) to assess eating psychopathology and

the Edinburgh Handedness Inventory (Oldfield, 1971) were also administered. All subjects were recruited at the Eating Disorder Unit of the Hospital of Padova, fulfilled the diagnosis for AN according to DSM-IV criteria and were medically stable at the time of scanning. Different diagnostic subtypes at the time of scanning were observed: 32 AN patients (84%) were restrictive, 6 AN patients fall under the binge eating/purging subtype and 7 patients who were restrictive at the time of the present study reported previous recurrent binge eating and/or purging. 14 AN patients and 4 recovered women were under treatment with antidepressant drugs at the time the study was conducted (acute AN: 1 case mirtazapine, 2 paroxetine, 2 escitalopram, 1 fluoxetine, 8 sertraline; recovered AN: 4 sertraline).

MRI Data Acquisition

Data were collected on a Philips Achieva 1.5 Tesla scanner equipped for echo-planar imaging. A high-resolution 3D T1-weighted anatomical image was also acquired, in a gradient-echo sequence (repetition-time520 s, echo time- 53.78 ms, flip angle 5208, 160 sagittal slices, acquisition voxel size 51 3 0.66 3 0.66 mm, field of view 21–22 cm).

Data Processing and Statistics

Data processing were performed using the FreeSurfer package (Martinos Center for Biomedical Imaging, Massachusetts General Hospital, Boston) version 5.3.0. Preprocessing, cortical reconstruction, segmentation, and cortical thickness estimation were performed following standard protocols, see Supplementary Materials for detailed information. Surface reconstruction and segmentation were inspected and minor manual intervention was performed according to FreeSurfer user guidelines. After cortical reconstruction, the cortex was divided into units based on individual gyral and sulcal structures (Destrieux et al., 2010)

A freely available MATLAB toolbox (http://cmadan.github.io/calcFD/). was used to compute the fractal dimensionality of the cortical ribbon and of parcellated regions of the cortex. The toolbox uses

intermediate files generated as part of the standard Freesurfer analysis pipeline to perform the calculation (Madan & Kensinger, 2016).

RESULTS

Demographic characteristics of the sample are reported in table 12.

FD in patients with AN vs. HC

Table 13 shows the average FD values in the whole-brain, the 4 lobes and the 21 brain areas (according to Destrieux parcellation) in the two groups. The whole-brain and lobar mean FD value was significantly lower in acute AN patients compared to HC.

The mean FD value computed for the whole brain was significantly lower in acute AN patients compared to HC. FD values of each brain lobe are lower in the AN group.

The mean FD value of the cortical ribbon was significantly lower both in the left and in the right hemisphere in paracentral, postcentral, superior parietal, superior frontal, middle frontal, inferior frontal, orbital, angular, and in superior and middle occipital gyri, in posterior transverse collateral sulcus, in the superior part of the precentral sulcus and in precuneus. In the left hemisphere, we found significantly decreased FD values in the frontal inferior opercular, supramarginal and precentral giri and in the posterior segment of lateral sulcus. In the right hemisphere, we found decreased FD values in the posterior ventral cingulate and in lateral superior temporal gyrus, in the lateral anterior fissure and in the superior and transverse occipital sulcus (Table 13).

FD in patients recovered from AN vs. HC

Table 14 shows the average FD values in the whole-brain, the 4 lobes and the 21 brain areas (according to Destrieux parcellation) in the two groups. Recovered AN patients didn’t show differences in the

global and lobar FD when compared to HC. However, there are some brain areas that showed FD values significantly higher than healthy women and brain areas with lower FD in comparison to controls (Table 14). It is interesting to observe that left middle occipital gyrus and right superior parietal gyrus showed significantly lower FD both acute and recovered AN in comparison to controls.

Association between FD values and clinical variables

Table 15 shows correlation (rho Spearman's rank correlation) between FD values and clinical variables in the three groups. Significant positive correlations emerged between whole-brain FD and BMI in acute AN, and between total FD and cortical volume in acute AN and in recovered patients. The FD value was also negatively correlated with duration of the illness in the AN group. Significant negative correlation between of age of onset of the disorder and FD emerged in the recovered group (table 15).

Table 13. Fractal Dimension differences analysis between AN and HC groups

			AN	HC	
	Lat	Lobe	Mean (SD)	Mean (SD)	F* (p)
Total FD			2.49 (0.02)	2.51 (0.01)	16.36 (0.000)
Frontal Lobe			2.43 (0.02)	2.44 (0.01)	13.07 (0.001)
Parietal Lobe			2.30 (0.02)	2.32 (0.01)	19.75 (0.000)
Temporal lobe			2.34 (0.02)	2.35 (0.01)	5.40 (0.023)
Occipital lobe			2.30 (0.02)	2.32 (0.01)	15.31 (0.000)
Paracentral lobule and S	L	Parietal	1.91 (0.04)	1.93 (0.03)	10.41 (0.002)
G Front Inf Operc	L	Frontal	2.01 (0.03)	2.03 (0.03)	7.71 (0.007)
Triangular part inferior frontal G	L	Frontal	2.00 (0.031)	2.01 (0.027)	5.89 (0.018)
Middle frontal G	L	Frontal	2.09 (0.03)	2.11 (0.02)	7.05 (0.010)
Superior frontal G	L	Frontal	2.17 (0.03)	2.18 (0.02)	6.81 (0.011)
Middle occipital G	L	Occipital	1.99 (0.04)	2.01 (0.03)	7.71 (0.007)
Superior occipital G	L	Occipital	1.90 (0.04)	1.92 (0.03)	6.81 (0.011)
Orbital G	L	Frontal	2.03 (0.03)	2.04 (0.02)	9.15 (0.003)
Angular G	L	Parietal	2.06 (0.03)	2.08 (0.02)	11.40 (0.001)
Supramarginal G	L	Parietal	2.09 (0.03)	2.11 (0.02)	6.00 (0.017)
Superior parietal G	L	Parietal	2.03 (0.04)	2.06 (0.03)	18.82 (0.000)
Postcentral G	L	Parietal	1.91 (0.05)	1.94 (0.03)	10.19 (0.002)
Precentral G	L	Frontal	1.98 (0.04)	2.01 (0.03)	8.68 (0.004)
Precuneus	L	Parietal	2.03 (0.02)	2.05 (0.02)	7.85 (0.007)
Posterior segment of lateral S	L	Temporal	1.87 (0.02)	1.89 (0.03)	6.47 (0.013)
Posterior transverse collateral S	L	Occipital	1.61 (0.07)	1.65 (0.06)	6.96 (0.010)
Anterior occipital S	L	Occipital	1.79 (0.08)	1.83 (0.06)	9.35 (0.003)
Superior part of the precentral S	L	Frontal	1.87 (0.04)	1.89 (0.04)	6.86 (0.011)

Paracentral lobule	R	Parietal	1.89 (0.04)	1.91 (0.03)	5.77 (0.019)
Posterior ventral cingulate G	R	Parietal	1.68 (0.05)	1.71 (0.05)	9.55 (0.003)
Triangular part inferior frontal G	R	Frontal	1.98 (0.03)	2.00 (0.03)	6.74 (0.011)
Middle frontal G	R	Frontal	2.08 (0.03)	2.10 (0.02)	8.64 (0.004)
Superior frontal G	R	Frontal	2.14 (0.03)	2.17 (0.02)	19.34 (0.000)
Lateral Anterior Fissure	R	Frontal	1.70 (0.04)	1.72 (0.05)	5.52 (0.022)
Middle occipital G	R	Occipital	2.01 (0.03)	2.03 (0.02)	9.61 (0.003)
Superior occipital G	R	Occipital	1.92 (0.04)	1.95 (0.03)	15.86 (0.000)
Orbital G	R	Frontal	2.04 (0.03)	2.06 (0.02)	6.10 (0.016)
Angular G	R	Parietal	2.09 (0.04)	2.11 (0.03)	8.72 (0.004)
Superior parietal G	R	Parietal	2.00 (0.04)	2.03 (0.03)	12.49 (0.001)
Postcentral G	R	Parietal	1.88 (0.04)	1.91 (0.04)	14.34 (0.000)
Precuneus	R	Parietal	2.03 (0.03)	2.05 (0.02)	7.33 (0.008)
Lateral superior temporal G	R	Temporal	2.02 (0.04)	2.04 (0.03)	5.91 (0.018)
Posterior transverse collateral S	R	Occipital	1.64 (0.07)	1.71 (0.09)	11.38 (0.001)
Sup. and transverse occipital S	R	Occipital	1.90 (0.04)	1.92 (0.04)	6.73 (0.011)
Superior part of the precentral S	R	Frontal	1.88 (0.05)	1.91 (0.04)	9.48 (0.003)

FD: Fractal Dimension; G: gyrus; S: sulcus; Lat: lateral; R: right; L: left

* F (GLM with age and hand lateralization as covariates of no interest; gl=3,72), p threshold according to FDR < 0,025

Table 14. Fractal Dimension differences analysis between Recovered AN and HC groups

	Lat	Lobe	Rec.AN Mean (SD)	HC Mean (SD)	F* (p)
Total FD			2.52 (0.02)	2.52 (0.01)	0.32 (0.573)
Frontal Lobe			2.44 (0.02)	2.45 (0.02)	0.05 (0.829)
Parietal Lobe			2.32 (0.02)	2.32 (0.01)	0.72 (0.400)
Temporal lobe			2.36 (0.01)	2.35 (0.01)	3.46 (0.068)
Occipital lobe			2.32 (0.02)	2.33 (0.01)	0.55 (0.462)
Subcentral G#	L	Frontal	2.03 (0.02)	2.02 (0.02)	5.57 (0.022)
Middle occipital G	L	Occipital	1.99 (0.03)	2.01 (0.03)	6.11 (0.017)
Inferior temporal G#	L	Temporal	2.11 (0.03)	2.09 (0.03)	5.75 (0.020)
Middle temporal G#	L	Temporal	2.11 (0.02)	2.09 (0.03)	6.68 (0.012)
Transverse occipital S#	L	Occipital	1.92 (0.03)	1.89 (0.05)	5.37 (0.024)
Parieto occipital S#	L	Occipital	1.79 (0.04)	1.75 (0.06)	12.47 (0.001)
Subparietal S#	L	Parietal	1.93 (0.05)	1.90 (0.04)	6.49 (0.014)
Temporal Inferior S#	L	Temporal	1.79 (0.04)	1.75 (0.05)	11.50 (0.001)
Superior temporal S#	L	Temporal	2.12 (0.03)	2.10 (0.03)	7.67 (0.008)
Superior parietal G	R	Parietal	2.01 (0.03)	2.03 (0.03)	5.88 (0.019)
Parieto-occipital S	R	Occipital	1.98 (0.03)	2.01 (0.03)	15.71 (0.000)
Subparietal S#	R	Parietal	1.96 (0.04)	1.92 (0.04)	7.65 (0.008)

G: gyrus; S: sulcus; Lat: lateral; R: right; L: left; ns: not significant

* F (GLM with age and hand lateralization as covariates of no interest; gl=3,54), p threshold according to FDR < 0,025

Table 15. Correlation between whole-brain FD and clinical variables in the 3 groups

	whole-brain FD		
	AN (n=38)	recovered AN (n=20)	Healthy women (n=38
	Rho (p)	Rho (p)	Rho (p)
Age	-0.608 (0.000)	-0.617 (0.004)	-0.527 (0.001)
Body mass index	0.380 (0.019)	-0.351 (0.130)	-0.209 (0.207)
Duration of illness	-0.406 (0.011)	-0,111 (0.642)	
Age of onset	-0.265 (0.108)	-0.586 (0.007)	
Cortex volume	0.638 (0.000)	0.537 (0.015)	0.496 (0.002)
Overall LGI rh	0.314 (0.055)	0.358 (0.121)	0.504 (0.001)
Overall LGI lh	0.247 (0.135)	0.332 (0.152)	0.522 (0.001)
	FD of the Left Middle Occipital Gyrus		
	AN (n=38)	recovered AN (n=20)	Healthy women (n=38)
Age	-0.317 (0.053)	-0.129 (0.587)	-0.579 (0.000)
Body mass index	0.359 (0.027)	-0.393 (0.086)	-0.136 (0.416)
Duration of illness	-0.203 (0.223)	0.126 (0.595)	
Age of onset	-0.286 (0.082)	-0.320 (0.168)	
Cortex volume	0.773 (0.000)	0.735 (0.000)	0.502 (0.001)
Overall LGI rh	0.467 (0.003)	0.508 (0.022)	0.240 (0.148)
Overall LGI lh	0.362 (0.025)	0.456 (0.043)	0.159 (0.341)
	FD of the Right Superior Parietal Gyrus		
	AN (n=38)	recovered AN (n=20)	Healthy women (n=38)
Age	-0.294 (0.073)	-0.189 (0.424)	-0.126 (0.451)
Body mass index	0.434 (0.006)	-0.301 (0.197)	0.144 (0.388)
Duration of illness	-0.160 (0.336)	-0.023 (0.925)	
Age of onset	-0.343 (0.035)	-0.395 (0.084)	
Cortex volume	0.642 (0.000)	0.006 (0.980)	0.312 (0.057)
Overall LGI rh	0.302 (0.65)	-0.096 (0.686)	0.264 (0.110)
Overall LGI lh	0.196 (0.239)	0.105 (0.659)	0.159 (0.341)

FD: Fractal Dimension; LGI: Local Gyrification Index; R: right; L: left; ns: not significant
Rho di Spearman; FDR < 0,025

DISCUSSION

To our knowledge, the present is the first study that investigate the cortical morphology in AN by means of FD, an index that is specifically designed to capture the complex morphological patterns of the cortex, thus integrating the structural information provided by other surface-based indexes.

In this paper we specifically evaluated cortical FD indices both globally and regionally and investigated the relationship between any morphological abnormalities and specific clinical variables.

Our results demonstrated the presence of a globally reduced FD in patients with acute AN compared to HC, while patients who recovered from AN didn't show any differences in FD when compared with HC on a global level. This observation, together with the presence of a correlation between FD and BMI, allows to hypothesize that a global reduction in cortical complexity may be an acute effect of malnutrition, and that it can improve with weight recovery. The ability to investigate the complex patterns of cortical morphology, together with the good sensitivity to the effects of underweight on cortical structure, points out the usefulness of this parameter in the structural imaging evaluation of AN and confirms its ability to describe cortical atrophy. The cortical structural modifications in AN are likely to depend on many factors, representing a consequence of underweight and malnutrition but also the outcome of neurodevelopmental trajectories alterations (Connan et al., 2003). The hypothesized developmental origin of the disorder and the effect of its onset in critical developmental phases highlight the importance to consider the relationship between any cortical alterations, the duration of the disorder and the patient's age and age of onset in the evaluation of structural MRI findings. Our results indicate that age of the patients and the duration of the disorder correlate inversely with FD, suggesting an impact of AN on the reduction of cortical complexity. Since cortical complexity, measured by FD, is likely to reduce from adolescence to adulthood as the results of cortical modeling mechanisms that physiologically occur with aging (Sandu et al., 2014), we could hypothesize an impact of the disorder in accelerating this process.

The relation between FD and gyrification index is consistent with previous researches that already evidenced that cortical folding is a high source of cortical complexity (R. D. King, Brown, Hwang, Jeon, & George, 2010; Madan & Kensinger, 2016). Gyrification appears to be largely determined during the earlier neurodevelopmental phases and alterations in this structural parameter have been already highlighted in AN (Bernardoni et al., 2018a; Angela Favaro et al., 2015). Since gyrification abnormalities are considered indicators of early neurodevelopmental anomalies and predictors of unfavorable outcome in AN as in other psychiatric disorders (Guo et al., 2015; Palaniyappan et al., 2016a), the finding of FD alterations could be also consistent with a neurodevelopmental hypothesis for AN (Angela Favaro, 2013).

From a regional analysis, we identified a FD reduction in the left middle occipital gyrus and in the right parietal superior gyrus both in acute and in recovered AN patients. These are the only areas in which a FD alteration persists after recovery. Parietal and occipital regions are crucial for the integration of body-image perception abilities and are probably susceptible to disorder-specific alterations.

The present study has several strengths, as well as important limitations. It is the first study to explore cortical complexity in AN by means of FD, a novel parameter that is demonstrated to show a good sensitivity to cortical atrophy and age-related brain differences. The evaluation of cortical morphology with FD allows to widen the horizons of surface-based cortical analysis, by integrating the information given by cortical thickness and gyrification with novel and non-redundant data. Furthermore, the presence of a correlation between FD alterations and the duration of the illness is a new and interesting finding over MRI surface-based analysis in AN and highlights the important potentialities of this morphological index in capturing the effects of prolonged starvation on cortical structure. A limitation of this study is represented by its cross-sectional design. In fact, longitudinal data could be particularly useful to understand how cortical complexity vary with the clinical course of the disorder and with weight recovery. Another limitation can be found in the absence of male patients in the sample. Any

inference about alteration in cortical complexity in male patients with AN cannot be made and would be an interesting topic to explore in future studies.

In conclusion, the present study evidences that FD should be considered particularly useful to investigate the morpho-structural properties of brain cortex in AN, since it demonstrated to be able in identifying the negative effects of different clinical variables on cortical structure and to give non-redundant information with respect to other surface-based indexes. Furthermore, the present study identifies the duration of the illness as a factor which directly correlates with cortical structural alteration in AN.

Shift toward randomness in Anorexia Nervosa: a structural connectivity study

INTRODUCTION

The neurobiological characterization of Anorexia Nervosa by means of structural and functional neuroimaging techniques evidenced the presence of multifaceted alterations, that are likely to reflects the complex psychopathological and cognitive underpinnings of the disorder (Guido K.W. Frank, 2014). Overall, neuroimaging studies suggest that the complex array of symptoms characterizing AN emerges from failures in the relations between multiple areas rather than from distinct regional alterations (Steward, Menchon, Jimenez-Murcia, Soriano-Mas, & Fernandez-Aranda, 2017). The brain networks that have been found to be altered in AN support different processes, which include cognitive control, reward processing, self-monitoring, visuospatial and somatosensory functions, emotion recognition and social/inter-personal abilities (Collantoni et al., 2016; Ehrlich et al., 2015; Angela Favaro et al., 2012; G K W Frank, Shott, Riederer, & Pryor, 2016; Seidel et al., 2018). All these functional networks are supported by spatially distributed neurocircuits. In recent years, the application of complex science tools to neuroimaging data has allowed to study the rules that govern the inter-relations between distinct brain areas and to explore how alterations in brain architecture could sustain specific psychological, cognitive and behavioral traits (Bullmore & Sporns, 2009).

The application of network-based statistics and graph theory to neuroimaging data allows to describe the organizational properties of neural networks. The global organization of a neural network can be described by its ability to efficiently integrate the communication between distant brain regions and to ensure, at the same time, an adequate processing of local information. The regional properties of a graph can be inferred from the segregation and integration characteristics of individual nodes or from their influence and centrality within the network (Rubinov & Sporns, 2010; Sporns, 2010).

Connectomic approaches have been recently used with both functional and anatomical data in different psychiatric disorders as Schizophrenia, Major Depressive Disorder, Obsessive Compulsive Disorder and

Attention Deficit Hyperactivity Disorder (Rubinov & Bullmore, 2013; Sidlauskaite, Caeyenberghs, Sonuga-Barke, Roeyers, & Wiersema, 2015; Taylor, 2014; Wang et al., 2016). In AN, three studies have evaluated the brain architecture by means of graph theory tools to date. Geisler and colleagues (2016) used a connectomic approach to study the functional architecture of the brain in a sample of 35 patients, evidencing both global and regional alterations. They specifically observed an increased overall path length, indicating the presence of a less integrated network, and an increase of assortativity, which suggests that nodes with similar degree are more likely to connect together. Regionally, they evidenced a lower integration of thalamus and insula. A recent research, conducted by our group (Collantoni et al., under review, 2018), confirmed an increase of global segregation properties by analyzing cortical thickness and gyrification co-variance patterns in a sample of 38 AN patients. In another recent study, Zhang et al (2016) used Diffusion Tensor Imaging to compare the modular organization of the brain in 24 patients recovered from AN and 31 healthy controls. They found an abnormal modular organization in frontal, basal ganglia and posterior cingulate nodes in recovered AN patients.

The neurodevelopmental origin of AN, its frequent onset during adolescence and its dramatic metabolic consequences make the study of white matter in this disorder particularly interesting. In fact, the maturation of WM proceeds from infancy to adulthood and is likely to be affected by alterations in neurodevelopmental trajectories (Lebel et al., 2012). Microstructural white matter (WM) alterations in AN have been observed by different studies employing TBSS and VBM to evaluate Fractional Anysotropy (FA) (Monzon, Hay, Foroughi, & Touyz, 2016). Results across these studies are quite inconsistent, due to low and heterogeneous sample sizes and to methodological issues (Kaufmann et al., 2017). Only few studies estimated WM by means of tractography techniques in patients with acute AN, but none of them used a connectomic approach to describe the topological properties of neural networks (G K W Frank et al., 2016; Pfuhl et al., 2016; Shott, Pryor, Yang, & Frank, 2016). Since WM architecture is fundamental to ensure a proper flow of information across the brain, the analysis of its organization in

AN may help in understanding if this disorder is sustained by alterations in structural connectivity patterns.

The identification of the most influential and connected regions within the brain seems to be particularly relevant when computing the overall architecture of the WM connectome. In fact, these regions appear to be particularly vulnerable and sensitive to pathogenic mechanisms that affect the brain and are also likely to spread disease-related processes to other brain areas (Fornito et al., 2017).

Aim of the present research is to analyze the global and regional WM architecture by means of graph theory tools in a sample of patients with acute AN, to observe the presence of any abnormalities in hubs distribution and to observe the presence of any correlation between clinical variables and the properties of the graph.

METHODS AND MATERIALS

The included sample was the same of a previous study (Favaro et al., 2013). A total of 38 patients with acute AN and 38 HC were included in this study. Table 16 describes the main characteristics of the sample. male gender, history of head trauma or injury with loss of consciousness, history of any serious neurological or medical illness, active use of systemic steroids, pregnancy, active suicidality or major depression, history of substance/alcohol abuse or dependence, bipolar disorder or schizophrenia spectrum disorder, moderate mental impairment (IQ<60) or learning disabilities, use of medications other than antidepressants, and known contraindications to conventional MRI were the exclusion criteria for both the AN and the HC groups. For healthy women, additional exclusion criteria for were history of any psychiatric disorder and the presence of any first- degree relatives with an eating disorder.

When recruiting subjects, some of them were not included in the study: five AN patients with AN, because of antipsychotic medication and/or severe comorbidity; one AN patient and one healthy subject, because of previous head trauma; one AN patient, 3 recovered AN and 2 healthy subjects, who

were not available to undergo MRI scanning when scheduled. The final sample comprised of 76 women (38 with AN, and 38 HC). No further subject was excluded due to problems with scan acquisition, gross brain alterations, or motion artifacts.

Ethical permission was obtained from the ethics committee of the Padova Hospital. After completely describing the study to the subjects, informed written informed consent was obtained.

Clinical assessment

All subjects were investigated for AN diagnosis with a diagnostic interview according to the Eating Disorders Section of the Structured Clinical Interview for DSM-5 (American Psychiatric Association, 2013). A semi-structured interview was also performed to collect socio-demographic and clinical variables (Angela Favaro et al., 2012, 2013). All the subjects completed the Hopkins Symptoms Checklist (Derogatis et al., 1974) to assess depressive and obsessive-compulsive symptoms, the Eating Disorders Inventory (Garner et al., 1983) to assess eating psychopathology and the Cloninger Tridimensional Personality Questionnaire (TPQ) (Cloninger, Przybeck, & Svrakic, 1991) to test personality traits. The Edinburgh Handedness Inventory (Oldfield, 1971) was used to assess handedness. All subjects were recruited at the Padova Hospital Eating Disorders Unit and all fulfilled all the DSM-5 criteria for AN. At the time of scanning, all of them were medically stable. The diagnostic subtype at the time of scanning was: restrictive in 32 patients (84%), binge eating/purging type in 6 patients. 7 patients who were restrictive at the time of the present study reported previous recurrent binge eating and/or purging. Concerning the use of medications, 14 AN patients were under treatment with antidepressant agents at the time the study was conducted (acute AN: 1 case mirtazapine, 2 paroxetine, 2 escitalopram, 1 fluoxetine, 8 sertraline).

Mri Data Acquisition

Data were collected on a Philips Achieva 1.5 Tesla scanner equipped for echo-planar imaging. A high-resolution 3D T1-weighted anatomical image was also acquired, in a gradient-echo sequence

(repetition-time520 s, echo time- 53.78 ms, flip angle 5208, 160 sagittal slices, acquisition voxel size51 3 0.66 3 0.66 mm, field of view 21–22 cm).

Image processing

All DICOM images were converted to NIfTI format. Diffusion gradients were extracted using mriconvert (http://lcni.uoregon.edu/~jolinda/MRIConvert) was used to extract the diffusion gradients. The package FMRIB Software Library (FSL)'s Diffusion Toolkit (FDT) was used to preprocess diffusion-weighted images (DWIs) and for the diffusion tensor estimation. Probtrackx was used for the probabilistic tracking with crossing fibers. The extraction of gray matter ROIs was performed using Freesurfer (http://surfer.nmr.mgh.harvard.edu/).

Connectivity matrices

The brain of each subjects was parcellated into 148 regions of interest (ROis) of the Destrieux atlas using Freesurfer to act as node labels. The quality of the parcellation was manually checked for each subject. Node labels were individually treated as seed regions, and the connectivity between ROIs was defined as the number of probabilistic streamlines arriving in one ROI when another ROI was seeded and vice-versa. Seeding and streamline counting was performed in the voxels within the ROI that were in the gray/white matter boundary. We used the default parameters of two fibers per voxel and 5000 sample streamlines for each tract to create a 148 x 148 matrix, P, of probability values. Each matrix entry Pij represents a scaled conditional probability of a pathway between the seed ROI, i, and the target ROI, j, given by Pij =(Si→j/Si) Ri, where Si→j denotes the number of the fibers reaching the target region j from the seed region I and Si is the number of streamlines seeded in i. This measure quantifies connectivity such that Pij ≈ Pji, which, on averaging, gives an undirected weighted connectivity measure. This now creates a 148 x 148 undirected symmetrical weighted connectivity network.

Network properties

Graph network properties of the connectome were computed using integration, segregation and centrality indices. Integration was measured using Global Efficiency and Characteristic Path Length; segregation was measured using Clustering Coefficient, Transitivity, Modularity and Local Efficiency. We also quantified Small-World Index (SWI), a measure of the balance between integration and segregation. The SWI is computed as the ratio between two key metrics: the normalized clustering coefficient and the characteristic path length of the network. The network measures were computed using Graph Analysis Toolbox (GAT) (http://brainlens.org/tools. html) (Hosseini et al., 2012). Significant differences between topological parameters were investigated using a nonparametric permutation test with 1000 repetition. The numerosity of the original groups were maintained in each repetition by randomly reassigning regional data (or residuals) of each participant to one of the two groups, so as to obtain an association matrix for each random group. Then, a range threshold of 0.02 to 0.2 with increments of 0.002 were applied to each random group to estimate the binary adjacency matrices. Topological measurements were calculated for all networks and the full density range were used to compare differences in network measurements. For each iteration, the values of each random group across the range of density were plotted and the differences of the different areas under the obtained curves (AUC) were used in order to compute the topological proprieties. p values were computed by comparing the results from the actual differences in the curve functions and the null distribution of differences. This nonparametric permutation test compared the shapes of the curves derived from multiple threshold points (and so from multiple comparisons) and is based on functional data analysis (FDA) that allowed to overcome limitations driven by the sensitivity of the analysis methodology.

RESULTS

Table 16. shows the main clinical characteristics of experimental and control groups.

	AN (n=38) Mean	SD	HC (n=38) Mean	SD	AN vs. HC *t* (p)
Age (years)	26.1	7.2	25.2	6.7	0.54 (0.59)
Baseline Body mass index (kg/m^2)	16.0	1.8	21.6	3.0	10.51 (<0.001)
Lowest Body mass index (kg/m^2)	14.0	1.8	19.8	2.5	11.56 (<0.001)
Weight loss (kg)	7.1	2.8	3.4	1.7	7.01 (<0.001)
Age of onset (years)	18.3	5.0	-	-	-
Duration of illness (months)	78.6	81.2	-	-	-
Duration of recovery (months)			-	-	-
Edinburgh laterality index	57.1	37.5	55.0	42.0	0.23 (0.82)
Education (years)	14.2	2.2	15.4	2.3	2.44 (0.02)
Drive to thinness	9.9	6.1	2.3	4.2	6.22 (<0.001)
Depression	1.4	0.8	0.7	0.6	4.06 (<0.001)
Trait anxiety	56.6	9.7	39.3	9.6	7.82 (<0.001)

Reduced Small world and clustering properties and their association with clinical variables

Between-group comparisons were performed using difference in areas under the curve (AUC). From a global perspective, patients with AN showed reduced Small-World Index (SWI) (p=0,031) and lower normalized clustering coefficient (p=0,029). Transitivity, which is estimates the relative number of triangles in the graph, compared to total number of connected triples of nodes, shows a tendency towards a reduction in patients with AN (p=0,054). No differences were observed in other network measures between patients with acute AN and HC. Figure 6 reports differences in AUC of characteristic path length, clustering coefficient and small-world index between AN patients and HC.

The SWI positively correlates with the lifetime lowest BMI ($p<0.001$) and with the BMI at the time of the evaluation ($p=0.024$). A regression analysis evidenced a relation between the lowest lifetime BMI and the SWI in patients with AN ($p=0.006$). Normalized clustering coefficient positively correlates with the lifetime lowest BMI ($p=0.027$).

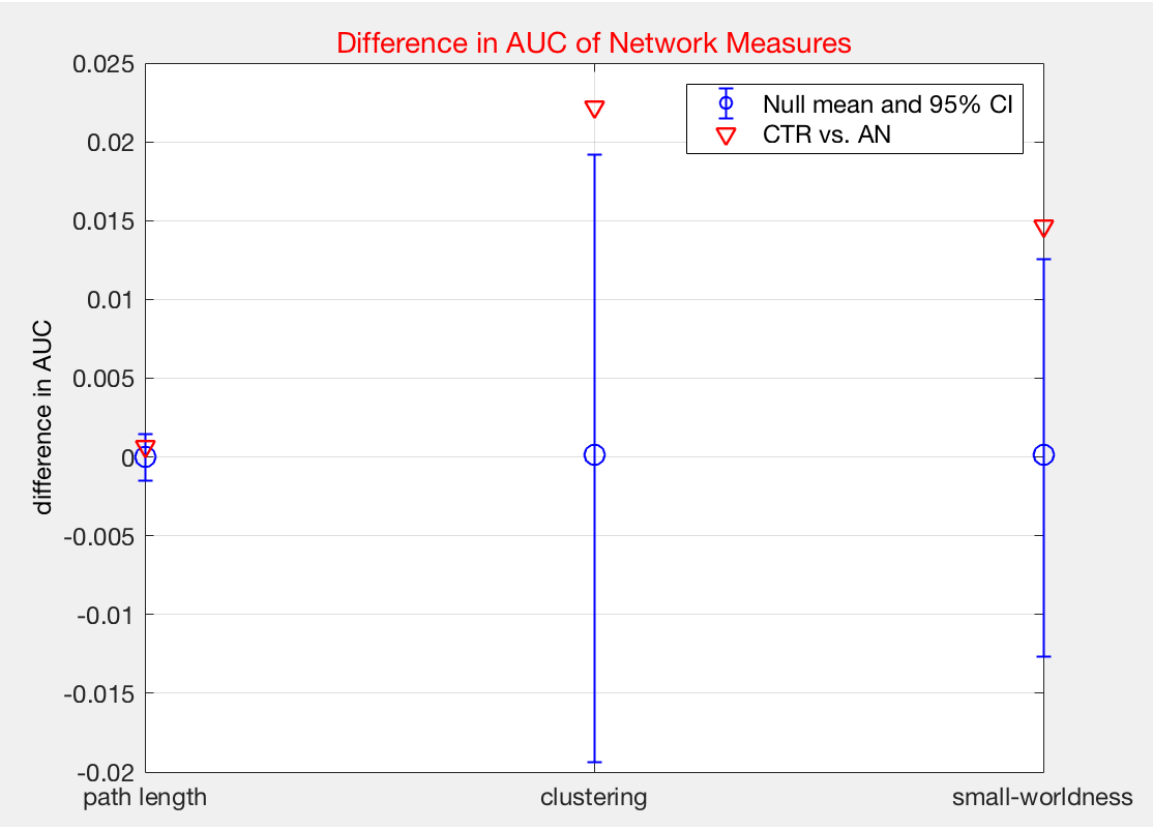

Figure 6. Difference in AUC in characteristic path length, clustering coefficient and small world index between patients with AN and HC.

Differences in regional properties between patients with AN and HC and their association with temperamental and psychopathological scores

From a regional analysis, patients with AN showed a higher clustering coefficient in right anterior cingulate gyrus and a higher betweenness in right fusiform gyrus. In the AN group, the clustering coefficient of the right anterior cingulate gyrus negatively correlates with novelty seeking score, measured by means of TPQ, in the AN group. A regression analysis shows a negative relation between

novelty seeking and the clustering of the right ACC (p=0.021). Moreover, the betweenness of the right fusiform gyrus positively correlates with somatization and depression indices, measured by SCL-90. In HC, the clustering coefficient of the right ACC correlates with the current BMI. Table x and xx report correlations values between network measures and clinical, psychopathological and temperamental variables in the AN group and in the HC one.

Table 17. Correlations analysis between network measures, clinical variables, SCL-90 indices and temperamental characteristics in the AN group

AN		Small-world index		Normalized Clustering coefficient		Anterior Cingulate cortex - Clustering coefficient		Fusiform Gyrus - Betweenness	
		Rho	p	Rho	p	Rho	p	Rho	p
Clinical variables	Lower BMI lifetime	0.568**	<0.001	0.476*	0.003	0.095	0.583	-0.168	0.329
	Current BMI	0.376*	0.024	0.323	0.054	0.089	0.605	-0.156	0.364
	Age	0.105	0.543	-0.005	0.975	0.054	0.752	-0.040	0.819
	Age of onset	-0.044	0.798	-0.223	0.190	0.270	0.110	0.125	0.468
	Illness duration	0.131	0.445	0.075	0.662	-0.054	0.752	-0.127	0.461
SCL-90	SCL-90 tot	0.152	0.375	0.039	0.817	-0.059	0.732	0.317	0.059
	OC	0.067	0.697	-0.058	0.737	-0.001	0.995	0.236	0.165
	IS	0.034	0.843	-0.078	0.651	-0.208	0.223	0.300	0.076
	SOM	0.262	0.123	0.232	0.172	-0.015	0.927	0.428*	0.009
	DEP	0.022	0.898	-0.065	0.705	-0.056	0.746	0.354*	0.033
	ANX	0.076	0.658	0.013	0.937	0.109	0.527	0.168	0.326
	HOS	0.195	0.254	0.056	0.745	-0.149	0.387	0.267	0.115
TPQ	Novelty seeking	0.253	0.136	0.175	0.308	-0.391*	0.018	0.014	0.932
	Harm Avoidance	0.043	0.800	-0.180	0.293	0.023	0.892	-0.047	0.783
	Reward Dependance	0.115	0.505	0.172	0.316	-0.234	0.170	-0.138	0.423

Spearman's Rho. p<0,05.

Table 18. Correlations analysis between network measures, clinical variables, SCL-90 indices and temperamental characteristics in the HC group

HC		Small-world index		Normalized Clustering coefficient		Anterior Cingulate cortex -Clustering coefficient		Fusiform Gyrus - Betweenness	
		Rho	p	Rho	p	Rho	p	Rho	p
Clinical variables	Lower BMI lifetime	0.227	0.190	0.032	0.857	-0.282	0.101	0.090	0.609
	Current BMI	0.105	0.543	0.185	0.279	-0.382*	0.022	0.054	0.754
	Age	-0.126	0.464	0.056	0.744	-0.106	0.538	-0.159	0.354
	Age of onset	-	-	-	-	-	-	-	-
	Illness duration	-	-	-	-	-	-	-	-
SCL-90	SCL-90 tot	0.024	0.955	0.168	0.691	-0.467	0.243	0.228	0.588
	OC	0.008	0.965	0.035	0.845	-0.066	0.712	0.222	0.207
	IS	0.103	0.651	0.172	0.330	0.038	0.833	0.105	0.553
	SOM	0.181	0.305	0.291	0.095	-0.094	0.596	0.025	0.888
	DEP	-0.225	0.200	-0.173	0.328	-0.129	0.467	0.138	0.436
	ANX	0.025	0.888	0.077	0.664	-0.049	0.784	0.152	0.391
	HOS	0.182	0.319	0.258	0.154	0.029	0.876	0.215	0.236
TPQ	Novelty seeking	0.210	0.218	0.209	0.221	-0.182	0.289	-0.166	0.333
	Harm Avoidance	-0.219	0.199	0.013	0.939	-0.147	0.393	-0.175	0.308
	Reward Dependance	-0.090	0.601	0.063	0.715	-0.156	0.354	-0.123	0.476

Spearman's Rho. p<0,05

Altered nodal centrality in AN

Alterations in nodal centrality were identified by analyzing the hub distribution. Hubs were computed both on degree and on betweenness values. Based on degree, we identified an identical hub distribution between AN group and HC, except for the Right Superior Frontal Gyrus, that is lacking in the experimental group. Hubs distribution based on nodes degree is reported in table 17.

Based on betweenness, we identified the same hubs in the two groups, except for the Left Superior parietal lobule and the Right Superior Occipital Gyrus. These two hubs are characterized by a high

betweenness in HC but not in patients with AN. Hubs distribution based on nodes betweenness is reported in table 17.

Table 17. Nodes with higher degree between AN patients and HC

NET HUB DEGREE (AN)	NET HUB DEGREE (HC)
Left Pericallosal Sulcus	Left Superior frontal gyrus
Left Putamen	Left Pericallosal sulcus
Left Thalamus	Left Putamen
Right Superior Frontal Gyrus	Left Thalamus
Right Pericallosal Sulcus	Right Superior frontal gyrus
Right Putamen	Right Pericallosal Sulcus
	Right Putamen

Table 18. Nodes with higher betweenness between AN patients and HC

NET HUB BETWEENNESS (AN)	NET HUB BETWEENNESS (HC)
Left Superior Frontal Gyrus	Left Superior frontal gyrus
Left Pericallosal Sulcus	Left Superior parietal lobule
Left Putamen	Left Pericallosal sulcus
Left Thalamus	Left Putamen
Right Superior Frontal Gyrus	Left Thalamus
Right Pericallosal sulcus	Right Superior frontal gyrus
Right Putamen	Right Superior occipital gyrus
	Right Pericallosal sulcus
	Right Putamen

DISCUSSION

For our knowledge, the present is the first paper that evaluate the WM architecture in patients with acute AN by means of connectomic tools. On a global level, our results evidence the presence of reduced small-world properties in AN, which are probably driven by a reduction in the clusterization of the network. A reduction in the segregation characteristics of the connectome does not seem to reflect in an increase of integration, since no integration measures show differences between AN patients and HC.

Clustering coefficient indicates the tendency of a network to be composed by densely connected and functionally coherent neuronal units. Higher levels of clustering contribute in increasing the regularity of a network, while lower levels of segregation result in a shift toward more random configurations (Rubinov & Sporns, 2010). SWI specifically quantify the balance between order and randomness of a network: lower levels of SWI indicates higher levels of randomness, while higher SWI values indicate higher regularity (Danielle Smith Bassett & Bullmore, 2006c).

Overall, the studies that evaluated how DTI networks change during development observed a reduction in segregation properties along maturational stages, but an increase of clustering coefficient with age has also been highlighted (Wierenga et al., 2016). Therefore, it is difficult to understand if the altered balance between integration and segregation in AN could be due to deviations in normal developmental trajectories or to alterations in already established network properties.

Interestingly, malnutrition seems to have a specific impact on the overall WM structure. In fact, the lowest lifetime BMI and the current BMI have shown to positively correlate with the small-world properties of the network, and the lowest lifetime BMI was also evidenced to positively correlate with the clustering coefficient in the AN group. These results suggest that malnutrition could negatively impact on the trade-off between integration and segregation characteristic in the WM structural connectome by reducing its regularity.

Regional results highlight increased segregation characteristics in two specific brain areas: the right anterior gyrus, which displays a higher clustering coefficient, and the right fusiform gyrus, which shows higher betweenness values. The clustering coefficient of a node quantifies the density of connections between the node's neighbors, while betweenness measures the fraction of all the network shortest paths that pass through a specific node (Sporns, 2010). The anterior cingulate cortex (ACC) is crucially involved in several self-referential and self-regulation processes (Carter et al., 1998). Anatomically, it connects with different cortical, limbic and paralimbic regions (Margulies et al., 2007). In AN, ACC was shown to be involved in the cognitive control of appetite, in perfectionism, in body image distortion, in cognitive inflexibility and in elevated performance monitoring (Bischoff-Grethe et al., 2013; Boehm et al., 2014; Friederich et al., 2010; Kaye et al., 2009; Lee et al., 2014b; Geisler et al., 2017). From a structural point of view, Bär and colleagues recently observed that reductions in cortical volume and thickness in the frontoparietal-cingulate network correlated both with symptoms severity and illness duration (Bär et al., 2015). The increased clustering properties of the ACC in the AN group suggests that the functional alterations of this area may be, at least partially, sustained by its structural segregation. On the other hand, the increased clusterization of ACC may lead to an increase in its centrality, which can in turn explain the relevance that this region has demonstrated in the psychopathology and in the cognitive functioning of AN. The negative correlation between ACC clusterization and novelty seeking in patients with AN suggests that a higher structural centrality of this regions could represent the structural basis for a reduced tendency of AN patients to explore unfamiliar stimuli and environments (Fassino et al., 2002).

The fusiform gyrus (FG) is highly involved in the recognition of bodies and faces and in the processing of emotions (Kawasaki et al., 2012; Schwarzlose, 2005). Interestingly, FG was observed to be peculiarly involved in integrating images of faces and bodies into an image of a person, while occipital areas are more involved in a separate categorization of these two elements (Bernstein, Oron, Sadeh, & Yovel, 2014). In AN, FG was evidenced to show higher levels of functional activation during the early

processing of happy facial expressions, suggesting a role in the implicit processing of emotions (Fonville, Giampietro, Surguladze, Williams, & Tchanturia, 2014). The higher structural centrality of FG could represent a structural substrate for the increased functional recruitment of this area during specific cognitive processes in AN, but may also lead to a reduction of its global integration. The positive correlation between FG betweenness and depression and somatization indices in patients with AN suggests that a higher centrality of this region could mediate for a more severe psychopathology in the disorder.

The architecture of the most central and influential nodes shows some differences between the experimental group and the HC one. Hubs constitute the architectural backbone of the neural network and facilitate the structural and functional integration of the connectome (Roberts et al., 2018). Several studies reported differences in the distribution of hubs in different psychiatric disorders (Rubinov & Bullmore, 2013; Wu et al., 2016), but no research analyzed the hubs distribution in AN to date. We identified the WM hubs separately in AN patients and in HC using two centrality measures: degree and betweenness. The degree of a node estimates the number of connections of that node. Nodes with a high degree manage more connections and are likely to influence many other network nodes. The betweenness centrality of an individual node indicates the fraction of all shortest paths in the network that pass through the node. The nodes with a higher betweenness are in the intersection of many short paths and, by virtue of this, are particularly able to control the flow of information within the network (Danielle S Bassett & Sporns, 2017).

The observed reduction of hubs in AN could indicate a structural weakness of the connectome. Since betweenness is a measure of the local influence of a node, the lack of two hubs with high betweenness in patients with AN suggests an impaired local information processing in the disorder and is also consistent with the observation of a more randomic and less locally organized WM architecture in the experimental group. Interestingly, Superior occipital gyrus and superior parietal gyrus, together with

precuneus, were observed to display the highest levels of betweenness centrality in a recent WM connectome analysis (Kwon, Choi, Seo, & Lee, 2017).

Since the highest central and connected nodes have high rates of glucose consumption and of cerebral blood flow, they are particularly vulnerable to several metabolic and pathogenic processes affecting the brain (Fornito et al., 2017). Therefore, in AN, the loss of two hubs with high centrality properties may reflect a pathological adaptation of the network to the effects of malnutrition and starvation. Nodes with a higher degree show a slightly different distribution in the two groups. In particular, the Left Superior Frontal Gyrus is lacking in the AN group. This area was showed to be peculiarly involved in those Working Memory functions that require a high level of executive processing (Du Boisgueheneuc et al., 2006) and therefore, its lower centrality in the overall DTI network may contribute to the executive impairments observed in AN.

The present study has both strengths and limitations, that need to be taken into consideration when interpreting its results. It is the first study to analyze the WM connective architecture using graph theory tools in patients with acute AN and to describe the relationships between connectomic indices and clinical, temperamental and psychopathological measures. However, the cross-sectional nature of our observations does not allow us to understand whether the observed alterations precede the onset of AN or represents a consequence of the disorder.

In conclusion, the present study evidenced the presence of a less regular organization of the overall WM network in patients with acute AN. Moreover, AN patients displayed regional differences in areas that are involved in different psychopathological and temperamental dimensions. The shift toward a more randomic configuration of the network in AN could be partially determined by the loss of some of the most integrative and influential hubs in the brain, that are located in prefrontal, parietal and occipital regions.

REFERENCES

Agarwal, V., Kumar, M., Singh, J. K., Rathore, R. K. S., Misra, R., & Gupta, R. K. (2009). Diffusion tensor anisotropy magnetic resonance imaging: A new tool to assess synovial inflammation. *Rheumatology*, *48*(4), 378–382. https://doi.org/10.1093/rheumatology/ken499

Alexander-Bloch, A., Giedd, J. N., & Bullmore, E. (2013). Imaging structural co-variance between human brain regions. *Nature Reviews Neuroscience*. https://doi.org/10.1038/nrn3465

Alexander-Bloch, A., Raznahan, A., Bullmore, E., & Giedd, J. (2013). The convergence of maturational change and structural covariance in human cortical networks. *The Journal of Neuroscience : The Official Journal of the Society for Neuroscience*, *33*(7), 2889–99. https://doi.org/10.1523/JNEUROSCI.3554-12.2013

American Psychiatric Association. (2013). *Diagnostic and Statistical Manual of Mental Disorders*. American Psychiatric Association. https://doi.org/10.1176/appi.books.9780890425596

Arcelus, J., Mitchell, A. J., Wales, J., & Nielsen, S. (2011). Mortality rates in patients with anorexia nervosa and other eating disorders: A meta-analysis of 36 studies. *Archives of General Psychiatry*, *68*(7), 724–731. https://doi.org/10.1001/archgenpsychiatry.2011.74

Armstrong, E., Schleicher, A., Omran, H., Curtis, M., & Zilles, K. (1995). The ontogeny of human gyrification. *Cerebral Cortex*, *5*(1), 56–63. https://doi.org/10.1093/cercor/5.1.56

Ashburner, J., & Friston, K. J. (2000). Voxel-Based Morphometry—The Methods. *NeuroImage*, *11*(6), 805–821. https://doi.org/10.1006/nimg.2000.0582

Bär, K.-J., de la Cruz, F., Berger, S., Schultz, C. C., & Wagner, G. (2015). Structural and functional differences in the cingulate cortex relate to disease severity in anorexia nervosa. *Journal of Psychiatry & Neuroscience : JPN*, *40*(4), 269–79. https://doi.org/10.1503/jpn.140193

Bassett, D. S., & Bullmore, E. (2006). Small-World Brain Networks. *The Neuroscientist*, *12*(6), 512–523. https://doi.org/10.1177/1073858406293182

Bassett, D. S., & Sporns, O. (2017). Network neuroscience. *Nature Neuroscience*, *20*(3), 353–364. https://doi.org/10.1038/nn.4502

Benoit B. Mandelbrot. (1983). The fractal geometry of nature. Benoit B. Mandelbrot. W. H. Freeman and co., San Francisco, 1982. No. of pages: 460. Price: £22.75 (hardback). *Earth Surface Processes and Landforms*, *8*(4), 406–406. https://doi.org/10.1002/esp.3290080415

Bernardoni, F., King, J. A., Geisler, D., Birkenstock, J., Tam, F. I., Weidner, K., … Ehrlich, S. (2018). Nutritional status affects cortical folding: Lessons learned from anorexia nervosa. *Biological Psychiatry*. https://doi.org/10.1016/J.BIOPSYCH.2018.05.008

Bernardoni, F., King, J. A., Geisler, D., Stein, E., Jaite, C., Nätsch, D., … Ehrlich, S. (2016). Weight restoration therapy rapidly reverses cortical thinning in anorexia nervosa: A longitudinal study. *NeuroImage*, *130*, 214–222. https://doi.org/10.1016/j.neuroimage.2016.02.003

Bernstein, M., Oron, J., Sadeh, B., & Yovel, G. (2014). An Integrated Face-Body Representation in the Fusiform Gyrus but Not the Lateral Occipital Cortex. https://doi.org/10.1162/jocn_a_00639

Bischoff-Grethe, A., McCurdy, D., Grenesko-Stevens, E., Irvine, L. E., Wagner, A., Wendy Yau, W.-Y., … Kaye, W. H. (2013). Altered brain response to reward and punishment in adolescents with Anorexia nervosa. *Psychiatry Research: Neuroimaging*, 1–10. https://doi.org/10.1016/j.pscychresns.2013.07.004

Boccaletti, S., Latora, V., Moreno, Y., Chavez, M., & Hwang, D. U. (2006). Complex networks: Structure and dynamics. *Physics Reports*. https://doi.org/10.1016/j.physrep.2005.10.009

Boehm, I., Geisler, D., King, J. A., Ritschel, F., Seidel, M., Araujo, Y. D., … Frank, G. (2014). Increased resting state functional connectivity in the fronto-parietal and default mode network in anorexia nervosa. https://doi.org/10.3389/fnbeh.2014.00346

Boehm, I., Geisler, D., Tam, F., King, J. A., Ritschel, F., Seidel, M., … Ehrlich, S. (2016). Partially restored resting-state functional connectivity in women recovered from anorexia nervosa. *J Psychiatry Neurosci*, *41*(6). https://doi.org/10.1503/jpn.150259

Brockmeyer, T., Holtforth, M. G., Bents, H., Kämmerer, A., Herzog, W., & Friederich, H. C. (2012). Starvation and emotion regulation in anorexia nervosa. *Comprehensive Psychiatry*, *53*(5), 496–501. https://doi.org/10.1016/j.comppsych.2011.09.003

Buchy, L., Barbato, M., Makowski, C., Bray, S., MacMaster, F. P., Deighton, S., & Addington, J. (2017). Mapping structural covariance networks of facial emotion recognition in early psychosis: A pilot study. *Schizophrenia Research*, *189*, 146–152. https://doi.org/10.1016/j.schres.2017.01.054

Bulik, C. M., Thornton, L., Pinheiro, A. P., Plotnicov, K., Klump, K. L., Brandt, H., … Kaye, W. H. (2008). Suicide Attempts in Anorexia Nervosa. *Psychosomatic Medicine*, *70*(3), 378–383. https://doi.org/10.1097/PSY.0b013e3181646765

Bullmore, E., & Sporns, O. (2009). Complex brain networks: graph theoretical analysis of structural and functional systems. *Nature Publishing Group*, *10*(3), 186–198. https://doi.org/10.1038/nrn2575

Bullmore, E., & Sporns, O. (2012, May 13). The economy of brain network organization. *Nature Reviews Neuroscience*. https://doi.org/10.1038/nrn3214

Burgoyne, R. D., Graham, M. E., & Cambray-Deakin, M. (1993). Neurotrophic effects of NMDA receptor activation on developing cerebellar granule cells. *Journal of Neurocytology*, *22*(9), 689–695. https://doi.org/10.1007/BF01181314

Cao, M., Huang, H., Peng, Y., Dong, Q., & He, Y. (2016). Toward Developmental Connectomics of the Human Brain. *Frontiers in Neuroanatomy*, *10*, 25. https://doi.org/10.3389/fnana.2016.00025

Cao, M., Wang, J. H., Dai, Z. J., Cao, X. Y., Jiang, L. L., Fan, F. M., … He, Y. (2014). Topological organization of the human brain functional connectome across the lifespan. *Developmental Cognitive Neuroscience*, *7*, 76–93. https://doi.org/10.1016/j.dcn.2013.11.004

Carter, C. S., Braver, T. S., Barch, T. S., Botvinick, M. M., Noll, D., & Cohen, J. D. (1998). Anterior cingulate cortex, error detection, and the online monitoring of performance. *Science*, *280*(May), 747–749.

Cha, J., Ide, J. S., Bowman, F. D., Simpson, H. B., Posner, J., & Steinglass, J. E. (2016). Abnormal reward circuitry in anorexia nervosa: A longitudinal, multimodal MRI study. *Human Brain Mapping*, *37*(11), 3835–3846. https://doi.org/10.1002/hbm.23279

Chen, Z., Deng, W., Gong, Q., Huang, C., Jiang, L., Li, M., … Li, T. (2014). Extensive brain structural network abnormality in first-episode treatment-naive patients with schizophrenia: Morphometrical and covariation study. *Psychological Medicine*, *44*(12), 2489–2501. https://doi.org/10.1017/S003329171300319X

Cloninger, C. R., Przybeck, T. R., & Svrakic, D. M. (1991). The Tridimensional Personality Questionnaire: U.S. Normative Data. *Psychological Reports*, *69*(3), 1047–1057. https://doi.org/10.2466/pr0.1991.69.3.1047

Collantoni, E., Michelon, S., Tenconi, E., Degortes, D., Titton, F., Manara, R., … Favaro, A. (2016). Functional connectivity correlates of response inhibition impairment in anorexia nervosa. *Psychiatry Research - Neuroimaging*, *247*. https://doi.org/10.1016/j.pscychresns.2015.11.008

Collin, G., de Reus, M. A., Cahn, W., Hulshoff Pol, H. E., Kahn, R. S., & van den Heuvel, M. P. (2013). Disturbed grey matter coupling in schizophrenia. *European Neuropsychopharmacology*, *23*(1), 46–54. https://doi.org/10.1016/j.euroneuro.2012.09.001

Collin, G., & Van Den Heuvel, M. P. (2013). The ontogeny of the human connectome: Development and dynamic changes of brain connectivity across the life span. *Neuroscientist*, *19*(6), 616–628. https://doi.org/10.1177/1073858413503712

Connan, F., Campbell, I. C., Katzman, M., Lightman, S. L., & Treasure, J. (2003). A neurodevelopmental model for anorexia nervosa. *Physiology & Behavior*, *79*(1), 13–24. Retrieved from http://www.ncbi.nlm.nih.gov/pubmed/12818706

Cook, M. J., Free, S. L., Manford, M. R. A., Fish, D. R., Shorvon, S. D., & Stevens, J. M. (1995). Fractal Description of Cerebral Cortical Patterns in Frontal Lobe Epilepsy. *European Neurology*, *35*(6), 327–335. https://doi.org/10.1159/000117155

Craig, A. D. (2009, January 1). How do you feel - now? The anterior insula and human awareness. *Nature Reviews Neuroscience*. Nature Publishing Group. https://doi.org/10.1038/nrn2555

Crossley, N. A., Mechelli, A., Ginestet, C., Rubinov, M., Bullmore, E. T., & Mcguire, P. (2016). Altered hub functioning and compensatory activations in the connectome: A meta- Analysis of functional neuroimaging studies in schizophrenia. *Schizophrenia Bulletin*, *42*(2), 434–442. https://doi.org/10.1093/schbul/sbv146

Crossley, N. A., Mechelli, A., Scott, J., Carletti, F., Fox, P. T., McGuire, P., & Bullmore, E. T. (2014). The hubs of the human connectome are generally implicated in the anatomy of brain disorders. *Brain : A Journal of Neurology*, *137*(Pt 8), 2382–95. https://doi.org/10.1093/brain/awu132

Damoiseaux, J. S., Rombouts, S. A. R. B., Barkhof, F., Scheltens, P., Stam, C. J., Smith, S. M., & Beckmann, C. F. (2006). Consistent resting-state networks across healthy subjects. *Proceedings of the National Academy of Sciences of the United States of America*, *103*(37), 13848–53. https://doi.org/10.1073/pnas.0601417103

Dauguet, J., Peled, S., Berezovskii, V., Delzescaux, T., Warfield, S. K., Born, R., & Westin, C. F. (2007). Comparison of fiber tracts derived from in-vivo DTI tractography with 3D histological neural tract tracer reconstruction on a macaque brain. *NeuroImage*, *37*(2), 530–538. https://doi.org/10.1016/j.neuroimage.2007.04.067

DeFelipe, J. (2006, October). Brain plasticity and mental processes: Cajal again. *Nature Reviews Neuroscience*. https://doi.org/10.1038/nrn2005

Dennis, E. L., Jahanshad, N., McMahon, K. L., de Zubicaray, G. I., Martin, N. G., Hickie, I. B., … Thompson, P. M. (2013). Development of brain structural connectivity between ages 12 and 30: A 4-Tesla diffusion imaging study in 439 adolescents and adults. *NeuroImage*, *64*(1), 161–684. https://doi.org/10.1016/j.neuroimage.2012.09.004

Derogatis, L. R., Lipman, R. S., Rickels, K., Uhlenhuth, E. H., & Covi, L. (1974). The Hopkins Symptom Checklist (HSCL): A Self Report Symptom Inventory. *Behavioral Science*, *19*(1), 1–15. https://doi.org/10.1002/bs.3830190102

Descoteaux, M., Deriche, R., Knösche, T. R., & Anwander, A. (2009). Deterministic and probabilistic tractography based on complex fibre orientation distributions. *IEEE Transactions on Medical Imaging*, *28*(2), 269–286. https://doi.org/10.1109/TMI.2008.2004424

Destrieux, C., Fischl, B., Dale, A., & Halgren, E. (2010). Automatic parcellation of human cortical gyri and sulci using standard anatomical nomenclature. *NeuroImage*, *53*(1), 1–15. https://doi.org/10.1016/j.neuroimage.2010.06.010

Di Ieva, A. (2016). *The Fractal Geometry of the Brain: An Overview*. *The Fractal Geometry of the Brain*. https://doi.org/10.1007/978-1-4939-3995-4

DiMartino, A., Fair, D. A., Kelly, C., Satterthwaite, T. D., Castellanos, F. X., Thomason, M. E., … Milham, M. P. (2014, September 17). Unraveling the miswired connectome: A developmental perspective. *Neuron*. https://doi.org/10.1016/j.neuron.2014.08.050

Dong, Q., Welsh, R. C., Chenevert, T. L., Carlos, R. C., Maly-Sundgren, P., Gomez-Hassan, D. M., & Mukherji, S. K. (2004, January). Clinical Applications of Diffusion Tensor Imaging. *Journal of Magnetic Resonance Imaging*. https://doi.org/10.1002/jmri.10424

Du Boisgueheneuc, F., Levy, R., Volle, E., Seassau, M., Duffau, H., Kinkingnehun, S., … Dubois, B.

(2006). Functions of the left superior frontal gyrus in humans: a lesion study. *Brain*, *129*, 3315–3328. https://doi.org/10.1093/brain/awl244

Ehrlich, S., Geisler, D., Ritschel, F., King, J. A., Seidel, M., Boehm, I., … Kroemer, N. B. (2015). Elevated cognitive control over reward processing in recovered female patients with anorexia nervosa. *J Psychiatry Neurosci*, *40*(5). https://doi.org/10.1503/jpn.140249

Fair, D. A., Dosenbach, N. U. F., Church, J. A., Cohen, A. L., Brahmbhatt, S., Miezin, F. M., … Schlaggar, B. L. (2007). Development of distinct control networks through segregation and integration. *Proceedings of the National Academy of Sciences*, *104*(33), 13507–13512. https://doi.org/10.1073/pnas.0705843104

Fassino, S., Abbate-Daga, G., Amianto, F., Leombruni, P., Boggio, S., & Rovera, G. G. (2002). Temperament and character profile of eating disorders: A controlled study with the temperament and character inventory. *International Journal of Eating Disorders*, *32*(4), 412–425. https://doi.org/10.1002/eat.10099

Favaro, A. (2013, July 1). Brain development and neurocircuit modeling are the interface between genetic/environmental risk factors and eating disorders. A commentary on keel & forney and friederich et al. *International Journal of Eating Disorders*. Wiley-Blackwell. https://doi.org/10.1002/eat.22131

Favaro, A., Caregaro, L., Tenconi, E., Bosello, R., & Santonastaso, P. (2009). Time trends in age at onset of anorexia nervosa and bulimia nervosa. *Journal of Clinical Psychiatry*, *70*(12), 1715–1721. https://doi.org/10.4088/JCP.09m05176blu

Favaro, A., Clementi, M., Manara, R., Bosello, R., Forzan, M., Bruson, A., … Santonastaso, P. (2013). Catechol-O-methyltransferase genotype modifies executive functioning and prefrontal functional connectivity in women with anorexia nervosa. *Journal of Psychiatry and Neuroscience*, *38*(4), 241–248. https://doi.org/10.1503/jpn.120068

Favaro, A., Santonastaso, P., Manara, R., Bosello, R., Bommarito, G., Tenconi, E., & Di Salle, F. (2012). Disruption of visuospatial and somatosensory functional connectivity in anorexia nervosa. *Biological Psychiatry*, *72*(10), 864–870. https://doi.org/10.1016/j.biopsych.2012.04.025

Favaro, A., Tenconi, E., Degortes, D., Manara, R., & Santonastaso, P. (2015). Gyrification brain abnormalities as predictors of outcome in anorexia nervosa. *Human Brain Mapping*, *36*(12), 5113–5122. https://doi.org/10.1002/hbm.22998

Favaro, A., Tenconi, E., & Santonastaso, P. (2006). Perinatal factors and the risk of developing anorexia nervosa and bulimia nervosa. *Arch Gen Psychiatry*, *63*(1), 82–88. https://doi.org/63/1/82 [pii]\r10.1001/archpsyc.63.1.82

Fernandez-Aranda, F., Pinheiro, A. P., Tozzi, F., La Via, M., Thornton, L., Plotnicov, K., … Bulik, C. (2007). Symptom profile of major depressive disorder in women with eating disorders. *Australian and New Zealand Journal of Psychiatry*, *41*(1), 24–31. https://doi.org/10.1080/00048670601057718

Fischl, B., & Dale, A. M. (2000). Measuring the thickness of the human cerebral cortex from magnetic resonance images. *Proceedings of the National Academy of Sciences*, *97*(20), 11050–11055. https://doi.org/10.1073/pnas.200033797

Fischl, B., Sereno, M. I., & Dale, A. M. (1999, February). Cortical surface-based analysis: II. Inflation, flattening, and a surface-based coordinate system. *NeuroImage*. https://doi.org/10.1006/nimg.1998.0396

Fonville, L., Giampietro, V., Surguladze, S., Williams, S., & Tchanturia, K. (2014). Increased BOLD signal in the fusiform gyrus during implicit emotion processing in anorexia nervosa. *NeuroImage: Clinical*, *4*, 266–273. https://doi.org/10.1016/j.nicl.2013.12.002

Fornito, A., & Bullmore, E. T. (2015). Connectomics: A new paradigm for understanding brain disease. *European Neuropsychopharmacology*, *25*(5), 733–748. https://doi.org/10.1016/j.euroneuro.2014.02.011

Fornito, A., Bullmore, E. T., & Zalesky, A. (2017). Opportunities and Challenges for Psychiatry in the Connectomic Era. *Biological Psychiatry: Cognitive Neuroscience and Neuroimaging*. https://doi.org/10.1016/j.bpsc.2016.08.003

Fornito, A., Zalesky, A., & Breakspear, M. (2015). The connectomics of brain disorders. *Nature Reviews Neuroscience*, *16*(3), 159–172. https://doi.org/10.1038/nrn3901

Fox, M. D., Snyder, A. Z., Vincent, J. L., Corbetta, M., Van Essen, D. C., & Raichle, M. E. (2005). From

The Cover: The human brain is intrinsically organized into dynamic, anticorrelated functional networks. *Proceedings of the National Academy of Sciences*, *102*(27), 9673–9678. https://doi.org/10.1073/pnas.0504136102

Frank, G. K. W. (2014). Advances from neuroimaging studies in eating disorders. *CNS Spectrums*. https://doi.org/10.1017/S1092852915000012

Frank, G. K. W., Favaro, A., Marsh, R., Ehrlich, S., & Lawson, E. A. (2018). Toward valid and reliable brain imaging results in eating disorders. *International Journal of Eating Disorders*, *51*(3), 250–261. https://doi.org/10.1002/eat.22829

Frank, G. K. W., Shott, M. E., Hagman, J. O., & Yang, T. T. (2013). Localized brain volume and white matter integrity alterations in adolescent anorexia nervosa. *Journal of the American Academy of Child and Adolescent Psychiatry*, *52*(10), 1066–1075.e5. https://doi.org/10.1016/j.jaac.2013.07.007

Frank, G. K. W., Shott, M. E., Riederer, J., & Pryor, T. L. (2016). Altered structural and effective connectivity in anorexia and bulimia nervosa in circuits that regulate energy and reward homeostasis. *Translational Psychiatry*, *6*(11), e932. https://doi.org/10.1038/tp.2016.199

Franko, D. L., & Keel, P. K. (2006). Suicidality in eating disorders: Occurrence, correlates, and clinical implications. *Clinical Psychology Review*, *26*(6), 769–782. https://doi.org/10.1016/j.cpr.2006.04.001

Fransson, P., Åden, U., Blennow, M., & Lagercrantz, H. (2011). The functional architecture of the infant brain as revealed by resting-state fMRI. *Cerebral Cortex*, *21*(1), 145–154. https://doi.org/10.1093/cercor/bhq071

Friederich, H.-C., Brooks, S., Uher, R., Campbell, I. C., Giampietro, V., Brammer, M., … Treasure, J. (2010). Neural correlates of body dissatisfaction in anorexia nervosa. *Neuropsychologia*, *48*(10), 2878–2885. https://doi.org/10.1016/J.NEUROPSYCHOLOGIA.2010.04.036

Fröhlich, F. (2016). *Network neuroscience*. *Elsevier*. https://doi.org/10.1038/nn.4502

Fuglset, T. S., Endestad, T., Hilland, E., Bang, L., Tamnes, C. K., Landrï¿½, N. I., & Rï¿½, Ï. (2016). Brain volumes and regional cortical thickness in young females with anorexia nervosa. *BMC Psychiatry*, *16*(1), 404. https://doi.org/10.1186/s12888-016-1126-9

Fujisawa, T. X., Yatsuga, C., Mabe, H., Yamada, E., Masuda, M., & Tomoda, A. (2015). Anorexia nervosa during adolescence is associated with decreased gray matter volume in the inferior frontal gyrus. *PLoS ONE*, *10*(6), e0128548. https://doi.org/10.1371/journal.pone.0128548

Gao, W., Alcauter, S., Elton, A., Hernandez-Castillo, C. R., Smith, J. K., Ramirez, J., & Lin, W. (2015). Functional network development during the first year: Relative sequence and socioeconomic correlations. *Cerebral Cortex*, *25*(9), 2919–2928. https://doi.org/10.1093/cercor/bhu088

Gao, W., Alcauter, S., Smith, J. K., Gilmore, J. H., & Lin, W. (2015). Development of human brain cortical network architecture during infancy. *Brain Structure and Function*, *220*(2), 1173–1186.

https://doi.org/10.1007/s00429-014-0710-3

Garner, D. M., Olmstead, M. P., & Polivy, J. (1983). Development and validation of a multidimensional eating disorder inventory for anorexia nervosa and bulimia. *International Journal of Eating Disorders*, *2*(2), 15–34. https://doi.org/10.1002/1098-108X(198321)2:2<15::AID-EAT2260020203>3.0.CO;2-6

Gaudio, S., Quattrocchi, C. C., Piervincenzi, C., Zobel, B. B., Montecchi, F. R., Dakanalis, A., … Carducci, F. (2017). White matter abnormalities in treatment-naive adolescents at the earliest stages of Anorexia Nervosa: A diffusion tensor imaging study. *Psychiatry Research - Neuroimaging*, *266*, 138–145. https://doi.org/10.1016/j.pscychresns.2017.06.011

Geisler, D., Borchardt, V., Lord, A. R., Boehm, I., Ritschel, F., Zwipp, J., … Ehrlich, S. (2016). Abnormal functional global and local brain connectivity in female patients with anorexia nervosa. *Journal of Psychiatry & Neuroscience*, *41*(1), 6–15. https://doi.org/10.1503/jpn.140310

Geisler, D., Ritschel, F., King, J. A., Bernardoni, F., Seidel, M., Boehm, I., … Ehrlich, S. (2017). Increased anterior cingulate cortex response precedes behavioural adaptation in anorexia nervosa. *Scientific Reports*, *7*(August 2016), 1–10. https://doi.org/10.1038/srep42066

Gong, G., He, Y., Chen, Z. J., & Evans, A. C. (2012). Convergence and divergence of thickness correlations with diffusion connections across the human cerebral cortex. *NeuroImage*, *59*(2), 1239–1248. https://doi.org/10.1016/j.neuroimage.2011.08.017

Greene, D. J., Laumann, T. O., Dubis, J. W., Ihnen, S. K., Neta, M., Power, J. D., … Schlaggar, B. L. (2014). Developmental Changes in the Organization of Functional Connections between the Basal Ganglia and Cerebral Cortex. *Journal of Neuroscience*, *34*(17), 5842–5854. https://doi.org/10.1523/JNEUROSCI.3069-13.2014

Griffiths, K. R., Grieve, S. M., Kohn, M. R., Clarke, S., Williams, L. M., & Korgaonkar, M. S. (2016). Altered gray matter organization in children and adolescents with ADHD: a structural covariance connectome study. *Translational Psychiatry*, *6*(11), e947. https://doi.org/10.1038/tp.2016.219

Guo, S., Iwabuchi, S., Balain, V., Feng, J., Liddle, P., & Palaniyappan, L. (2015). Cortical folding and the potential for prognostic neuroimaging in schizophrenia. *British Journal of Psychiatry*, *207*(5), 458–459. https://doi.org/10.1192/bjp.bp.114.155796

Ha, T. H., Yoon, U., Lee, K. J., Shin, Y. W., Lee, J.-M., Kim, I. Y., … Kwon, J. S. (2005). Fractal dimension of cerebral cortical surface in schizophrenia and obsessive–compulsive disorder. *Neuroscience Letters*, *384*, 172–176. https://doi.org/10.1016/j.neulet.2005.04.078

Hagmann, P., Kurant, M., Gigandet, X., Thiran, P., Wedeen, V. J., Meuli, R., & Thiran, J. P. (2007). Mapping human whole-brain structural networks with diffusion MRI. *PLoS ONE*, *2*(7). https://doi.org/10.1371/journal.pone.0000597

Hagmann, P., Sporns, O., Madan, N., Cammoun, L., Pienaar, R., Wedeen, V. J., … Grant, P. E. (2010). White matter maturation reshapes structural connectivity in the late developing human brain.

Proceedings of the National Academy of Sciences, *107*(44), 19067–19072. https://doi.org/10.1073/pnas.1009073107

Halmi, K. A., Sunday, S. R., Klump, K. L., Strober, M., Leckman, J. F., Fichter, M., … Kaye, W. H. (2003). Obsessions and compulsions in anorexia nervosa subtypes. *International Journal of Eating Disorders*, *33*(3), 308–319. https://doi.org/10.1002/eat.10138

Hensch, T. K. (2004a). CRITICAL PERIOD REGULATION. *Annual Review of Neuroscience*, *27*(1), 549–579. https://doi.org/10.1146/annurev.neuro.27.070203.144327

Hofman, M. A. (1991). The fractal geometry of convoluted brains. *Journal Fur Hirnforschung*, *32*(1), 103–11. Retrieved from http://www.ncbi.nlm.nih.gov/pubmed/1811015

Hong, S. B., Zalesky, A., Fornito, A., Park, S., Yang, Y. H., Park, M. H., … Kim, J. W. (2014). Connectomic disturbances in attention-deficit/hyperactivity disorder: A whole-brain tractography analysis. *Biological Psychiatry*, *76*(8), 656–663. https://doi.org/10.1016/j.biopsych.2013.12.013

Hosseini, S. M. H., Hoeft, F., & Kesler, S. R. (2012). Gat: A graph-theoretical analysis toolbox for analyzing between-group differences in large-scale structural and functional brain networks. *PLoS ONE*, *7*(7), e40709. https://doi.org/10.1371/journal.pone.0040709

Hyde, K. L., Lerch, J., Norton, A., Forgeard, M., Winner, E., Evans, A. C., & Schlaug, G. (2009). Musical Training Shapes Structural Brain Development. *Journal of Neuroscience*, *29*(10), 3019–3025.

https://doi.org/10.1523/JNEUROSCI.5118-08.2009

Javaras, K. N., Runfola, C. D., Thornton, L. M., Agerbo, E., Birgegård, A., Norring, C., … Bulik, C. M. (2015). Sex- and age-specific incidence of healthcare-register-recorded eating disorders in the complete swedish 1979-2001 birth cohort. *International Journal of Eating Disorders*, *48*(8), 1070–1081. https://doi.org/10.1002/eat.22467

Jelinek, H. F., & Fernandez, E. (1998). Neurons and fractals: How reliable and useful are calculations of offractal dimensions? *Journal of Neuroscience Methods*, *81*(1–2), 9–18. https://doi.org/10.1016/S0165-0270(98)00021-1

Katz, L. C., & Shatz, C. J. (1996, November 15). Synaptic activity and the construction of cortical circuits. *Science*. https://doi.org/10.1126/science.274.5290.1133

Kaufmann, L. K., Baur, V., Hänggi, J., Jäncke, L., Piccirelli, M., Kollias, S., … Milos, G. (2017). Fornix Under Water? Ventricular Enlargement Biases Forniceal Diffusion Magnetic Resonance Imaging Indices in Anorexia Nervosa. *Biological Psychiatry: Cognitive Neuroscience and Neuroimaging*, *2*(5), 430–437. https://doi.org/10.1016/j.bpsc.2017.03.014

Kawasaki, H., Tsuchiya, N., Kovach, C. K., Nourski, K. V, Oya, H., Howard, M. A., & Adolphs, R. (2012). Processing of facial emotion in the human fusiform gyrus. *Journal of Cognitive Neuroscience*, *24*(6), 1358–1370. https://doi.org/10.1162/jocn_a_00175

Kaye, W. H., Fudge, J. L., & Paulus, M. (2009). New insights into symptoms and neurocircuit function

of anorexia nervosa. *Nature Publishing Group*, *10*. https://doi.org/10.1038/nrn2682

Keski-Rahkonen, A., Hoek, H. W., Susser, E. S., Linna, M. S., Sihvola, E., Raevuori, A., … Rissanen, A. (2007). Epidemiology and Course of Anorexia Nervosa in the Community. *American Journal of Psychiatry*, *164*(8), 1259–1265. https://doi.org/10.1176/appi.ajp.2007.06081388

Khundrakpam, B. S., Reid, A., Brauer, J., Carbonell, F., Lewis, J., Ameis, S., … Evans, A. C. (2013). Developmental changes in organization of structural brain networks. *Cerebral Cortex*, *23*(9), 2072–2085. https://doi.org/10.1093/cercor/bhs187

Kim, S.-G., Jung, W. H., Kim, S. N., Jang, J. H., & Kwon, J. S. (2013). Disparity between dorsal and ventral networks in patients with obsessive-compulsive disorder: evidence revealed by graph theoretical analysis based on cortical thickness from MRI. *Frontiers in Human Neuroscience*, *7*, 302. https://doi.org/10.3389/fnhum.2013.00302

King, J. A., Frank, G. K. W., Thompson, P. M., & Ehrlich, S. (2018, February 1). Structural Neuroimaging of Anorexia Nervosa: Future Directions in the Quest for Mechanisms Underlying Dynamic Alterations. *Biological Psychiatry*. Elsevier. https://doi.org/10.1016/j.biopsych.2017.08.011

King, J. A., Geisler, D., Ritschel, F., Boehm, I., Seidel, M., Roschinski, B., … Ehrlich, S. (2015). Global cortical thinning in acute anorexia nervosa normalizes following long-term weight restoration. *Biological Psychiatry*, *77*(7), 624–632. https://doi.org/10.1016/j.biopsych.2014.09.005

King, R. D., Brown, B., Hwang, M., Jeon, T., & George, A. T. (2010). Fractal dimension analysis of the cortical ribbon in mild Alzheimer's disease. *NeuroImage*, *53*(2), 471–479. https://doi.org/10.1016/j.neuroimage.2010.06.050

King, R. D., Brown, B., Hwang, M., Jeon, T., & George, A. T. (2010). Fractal dimension analysis of the cortical ribbon in mild Alzheimer's disease. https://doi.org/10.1016/j.neuroimage.2010.06.050

Kiselev, V. G., Hahn, K. R., & Auer, D. P. (2003). Is the brain cortex a fractal? *NeuroImage*, *20*(3), 1765–74. Retrieved from http://www.ncbi.nlm.nih.gov/pubmed/14642486

Korgaonkar, M. S., Fornito, A., Williams, L. M., & Grieve, S. M. (2014). Abnormal structural networks characterize major depressive disorder: A connectome analysis. *Biological Psychiatry*, *76*(7), 567–574. https://doi.org/10.1016/j.biopsych.2014.02.018

Kwon, H., Choi, Y. H., Seo, S. W., & Lee, J. M. (2017). Scale-integrated Network Hubs of the White Matter Structural Network. *Scientific Reports*, *7*(1), 1–10. https://doi.org/10.1038/s41598-017-02342-7

Landman, B. A., Farrell, J. A. D., Jones, C. K., Smith, S. A., Prince, J. L., & Mori, S. (2007). Effects of diffusion weighting schemes on the reproducibility of DTI-derived fractional anisotropy, mean diffusivity, and principal eigenvector measurements at 1.5T. *NeuroImage*, *36*(4), 1123–1138. https://doi.org/10.1016/j.neuroimage.2007.02.056

Latora, V., & Marchiori, M. (2001). Efficient behavior of small-world networks. *Physical Review*

Letters, *87*(19), 198701-1-198701–4. https://doi.org/10.1103/PhysRevLett.87.198701

Lavagnino, L., Amianto, F., Mwangi, B., D'Agata, F., Spalatro, A., Zunta Soares, G. B., … Soares, J. C. (2016). The relationship between cortical thickness and body mass index differs between women with anorexia nervosa and healthy controls. *Psychiatry Research - Neuroimaging*, *248*, 105–109. https://doi.org/10.1016/j.pscychresns.2016.01.002

Lavagnino, L., Mwangi, B., Cao, B., Shott, M. E., Soares, J. C., & Frank, G. K. W. (2018). Cortical thickness patterns as state biomarker of anorexia nervosa. *International Journal of Eating Disorders*, *51*(3), 241–249. https://doi.org/10.1002/eat.22828

Lebel, C., Gee, M., Camicioli, R., Wieler, M., Martin, W., & Beaulieu, C. (2012). Diffusion tensor imaging of white matter tract evolution over the lifespan. *NeuroImage*, *60*(1), 340–352. https://doi.org/10.1016/J.NEUROIMAGE.2011.11.094

Lee, S., Ran Kim, K., Ku, J., Lee, J.-H., Namkoong, K., & Jung, Y.-C. (2014). Resting-state synchrony between anterior cingulate cortex and precuneus relates to body shape concern in anorexia nervosa and bulimia nervosa. *Psychiatry Research: Neuroimaging*, *221*(1), 43–48. https://doi.org/10.1016/j.pscychresns.2013.11.004

Li, X., Jiang, J., Zhu, W., Yu, C., Sui, M., Wang, Y., & Jiang, T. (2007). Asymmetry of prefrontal cortical convolution complexity in males with attention-deficit/hyperactivity disorder using fractal information dimension. *Brain and Development*, *29*(10), 649–655. https://doi.org/10.1016/j.braindev.2007.04.008

Lv, Y.-T., Yang, H., Wang, D.-Y., Li, S.-Y., Han, Y., Zhu, C.-Z., … Zang, Y.-F. (2008). Correlations in spontaneous activity and gray matter density between left and right sensoritmotor areas of pianists. *NeuroReport*, *19*(6), 631–634. https://doi.org/10.1097/WNR.0b013e3282fa6da0

Madan, C. R., & Kensinger, E. A. (2016). Cortical complexity as a measure of age-related brain atrophy. *NeuroImage*, *134*, 617–629. https://doi.org/10.1016/j.neuroimage.2016.04.029

Maguire, E. A., Gadian, D. G., Johnsrude, I. S., Good, C. D., Ashburner, J., Frackowiak, R. S. J., & Frith, C. D. (2000). Navigation-related structural change in the hippocampi of taxi drivers. *Proceedings of the National Academy of Sciences*, *97*(8), 4398–4403. https://doi.org/10.1073/pnas.070039597

Mandelbrot, B. B. (1983). *The Fractal Geometry of Nature*. W.H. Freeman. https://doi.org/10.1119/1.13295

Margulies, D. S., Kelly, A. M. C., Uddin, L. Q., Biswal, B. B., Castellanos, F. X., & Milham, M. P. (2007). Mapping the functional connectivity of anterior cingulate cortex. *NeuroImage*, *37*(2), 579–588. https://doi.org/10.1016/j.neuroimage.2007.05.019

Menon, V. (2013, December 1). Developmental pathways to functional brain networks: Emerging principles. *Trends in Cognitive Sciences*. Elsevier. https://doi.org/10.1016/j.tics.2013.09.015

Monzon, B. M., Hay, P., Foroughi, N., & Touyz, S. (2016). White matter alterations in anorexia

nervosa: A systematic review of diffusion tensor imaging studies. *World Journal of Psychiatry*, *6*(1), 177. https://doi.org/10.5498/wjp.v6.i1.177

Morgan, S. E., White, S. R., Bullmore, E. T., & Vértes, P. E. (2018). A Network Neuroscience Approach to Typical and Atypical Brain Development. *Biological Psychiatry: Cognitive Neuroscience and Neuroimaging*. https://doi.org/10.1016/j.bpsc.2018.03.003

Mustelin, L., Silén, Y., Raevuori, A., Hoek, H. W., Kaprio, J., & Keski-Rahkonen, A. (2016). The DSM-5 diagnostic criteria for anorexia nervosa may change its population prevalence and prognostic value. *Journal of Psychiatric Research*, *77*, 85–91. https://doi.org/10.1016/j.jpsychires.2016.03.003

Nenadic, I., Yotter, R. A., Sauer, H., & Gaser, C. (2014). Cortical surface complexity in frontal and temporal areas varies across subgroups of schizophrenia. *Human Brain Mapping*, *35*(4), 1691–1699. https://doi.org/10.1002/hbm.22283

Newman, M. E. J., & Girvan, M. (2004). Finding and evaluating community structure in networks. *Physical Review E*, *69*(2), 26113. https://doi.org/10.1103/PhysRevE.69.026113

Noldus, R., & Mieghem, P. Van. (2014). Assortativity in complex networks. *Journal of Complex Networks*, *3*(4), 507–542. https://doi.org/10.1093/comnet/cnv005

Oldfield, R. C. (1971). The assessment and analysis of handedness: The Edinburgh inventory. *Neuropsychologia*, *9*(1), 97–113. https://doi.org/10.1016/0028-3932(71)90067-4

Onnela, J. P., Saramäki, J., Kertész, J., & Kaski, K. (2005). Intensity and coherence of motifs in weighted complex networks. *Physical Review E - Statistical, Nonlinear, and Soft Matter Physics*, *71*(6). https://doi.org/10.1103/PhysRevE.71.065103

Palaniyappan, L., Marques, T. R., Taylor, H., Mondelli, V., Reinders, A. A. T. S., Bonaccorso, S., … Dazzan, P. (2016a). Globally Efficient Brain Organization and Treatment Response in Psychosis: A Connectomic Study of Gyrification. *Schizophrenia Bulletin*, *42*(6), 1446–1456. https://doi.org/10.1093/schbul/sbw069

Palaniyappan, L., Marques, T. R., Taylor, H., Mondelli, V., Reinders, A. A. T. S., Bonaccorso, S., … Dazzan, P. (2016b). Globally Efficient Brain Organization and Treatment Response in Psychosis: A Connectomic Study of Gyrification. *Schizophrenia Bulletin*, *42*(6), 1446–1456. https://doi.org/10.1093/schbul/sbw069

Palaniyappan, L., Park, B., Balain, V., Dangi, R., & Liddle, P. (2015). Abnormalities in structural covariance of cortical gyrification in schizophrenia. *Brain Structure and Function*, *220*(4), 2059–2071. https://doi.org/10.1007/s00429-014-0772-2

P Lerch, J., Worsley, K., Philip Shaw, W., Greenstein, D. (Dede, K Lenroot, R., Giedd, J., & Evans, A. (2006). *Mapping anatomical correlations across cerebral cortex (MACACC) using cortical thickness from MRI*. *NeuroImage* (Vol. 31). https://doi.org/10.1016/j.neuroimage.2006.01.042

Paus, T., Keshavan, M., & Giedd, J. N. (2008). Why do many psychiatric disorders emerge during

adolescence? *Nature Reviews Neuroscience*, *9*(12), 947–957. https://doi.org/10.1038/nrn2513

Pezawas, L., Meyer-Lindenberg, A., Drabant, E. M., Verchinski, B. A., Munoz, K. E., Kolachana, B. S., … Weinberger, D. R. (2005). 5-HTTLPR polymorphism impacts human cingulate-amygdala interactions: a genetic susceptibility mechanism for depression. *Nature Neuroscience*, *8*(6), 828–834. https://doi.org/10.1038/nn1463

Pfuhl, G., King, J. A., Geisler, D., Roschinski, B., Ritschel, F., Seidel, M., … Ehrlich, S. (2016). Preserved white matter microstructure in young patients with anorexia nervosa? *Human Brain Mapping*, *37*(11), 4069–4083. https://doi.org/10.1002/hbm.23296

Phillipou, A., Carruthers, S. P., Di Biase, M. A., Zalesky, A., Abel, L. A., Castle, D. J., … Rossell, S. L. (2018). White matter microstructure in anorexia nervosa. *Human Brain Mapping*, (March), 1–8. https://doi.org/10.1002/hbm.24279

Raznahan, A., Lerch, J. P., Lee, N., Greenstein, D., Wallace, G. L., Stockman, M., … Giedd, J. N. (2011). Patterns of coordinated anatomical change in human cortical development: A longitudinal neuroimaging study of maturational coupling. *Neuron*, *72*(5), 873–884. https://doi.org/10.1016/j.neuron.2011.09.028

Rimol, L. M., Panizzon, M. S., Fennema-Notestine, C., Eyler, L. T., Fischl, B., Franz, C. E., … Dale, A. M. (2010). Cortical Thickness Is Influenced by Regionally Specific Genetic Factors. *Biological Psychiatry*, *67*(5), 493–499. https://doi.org/10.1016/j.biopsych.2009.09.032

Ristanović, D., & Milošević, N. T. (2012). Fractal analysis: Methodologies for biomedical researchers. *Theoretical Biology Forum*, *105*(2), 99–118. Retrieved from http://www.ncbi.nlm.nih.gov/pubmed/23757956

Ristanović, D., Stefanović, B. D., & Puskas, N. (2013). Fractal analysis of dendrites morphology using modified Richardson's and box counting method. *Theoretical Biology Forum*, *106*(1–2), 157–168. Retrieved from http://www.ncbi.nlm.nih.gov/pubmed/24640426

Roberts, G., Perry, A., Lord, A., Frankland, A., Leung, V., Holmes-Preston, E., … Breakspear, M. (2018). Structural dysconnectivity of key cognitive and emotional hubs in young people at high genetic risk for bipolar disorder. *Molecular Psychiatry*, *23216*, 413–421. https://doi.org/10.1038/mp.2016.216

Rose, M., & Frampton, I. (2011). Conceptual Models. In *Eating Disorders and the Brain* (pp. 142–163). Chichester, UK: John Wiley & Sons, Ltd. https://doi.org/10.1002/9781119998402.ch7

Rubinov, M., & Bullmore, E. (2013). Schizophrenia and abnormal brain network hubs. *Dialogues in Clinical Neuroscience*, *15*(3), 339–349. https://doi.org/10.1016/j.siny.2015.10.004

Rubinov, M., & Sporns, O. (2010). Complex network measures of brain connectivity: Uses and interpretations. *NeuroImage*, *52*(3), 1059–1069. https://doi.org/10.1016/j.neuroimage.2009.10.003

Saad, J. F., Griffiths, K. R., Kohn, M. R., Clarke, S., Williams, L. M., & Korgaonkar, M. S. (2017). Regional brain network organization distinguishes the combined and inattentive subtypes of

Attention Deficit Hyperactivity Disorder. *NeuroImage: Clinical*, *15*, 383–390. https://doi.org/10.1016/j.nicl.2017.05.016

Salbach-Andrae, H., Lenz, K., Simmendinger, N., Klinkowski, N., Lehmkuhl, U., & Pfeiffer, E. (2008). Psychiatric Comorbidities among Female Adolescents with Anorexia Nervosa. *Child Psychiatry and Human Development*, *39*(3), 261–272. https://doi.org/10.1007/s10578-007-0086-1

Sandu, A.-L., Izard, E., Specht, K., Beneventi, H., Lundervold, A., & Ystad, M. (2014). Post-adolescent developmental changes in cortical complexity. *Behavioral and Brain Functions*, *10*(1), 44. https://doi.org/10.1186/1744-9081-10-44

Sandu, A.-L., Rasmussen, I.-A., Lundervold, A., Kreuder, F., Neckelmann, G., Hugdahl, K., & Specht, K. (2008). Fractal dimension analysis of MR images reveals grey matter structure irregularities in schizophrenia. *Computerized Medical Imaging and Graphics*, *32*, 150–158. https://doi.org/10.1016/j.compmedimag.2007.10.005

Schaer, M., Bach Cuadra, M., Tamarit, L., Lazeyras, F., Eliez, S., & Thiran, J. P. (2008). A Surface-based approach to quantify local cortical gyrification. *IEEE Transactions on Medical Imaging*, *27*(2), 161–170. https://doi.org/10.1109/TMI.2007.903576

Schmitt, J. E., Lenroot, R. K., Wallace, G. L., Ordaz, S., Taylor, K. N., Kabani, N., … Giedd, J. N. (2008). Identification of genetically mediated cortical networks: A multivariate study of pediatric twins and siblings. *Cerebral Cortex*, *18*(8), 1737–1747. https://doi.org/10.1093/cercor/bhm211

Schultz, C. C., Wagner, G., de la Cruz, F., Berger, S., Reichenbach, J. R., Sauer, H., & Bär, K. J. (2017).

Evidence for alterations of cortical folding in anorexia nervosa. *European Archives of Psychiatry and Clinical Neuroscience*, *267*(1), 41–49. https://doi.org/10.1007/s00406-015-0666-1

Schwarzlose, R. F. (2005). Separate Face and Body Selectivity on the Fusiform Gyrus. *Journal of Neuroscience*, *25*(47), 11055–11059. https://doi.org/10.1523/JNEUROSCI.2621-05.2005

Seidel, M., King, J. A., Ritschel, F., Boehm, I., Geisler, D., Bernardoni, F., … Ehrlich, S. (2018). Processing and regulation of negative emotions in anorexia nervosa: An fMRI study. *NeuroImage: Clinical*, *18*, 1–8. https://doi.org/10.1016/j.nicl.2017.12.035

Seitz, J., Bühren, K., Von Polier, G. G., Heussen, N., Herpertz-Dahlmann, B., & Konrad, K. (2014). Morphological Changes in the Brain of Acutely Ill and Weight-Recovered Patients with Anorexia Nervosa A Meta-Analysis and Qualitative Review. *Anorexia Nervosa Z. Kinder-Jugendpsychiatr. Psychother. Anorexia Nervosa Z. Kinder-Jugendpsychiatr. Psychother*, *42*(421), 7–18. https://doi.org/10.1024/1422-4917/a000265

Seitz, J., Herpertz-Dahlmann, B., & Konrad, K. (2016). Brain morphological changes in adolescent and adult patients with anorexia nervosa. *Journal of Neural Transmission*, *123*(8), 949–959. https://doi.org/10.1007/s00702-016-1567-9

Shott, M. E., Pryor, T. L., Yang, T. T., & Frank, G. K. W. (2016). Greater Insula White Matter Fiber Connectivity in Women Recovered from Anorexia Nervosa. *Neuropsychopharmacology : Official Publication of the American College of Neuropsychopharmacology*, *41*(2), 498–507. https://doi.org/10.1038/npp.2015.172

Sidlauskaite, J., Caeyenberghs, K., Sonuga-Barke, E., Roeyers, H., & Wiersema, J. R. (2015). Whole-brain structural topology in adult attention-deficit/hyperactivity disorder: Preserved global - Disturbed local network organization. *NeuroImage: Clinical*, *9*, 506–512. https://doi.org/10.1016/j.nicl.2015.10.001

Smink, F. R. E., van Hoeken, D., & Hoek, H. W. (2013). Epidemiology, course, and outcome of eating disorders. *Current Opinion in Psychiatry*, *26*(6), 543–548. https://doi.org/10.1097/YCO.0b013e328365a24f

Sporns, O. (2006). Small-world connectivity, motif composition, and complexity of fractal neuronal connections. *BioSystems*, *85*(1), 55–64. https://doi.org/10.1016/j.biosystems.2006.02.008

Sporns, O. (2010). *Networks of the Brain*. *Networks of the brain* (Vol. 52). MIT Press. https://doi.org/10.1097/WNQ.0b013e31820f1a98

Squarcina, L., De Luca, A., Bellani, M., Brambilla, P., Turkheimer, F. E., & Bertoldo, A. (2015). Fractal analysis of MRI data for the characterization of patients with schizophrenia and bipolar disorder. *Physics in Medicine and Biology*, *60*(4), 1697–1716. https://doi.org/10.1088/0031-9155/60/4/1697

Steinhausen, H.-C. (2002). The Outcome of Anorexia Nervosa in the 20th Century. *American Journal of Psychiatry*, *159*(8), 1284–1293. https://doi.org/10.1176/appi.ajp.159.8.1284

Steward, T., Menchon, J. M., Jimenez-Murcia, S., Soriano-Mas, C., & Fernandez-Aranda, F. (2017). Neural network alterations across eating disorders: a narrative review of fMRI studies. *Current Neuropharmacology*, *15*, 1–13. https://doi.org/10.2174/1570159X15666171017111532

Supekar, K., Musen, M., & Menon, V. (2009). Development of large-scale functional brain networks in children. *PLoS Biology*, *7*(7), e1000157. https://doi.org/10.1371/journal.pbio.1000157

Swinbourne, J., Hunt, C., Abbott, M., Russell, J., St Clare, T., & Touyz, S. (2012). The comorbidity between eating disorders and anxiety disorders: Prevalence in an eating disorder sample and anxiety disorder sample. *Australian and New Zealand Journal of Psychiatry*, *46*(2), 118–131. https://doi.org/10.1177/0004867411432071

Tau, G. Z., & Peterson, B. S. (2010, January 30). Normal development of brain circuits. *Neuropsychopharmacology*. https://doi.org/10.1038/npp.2009.115

Taylor, S. F. (2014, April 15). Using graph theory to connect the dots in obsessive-compulsive disorder. *Biological Psychiatry*. Elsevier. https://doi.org/10.1016/j.biopsych.2014.01.012

Thambisetty, M., Wan, J., Carass, A., An, Y., Prince, J. L., & Resnick, S. M. (2010). Longitudinal changes in cortical thickness associated with normal aging. *NeuroImage*, *52*(4), 1215–1223. https://doi.org/10.1016/j.neuroimage.2010.04.258

Thomason, M. E., Brown, J. A., Dassanayake, M. T., Shastri, R., Marusak, H. A., Hernandez-Andrade, E., … Romero, R. (2014). Intrinsic functional brain architecture derived from graph theoretical

analysis in the human fetus. *PLoS ONE*, *9*(5), e94423. https://doi.org/10.1371/journal.pone.0094423

Thompson, P. M., Cannon, T. D., Narr, K. L., van Erp, T., Poutanen, V.-P., Huttunen, M., … Toga, A. W. (2001). Genetic influences on brain structure. *Nature Neuroscience*, *4*(12), 1253–1258. https://doi.org/10.1038/nn758

Titova, O. E., Hjorth, O. C., Schiöth, H. B., & Brooks, S. J. (2013). Anorexia nervosa is linked to reduced brain structure in reward and somatosensory regions: A meta-analysis of VBM studies. *BMC Psychiatry*, *13*. https://doi.org/10.1186/1471-244X-13-110

Travis, K. E., Golden, N. H., Feldman, H. M., Solomon, M., Nguyen, J., Mezer, A., … Dougherty, R. F. (2015). Abnormal white matter properties in adolescent girls with anorexia nervosa. *NeuroImage: Clinical*, *9*, 648–659. https://doi.org/10.1016/j.nicl.2015.10.008

Treasure, J., Stein, D., & Maguire, S. (2015, June). Has the time come for a staging model to map the course of eating disorders from high risk to severe enduring illness? An examination of the evidence. *Early Intervention in Psychiatry*. https://doi.org/10.1111/eip.12170

Tzourio-Mazoyer, N. (2016). Intra- and inter-hemispheric connectivity supporting hemispheric specialization. In *Research and Perspectives in Neurosciences* (pp. 129–146). Springer. https://doi.org/10.1007/978-3-319-27777-6_9

van den Heuvel, M. P., & Sporns, O. (2011). Rich-Club Organization of the Human Connectome.

Journal of Neuroscience, *31*(44), 15775–15786. https://doi.org/10.1523/JNEUROSCI.3539-11.2011

van den Heuvel, M. P., & Sporns, O. (2013). Network hubs in the human brain. *Trends in Cognitive Sciences*. https://doi.org/10.1016/j.tics.2013.09.012

Van Den Heuvel, M. P., Sporns, O., Collin, G., Scheewe, T., Mandl, R. C. W., Cahn, W., … Kahn, R. S. (2013). Abnormal rich club organization and functional brain dynamics in schizophrenia. *JAMA Psychiatry*, *70*(8), 783–792. https://doi.org/10.1001/jamapsychiatry.2013.1328

Van Essen, D. C. (n.d.). A tension-based theory of morphogenesis and compact wiring in the central nervous system.pdf. Retrieved from https://pdfs.semanticscholar.org/ba94/1626846d02d86fd9011e9b9a0b83922f846f.pdf

Vander Wyk, B. C., Hudac, C. M., Carter, E. J., Sobel, D. M., & Pelphrey, K. A. (2009). Action Understanding in the Superior Temporal Sulcus Region. *Psychological Science*, *20*(6), 771–777. https://doi.org/10.1111/j.1467-9280.2009.02359.x

Vara, A. S., Pang, E. W., Vidal, J., Anagnostou, E., & Taylor, M. J. (2014). Neural mechanisms of inhibitory control continue to mature in adolescence. *Developmental Cognitive Neuroscience*, *10*, 129–139. https://doi.org/10.1016/j.dcn.2014.08.009

Vogel, K., Timmers, I., Kumar, V., Nickl-Jockschat, T., Bastiani, M., Roebroek, A., … Seitz, J. (2016). White matter microstructural changes in adolescent anorexia nervosa including an exploratory

longitudinal study. *NeuroImage: Clinical*, *11*, 614–621. https://doi.org/10.1016/j.nicl.2016.04.002

Wang, T., Wang, K., Qu, H., Zhou, J., Li, Q., Deng, Z., … Xie, P. (2016). Disorganized cortical thickness covariance network in major depressive disorder implicated by aberrant hubs in large-scale networks. *Scientific Reports*, *6*. https://doi.org/10.1038/srep27964

Watts, D. J., & Strogatz, S. H. (1998). Collective dynamics of "small-world" networks. *Nature*, *393*(6684), 440–442. https://doi.org/10.1038/30918

White, T., Su, S., Schmidt, M., Kao, C. Y., & Sapiro, G. (2010, February). The development of gyrification in childhood and adolescence. *Brain and Cognition*. NIH Public Access. https://doi.org/10.1016/j.bandc.2009.10.009

Wierenga, L. M., van den Heuvel, M. P., van Dijk, S., Rijks, Y., de Reus, M. A., & Durston, S. (2016). The development of brain network architecture. *Human Brain Mapping*, *37*(2), 717–729. https://doi.org/10.1002/hbm.23062

Wu, H., Sun, H., Xu, J., Wu, Y., Wang, C., Xiao, J., … Liu, J. (2016). Changed Hub and Corresponding Functional Connectivity of Subgenual Anterior Cingulate Cortex in Major Depressive Disorder. *Front. Neuroanat*, *10*, 120. https://doi.org/10.3389/fnana.2016.00120

Yap, P. T., Fan, Y., Chen, Y., Gilmore, J. H., Lin, W., & Shen, D. (2011). Development trends of white matter connectivity in the first years of life. *PLoS ONE*, *6*(9), e24678.

https://doi.org/10.1371/journal.pone.0024678

Zhang, A., Leow, A., Zhan, L., Gadelkarim, J., Moody, T., Khalsa, S., … Feusner, J. D. (2016). Brain connectome modularity in weight-restored anorexia nervosa and body dysmorphic disorder. *Psychological Medicine*, *46*(13), 2785–2797. https://doi.org/10.1017/S0033291716001458

Zhang, Y., Lin, L., Lin, C. P., Zhou, Y., Chou, K. H., Lo, C. Y., … Jiang, T. (2012). Abnormal topological organization of structural brain networks in schizophrenia. *Schizophrenia Research*, *141*(2–3), 109–118. https://doi.org/10.1016/j.schres.2012.08.021

Zielinski, B. A., Gennatas, E. D., Zhou, J., & Seeley, W. W. (2010). Network-level structural covariance in the developing brain. *Proceedings of the National Academy of Sciences of the United States of America*, *107*(42), 18191–6. https://doi.org/10.1073/pnas.1003109107

Zilbovicius, M., Meresse, I., Chabane, N., Brunelle, F., Samson, Y., & Boddaert, N. (2006, July 1). Autism, the superior temporal sulcus and social perception. *Trends in Neurosciences*. Elsevier Current Trends. https://doi.org/10.1016/j.tins.2006.06.004

Zipfel, S., Giel, K. E., Bulik, C. M., Hay, P., & Schmidt, U. (2015). Anorexia nervosa: Aetiology, assessment, and treatment. *The Lancet Psychiatry*, *2*(12), 1099–1111. https://doi.org/10.1016/S2215-0366(15)00356-9